Distribution Agreement

In presenting this thesis or dissertation as a partial fulfillment of the requirements for an advanced degree from Emory University, I hereby grant to Emory University and its agents the non-exclusive license to archive, make accessible, and display my thesis or dissertation in whole or in part in all forms of media, now or hereafter known, including display on the world wide web. I understand that I may select some access restrictions as part of the online submission of this thesis or dissertation. I retain all ownership rights to the copyright of the thesis or dissertation. I also retain the right to use in future works (such as articles or books) all or part of this thesis or dissertation.

Signature:

_____ _____

Oluwaseyi Adekunle Date

Analysis of Human B Cell Development and Antibody Responses Following Immunization with a Live Attenuated Cholera Vaccine

Oluwaseyi Adekunle Doctor of Philosophy

Graduate Division of Biological and Biomedical Sciences
Immunology and Molecular Pathogenesis

Jens P. Wrammert, Ph.D.
Advisor

Frances Eun-Hyung Lee, M.D.
Committee Member

Joshy Jacob, Ph.D.
Committee Member

Periasamy Selvaraj, Ph.D.
Committee Member

William Shafer, Ph.D.
Committee Member

Accepted:

Lisa A. Tedesco, Ph.D.
Dean of the James T. Laney School of Graduate Studies

Date

Analysis of Human B Cell Development and Antibody Responses Following Immunization with a Live Attenuated Cholera Vaccine

By

Oluwaseyi Adekunle
B.S. Georgia Southern University 2010
M.S., Georgia State University 2015

Advisor: Jens Wrammert, Ph.D.

An abstract of
A dissertation submitted to the Faculty of the
James T. Laney School of Graduate Studies of Emory University
in partial fulfillment of the requirements for the degree of
Doctor of Philosophy
in Immunology and Molecular Pathogenesis 2021

Abstract

Analysis of Human B Cell Development and Antibody Responses Following Immunization with a Live Attenuated Cholera Vaccine

By Oluwaseyi Adekunle

B cells are important mediators of protection that provide immunity against infectious pathogens like *Vibrio cholerae*. Both infection and the inactivated oral cholera vaccines (OCV) generate humoral responses, however infection provides durable immunity and the OCV do not. To better understand the immune factors that are important for the generation and maintenance of cholera immunity, we utilized a live attended cholera vaccine as a model of *V. cholerae* exposure.

First, we examined the kinetics of serum and plasmablasts responses following vaccination. We observed that the vaccine induced durable antibody titers that were maintained one year after vaccination. We found that the plasmablast responses were primarily specific for the two immunodominant antigens lipopolysaccharide (LPS) and cholera toxin (CT). The acute responses displayed preferential immunoglobulin isotype usage, with LPS specific cells being largely IgM or IgA producing, while CT responses were predominantly IgG. CCR9 was highly expressed on vaccine induced plasmablasts, especially on the LPS specific cells, suggesting a role in migration to the gastrointestinal tract. Finally, using single cell approaches we observed that the LPS specific plasmablasts also displayed hallmarks of ongoing affinity maturation.

Next, we examined the properties of LPS specific antibodies and how immunoglobulin isotype and subclass effects their functional attributes. To approach this, we utilized a panel of monoclonal antibodies that we expressed in different immunoglobulin backbones. We then characterized the impact of these changes on their binding and functional capabilities. We observed that isotype had a profound impact by increasing the low-affinity antibodies binding and functional properties. We found that pentameric IgM, dimeric IgA, and monomeric IgA were more potent than their IgG counterparts at inhibiting motility. Finally, by analyzing the F(ab) versions of these antibodies, we showed that LPS crosslinking was essential for motility inhibition.

Collectively, these findings provide key insights into cholera specific B cells development, the role of mucosal homing, and mechanisms of antibody mediated immunity. We believe that these findings will help inform future vaccine development by highlighting aspects of the response that are associated with protection and raise important questions on the relationship between peripheral and mucosal humoral responses.

Analysis of Human B Cell Development and Antibody Responses Following Immunization with a Live Attenuated Cholera Vaccine

By

Oluwaseyi Adekunle
B.S. Georgia Southern University 2010
M.S., Georgia State University 2015

Advisor: Jens Wrammert, Ph.D.

A dissertation submitted to the Faculty of the
James T. Laney School of Graduate Studies of Emory University
in partial fulfillment of the requirements for the degree of
Doctor of Philosophy
in Immunology and Molecular Pathogenesis 2021

Table of Contents

Chapter 1: Introduction

B cell Immune responses

Early B Cell Development

The adaptive immune system, through a variety of complex mechanisms, is able to provide long term protection against specific pathogens targets. The distinction of the two arms which comprise this system was elucidated by Dr. Max Cooper's early pivotal experiments examining the chicken immune system [1]. In the early 1960s it was known that removal of the bursa resulted in poor antibody production, although studies described conflicting results on the efficacy of the reduction [1]. Dr. Cooper paired bursa and thymus removal with radiation, thereby removing any cells which had migrated before the organs were removed. With this approach he was able to elegantly show that removal of the bursa and their associated lymphocytes resulted in the complete loss of antibody responses, while leaving the small thymus-derived lymphocytes intact. The inverse experiment with the removal of the thymus resulted in the loss of the small lymphocyte population while the antibody titers persisted [2, 3]. Thus, Dr. Cooper's experiments help to identify the two distinct branches which comprise the lymphocyte population, cellular immunity driven by thymus derived cells, or T-cells, and humoral immunity mediated by bursa-derived cells, also known as B cells.

Since those early pivotal experiments, subsequent research efforts have provided key insights on the origin and function of B cells. In mammals, the development of B cells begins within the bone marrow from progenitor hematopoietic stem cells [4]. Common lymphoid progenitors start to express the transcription factors PU.1 and ikaros which lead to the expression of the surface receptors FLT3 and IL-7R [5]. These receptors bind to surface and soluble factors in the stromal environment. The resulting signal cascade leads to an upregulation of the

transcription factors EBF and Pax-5, a master regulator which commits cells to the Pro-B cell pathway by inducing expression of CD19, BLNK, and Igα [6].

During the early development process complex recombination events within the cell lead to the generation of the B cell receptor (BCR), which plays a pivotal role guiding B cell development [7]. An important part of this process is VDJ rearrangement, which is mediated by the enzymes RAG-1 and RAG-2 [8]. This is the process by which the different variable (V), diversity (D), and joining (J) gene segments are recombined to form the BCR [9, 10]. Combined with the junctional diversity generated by p and n nucleotide addition, VDJ rearrangement allows for the generation of a multitude of diverse receptors that can recognize an incredibly wide array of antigens [11]. Studies have estimated the potential number of unique B cell receptors can reach over 11 million [12, 13]. Because of the diverse array of BCR that are generated, receptors that are reactive to self-antigens can also be assembled during this process.

There are checks during the development process which prevent the generation and release of self-reactive cells. B cells which strongly bind self-antigens are induced to undergo further gene rearrangements to produce non-self-reactive BCR [14]. B cells which are unable to generate non-self-reactive BCR undergo apoptosis within the bone marrow. Cells which weakly bind self-proteins can go into circulation. However, they become anergic and are unable to respond to further stimulation [15]. Additionally, for optimal activation B cells typically require T cell help. Therefore, for an autoreactive B cell to activate it must pair with an autoreactive T cell. This extra step further reduces the likelihood of these cells becoming active [16]. Naïve non-self-reactive B cells are able to enter circulation where they screen for antigens their BCR can recognize [4].

Activation of B cells

Antigen recognition typically takes in lymph nodes, specialized tissue structures which house B cells, T cells, and myeloid cells such as macrophages and dendritic cells. CXCR5 expression on the B cells allows them to migrate into follicles within the lymph node by following the gradient of CXCL13 released by follicular dendritic cells [17]. Lymph drains into the follicle and brings antigens from the distal sites of the body, allowing B cells to screen them for potential threats. In addition to soluble antigens, macrophages and follicular dendritic cells can bind antigen to their surface and allow the B cells to screen them [18, 19]. B cells which do not encounter their antigen upregulate S1PR1 receptor and exit back into the circulation to repeat the process in another lymph node [20]. B cells which encounter their cognate antigen undergo a series of steps which can lead to their activation.

Antigens that lead to B cell activation are broadly separated into two categories based on their requirement for T cell help. They are classified as T-dependent antigens, usually proteins, and T-independent antigens, which are typically made up of non-protein antigens such as polysaccharides [21]. Upon encountering a T-dependent antigen, the cell presents it on major histocompatibility complex II (MHC-II) [22]. Typically, antigen binding of the BCR alone is insufficient to activate a naive B cell and therefore a secondary stimulus is also required. Secondary signaling is typically provided by innate immune receptors like toll like receptors (TLR). TLR recognize a broad range of pathogen associated molecular patterns (PAMPs) such as lipopolysaccharide (LPS) and flagellin. TLR engagement results in recruitment of transcription factors such as NFκB, IRF, and AP-1 which prime the cell for activation [23]. Following the binding of a T-dependent antigen and activation of secondary signaling pathways, these

stimulated B cells move from the center of the follicle to the border of the T cell zone for antigen presentation.

When the B cell encounters its cognate T cell, interactions between the TCR/MHC-II in addition to secondary signaling from CD28/CD80 and CD40L/CD40 leads to the activation of the cell [24]. The B cell begins to proliferate and undergo changes to its transcriptional programing that have an important impact on its eventual fate [25]. Traditionally, CSR is thought to occur within the germinal center, due its association with AID and RAG expression [26, 27]. However, recent experiments by Roco *et al.* have demonstrated that this process can occur shortly after the initial T cell engagement [28, 29]. The group utilized an adoptive transfer model in which C57BL/6 mice, which had been adoptively transferred with SW_{HEL} B cells, were immunized with HEL conjugated sheep red blood cells. The researchers then measured germ line transcripts, which are makers of CSR, in the various B cells populations as they responded to the foreign antigen. By measuring these transcripts, the group was able to show that the majority of CSR occurred 2 days prior to germinal center formation and was significantly reduced within the germinal center [28]. These findings highlight the role that affinity and T cell assistance play in shaping the kind of humoral response that is generated following exposure. The study also described the presence of IgM dominated germinal centers. This is a very intriguing finding as it provides insight as to how IgM memory cells may be generated and maintained, thereby providing a pool of antigen experienced cells that retain the capacity to differentiate into the various isotypes depending on the circumstance.

Following the initial proliferative expansion, the B cell can differentiate into different subsets each with their own unique functions. These include forming a germinal center reaction, differentiating into antibody secreting cells (ASC), and memory B cell (MBC) formation [30].

Signals from cytokines, the inducing antigen, other cells, and intrinsic transcriptional and epigenetic factors within the B cell all play a role in determining its fate [31, 32]. For instance, higher affinity for the antigen leads to prolonged contact with helper T cells. This results in higher affinity B cells entering the germinal center while lower affinity cells enter the memory pool [24]. The precise combination of signals that control the future of the cell is an area of active research.

Germinal Center Reaction

B cells which receive the correct signaling milieu return to the follicle where they proliferate into a mass of cells called a germinal center. The germinal center is a structure which primarily consist of antigen specific activated B cells with a small number of T cells and follicular dendritic cells [18, 33, 34]. Surrounding this structure is a mantle zone consisting of inactivated B cells [24]. The germinal center consists of a dark zone where activated B cells differentiate into centroblasts and are actively undergoing somatic hypermutation (SHM) and proliferation. SHM is a process by which the BCR acquires mutations [35]. The mutations are random and can potentially increase or decrease the affinity of the BCR. These cells are held in the dark zone by expression of the receptor CXCR4 [36, 37]. Once a certain number of divisions has been reached the centroblasts down regulate CXCR4 and upregulate CXCR5, which allows for their egress into the light zone as centrocytes.

Once in the light zone the cells compete for the antigen found on the surface of follicular dendritic cells [18, 19, 38]. The B cells which have the highest affinity for the antigen can capture and present it on their MHC II to T follicular helper cells. Higher affinity leads to more antigen capture and presentation which results in more T cell help in the form of survival signals and prolonged contact. Cells with low affinity BCR are unable to compete for T cell help,

receive fewer signals that promote survival, and undergo apoptosis [34]. Centrocytes have three pathways through which they can proceed. They can return to the dark zone to undergo further rounds of SHM. They can form quiescent memory B cells, ready to rapidly respond to the next encounter with the antigen [30, 31]. Finally, a portion will differentiate into antibody secreting cells and return to circulation.

Antibody Secreting Cells

Plasmablasts are antibody secreting cells that are transiently found in circulation shortly after infection or vaccination [39]. These cells represent an induced response, and a substantial number of them are specific towards the immunizing agent [40]. In the absence of an infection, these cells typically represent 1-3% of the total B cells. Following either infection or vaccination, however, these cells can comprise over 50% of the B cell population [39]. Plasmablasts can be detected as early as 4 days post exposure, but typically peak between day 7 and 10 [41, 42]. The duration of the response generally depends on antigen persistence. Levels return to baseline approximately two weeks following vaccination [43]. In infection, plasmablasts levels can remain elevated until the pathogen is cleared [39]. Plasmablasts can be found in both primary and secondary responses, mediated either by naïve or memory B cells respectively [44, 45]. Primary response will see a large induction of IgM cells with relatively low levels of mutation compared to secondary responses which are typically class switched and have a larger number of mutations [40].

The fate of these cells following circulation is unclear, with many of them shortly undergoing apoptosis [46]. There is also evidence that early antibody secreting cell responses have the potential to enter the long-lived ASC pool [47]. Plasmablasts are typically defined as $CD3^{neg}/CD19^{+}/CD20^{low}/CD27^{+}/CD38^{hi}$ cells seen in circulation. However, some research has

shown that plasmablasts form a heterogeneous population that can be further subdivided based on CD19 and CD138 expression. $CD19^{low}$ and $CD138^{hi}$ share a similar phenotypic profile to long lived plasma cells (LLPC) [38, 48, 49]. While phenotypically distinct, it is not clear if these subsets have differential survival in long term niches [47]. It is also uncertain if plasmablasts sequentially proceed from early ASC into LLPC or, if LLPC potential is restricted to a specific subset within the overall plasmablast population [50].

Plasma cells, in contrast to plasmablasts, are terminally differentiated ASC that are primarily found within the bone marrow or intestine [46]. These cells are long lived, non-proliferating, continually secrete antibody, and do not require the presence of the inducing antigen for their survival [51]. It is the constitutive expression of the antibodies from these cells that result in the long-lived protection seen in vaccines such as smallpox. Within the bone marrow the stromal cells, hypoxic environment, and cytokine milieu contribute to the long-term maintenance of these cells [52]. The population of plasma cells that reside in the human bone marrow are identified by their expression of $CD19^{-}/CD38^{hi}/CD138^{+}$ [53].

Plasma cells within the gut serve a similar role to those in the bone marrow, with the antibodies they produce primarily secreted into the intestinal lumen. Like their bone marrow counter parts, intestinal plasma cells can also be identified by their expression of $CD19/CD38^{hi}/CD138^{+}$. Initially, plasma cells in the gut were thought to undergo high rates of turnover. However, recent experiments by Landsverk *et al.* looking at human intestinal plasma cells from transplant recipients have identified a population of long-lived plasma cells [54]. By examining CD19 and CD45 expression on the plasma cells, they were able to divide the cells into three distinct groups. Plasma cells which were $CD19^{+}/CD45^{+}$ expressed higher levels of Ki67, which indicates recent proliferation. In addition, a significant amount of the $CD19^{+}/CD45^{+}$

cells found within the donor tissue originated from the recipient, suggesting a high rate of turnover in this population. In contrast cells which were $CD19^{-}/CD45^{-}$ had low Ki67 expression, high Bcl2 expression, and consisted solely of donor cells within the donor tissue, even up to a year post transplant. This, with the addition of carbon dating, definitively showed that these cells can persist many decades within the gut mucosal environment. The authors also speculated that the $CD19^{-}/CD45^{+}$ subset may represent an intermediate phase and that a portion of these cells could transition into the LLPC population [54]. Given the limited space capable of housing LLPC in both the bone marrow and intestine, identifying factors which are important for the establishment of cells into the long-term survival niches is of great interest [54-56].

Memory B cells

Memory B cells (MBC) are another pathway B cells can differentiate into following activation. They are antigen experienced cells which proliferate rapidly following secondary exposure to antigens, either entering germinal center reactions or differentiating directly into plasmablasts [57]. MBC typically arise prior to or shortly after germinal center formation [58]. Because of the limited time they spend in germinal centers, they typically have lower levels of SHM and affinity when compared to their ASC counter parts [39]. However, the lower affinity allows the body to maintain a repertoire of experienced cells that can quickly react to the inducing antigen or related variants [59].

Primary exposure generates a wide range of MBC clones that have varying affinity for the inducing antigen. Classically, it is believed that these cells are recruited into forming germinal centers following repeat exposure. However, some research has described that many of these cells do not undergo reentry into GC following secondary exposure [60]. A study by Mesin *et al.,* demonstrated that during secondary immunization most of the cells within the germinal

centers were antigen inexperienced clones [60]. Additionally, they found that only a few of the high affinity MBC clones were recruited into secondary germinal center reactions. It is possible that MBC with lower affinity do not undergo GC reactions upon stimulation, but instead immediately proliferate into ASC while those with higher affinity preferentially enter germinal center reactions. This thought may be supported by another study which showed that the expression of CD80 and PDL2 were the best predictors of GC vs ASC formation. In that study, the researchers observed that $CD80^{+}PDL2^{+}$ MBC differentiated into ASC while $CD80^{-}PDL2^{-}$ cells formed GC [61]. The affinity of the two subsets for the inducing antigen was not examined. However, it is possible that the initial affinity of the B cell receptor for its antigen could affect expression of surface receptors. Isotype can also have impact on the decision to differentiate into ASC or undergo germinal center reactions [30]. This is likely due to transcriptional and epigenetic changes that occur within these cells during memory cell development [62].

While naïve B cells typically require T cell assistance for activation, this is not always prerequisite for MBC activation. They can respond to some antigens in the absence of T cell assistance, depending on the nature of the antigen [57, 63]. Additionally, in some circumstances both antigen experienced and naïve T cells are able to provide the necessary signaling for activation [64]. For instance, naïve T cells are able to assist in MBC activation in the case of some monomeric protein antigens and absence of these cells severely inhibits the ability of the MBC to differentiate [65].

Response to non-protein antigens

T-independent antigens can activate B cells without T cell help and come in two variations. T-independent type 1 antigens can activate cells via mitogen and T-independent type 2 antigens activate cells via repeated epitopes [21]. Classically, T-independent antigens were not

thought to induce robust germinal center responses, and it was believed that they were incapable of generating long term immunity [66, 67].However, more recent studies using whole bacteria, LPS, and haptenated ficoll have all shown the presence of LLPC and MBC following immunization [68-70]. T cell depletion experiments have also demonstrated that germinal center reactions, CSR, and SHM were not necessary for the generation of these responses [71]. Moreover, B1 which release IgM in response to T-independent antigens have been shown to differentiate into MBC and thus provide long term protection [72].

B cells activated by T-independent antigens are also able to accumulate mutations and in the absence of germinal centers [72-74]. A study by Roberto Di Niro *et al.* showed that *Salmonella typhimurium* infection in mice leads to the generation of extra follicular responses, and that these responses could occur in the absence of germinal centers [75]. Interestingly, these responses still exhibited hallmarks of CSR and SHM, demonstrating that these functions can occur outside germinal centers reactions. Whether these responses are limited to *Salmonella* or if they can be applied to other T-independent antigens requires further study. While the mechanism behind this process are still uncertain, it is clear that T-independent antigens are capable of inducing long term, affinity mature responses that contribute to the maintenance of humoral immunity.

Antibodies, functional response of B cells

Antibodies are a secreted form of the BCR responsible for the effector functions of the humoral response. They are typically Y shaped proteins comprised of two identical heavy and light chains. Each chain contains a variable and constant domain. Within the variable domain is the complementary determining region which is the part of the antibody that interacts with the antigen. The heavy chain constant domain can come in a variety of forms called isotypes, each

providing unique effector functions due to their structure and interactions with various receptors and proteins [76]. Two of these isotypes, IgG, and IgA, can be further subdivided into various subclasses [77]. Antibodies provide protection by binding and neutralizing the target, enhancing opsonization for phagocytic cells, interacting with complement proteins, and mediating cell signaling via various Fc receptors [78]. While all isotypes play important roles in the immune response, the ones typically associated with infectious disease are IgM, IgG, and IgA.

IgG is the dominant isotype found within serum. Human IgG can be subdivided into 4 subclasses, each differing in their affinity to different Fc receptors and accessory proteins such as complement. IgG1 and IgG3, for example, are efficient activators of the complement system which makes them efficient at enhancing opsonin and lysing microbial targets. IgG ability to bind to the neonatal fc receptor (FcRn) grants them a half-life of 28 days in serum [77]. IgG responses are also typically associated with secondary exposure, as it takes time for CSR to produce large quantities of these antibodies during primary exposure.

IgM is the first isotype produced during a primary immune response. It is comprised of a pentamer connected with the J chain. IgM has the highest avidity of all the antibody isotypes and the pentamer makes it an extremely efficient activator of complement. Although primarily located in serum, it can also be found in the gut lumen due to transport by the polymeric immunoglobulin receptor (pIgR). IgM is not typically found in high amounts during a secondary response due to IgM cells being outcompeted by the higher affinity class switched clones [78].

IgA is the dominant isotype found within the intestinal track and the most abundant isotype produced. In intestinal tissues it is found as a dimer joined together via the j-chain while serum fractions are primarily monomeric. The j-chain is able to bind the polymeric Ig receptor which is found on the basal side of epithelia cells [79]. The Ig is then transported through the cell

to the apical surface where it is cleaved and released into the mucosa [80]. There are two subclasses of IgA, IgA1 and IgA2. IgA1 is more abundant than IgA2 is in the small intestine while there are equal levels of IgA1 and IgA2 within the colon [81]. IgA1 has a larger hinge region compared to IgA2 which makes it more susceptible to microbial proteases [82]. This susceptibility is likely the reason IgA1 is more predominantly found within the microbially less dense regions of the intestinal lumen. The two subclasses also differ in their binding and signaling functions. IgA2 lacks sialic acid and is more pro-inflammatory, compared to IgA1. This effect seems to be dependent on the sialic acids, as removal of them from IgA1 increases its inflammatory potential [83]. There is a large amount of IgA production in the body. In fact, the number of IgA producing cells exceeds the number of the other isotypes combined [81]. SIgA is generally non inflammatory, while monomeric IgA immune complexes can crosslink to the receptor FcaRI and lead to cellular activation, resulting in phagocytosis, ADCC, cytokine secretion, and other outcomes [84].

Intestinal B cell responses

The intestinal immune system is in constant contact with an extraordinary variety of foreign antigens. In contrast to other tissues, cells at this location preferentially sample antigens from the outside environment. Due to these features B cells in this location are under constant stimulation from the microbiota. B cells in this tissue must work to maintain the balance of commensal organisms, inhibit overt inflammatory responses, and prevent infectious by opportunistic and pathogenic microbes.

The naïve and memory B cells reside in gut associated lymphoid tissue (GALT) such as peyers patches or follicle associated epithelium (FAE) [85]. These are areas located primarily within the small intestine and are typically associated with M cells, which can sample luminal

antigens and transfer them into the follicle. [86]. Naïve and MBC located within the follicle sample antigens brought in by M cells or other APC. When activated, the presence of retinoic acid causes B cells to upregulate the surface receptors CCR9, CCR10, and a4b7 [87]. CCR9 and CCR10 bind to the chemokines CCL25, CCL28 released by intestinal enterocytes, allowing them to home to the lamina propria. In addition to promoting gut homing, the environmental milieu of the intestine also has a profound impact on CSR. TGF-B, IL-10, IL-4, APRIL, and IgA-inducing protein secreted by the intestinal cells have been demonstrated to stimulate CSR to IgA [88]. Because of those factors, IgA is primary isotype produced within the gut [89].

A modest percentage of the ASC located in this region secrete antibodies which are polyreactive [90]. However, many of the of the antibodies in the intestine seem are antigen specific, have high levels of mutations in the CDR indicating selective pressure, and have a preference for VH3 family gene usage [91]. These findings imply that the gut has a pool of naïve and polyreactive cells which can be recruited when encountering novel antigens [92]. The presence of a population of antigen experienced, polyreactive MBC and ASC may play key roles in maintaining commensal microbes while retaining the ability to quickly mount immune responses to foreign pathogens.

The role of memory B cells within the gut is also an area of active research. A study by Williams *et al.* has shown that the homing capabilities of MBC has a profound impact on their ability to induce protective intestinal immunity [93]. In the study, rotavirus specific $\alpha4\beta7^{+}$ and $\alpha4\beta7^{-}$ MBC were adoptively transferred into RAG KO mice which were then challenged with rotavirus. The mice that received $\alpha4\beta7^{+}$ MBC produced rotavirus specific antibody within the stool, cleared the virus, and remained protected from infection for up to 7 months post transfer. Mice which received $\alpha4\beta7^{-}$ MBC produced rotavirus specific serum antibody, but were unable to

clear the virus even 2 months post infection [93]. This study highlights the role of MBC in protection and critically how important tissue homing is in ameliorating disease.

While memory cells have are known to circulate searching for antigen, research has also been ongoing to identify the presence and role of tissue resident MBC. A recently study identified subsets of the overall MBC population which seemed to be exclusively found in tissues, but not in circulation [94]. These different subpopulations could be readily identified by their CD69 and CD45RB expression. While MBC in circulation were $CD45RB^{+/-}CD69^{-}$, MBC in the intestine were almost exclusively $CD45RB^{+}CD69^{+}$. The double positive cells were more likely to differentiate into antibody secreting cells upon stimulation and had a gene expression profile which had increased expression of plasma cell related genes. In contrasts the circulating MBC population were less likely to form antibody secreting cells and had a gene expression profile that was more suggestive of germinal center formation. The source of these tissue resident MBC, the role they play in infection, and their relationship with the gut homing MBC seen in circulation needs further examination.

Memory to mucosal pathogens is mediated by long lived ASC, proliferating ASC, or MBC. Recent studies have identified LLPC and matching MBC clones within the intestine of both mice and humans. In a study by Lemke *et al.*, mice were orally given cholera toxin and ASC responses were measured up to 9 months post vaccination [95]. They were able to detect CT specific ASC were found both tissues, but surprisingly, there seemed to be an isotype preference for the tissues. IgG and IgM ASC were restricted to the bone marrow while IgA ASC were found in both compartments [95]. The relationship between gut ASC and MBC are also an area of active research. A recent study examined the clonal relationship between IgM MBC and the ASC within the intestinal tissue [91]. The gut homing IgM MBC were clonally related to

both intestinal IgM and IgA ASC. Additionally, the antibodies they secreted bound to members of the microbiota. This indicates the role that gut MBC may play in modulating the host microbiota.

Cholera

Cholera, caused by the bacteria *Vibrio cholerae*, is a severe diarrheal disease endemic in over 50 countries worldwide [96]. Approximately three million people are infected each year which results in over 100,000 deaths annually [97-99]. Lack of access to clean water can render communities susceptible to outbreaks of the disease. For example, the destruction of infrastructure following the 2010 earthquake in Haiti led to a large outbreak of cholera on the island [100]. While severe, a symptomatic case of cholera can lead to protective immunity lasting up to a decade [101]. Inactivated oral cholera vaccines have been developed and are widely used, however they are not able to replicate the protection seen following infection and the reason for this discrepancy is not known [102]. Limited understanding on the aspects of the immune system which are responsible for the generation, duration, and mechanisms of cholera immunity have impeded vaccine development efforts. Without a better understanding of the factors that drive cholera immunity, the development of effective vaccines remains difficult prospect.

Pathogenesis of V. cholerae

V. cholerae is divided into over 200 different serogroups, each distinguished by the terminal O antigen on the LPS. Of these serogroups only O1 and O139 are known to cause epidemics in humans. The O1 serogroup is further divided into two biotypes, Classical and El tor [103]. These biotypes differ in their ability to produce toxins, and antibiotic resistance. Furthermore, these biotypes can be subdivided into Inaba and Ogawa serotypes. These two

strains differ in the in the presences or absence of a functional methyltransferase. The Ogawa serotype contains a methyl group on the terminal O antigen while the Inaba serotype lacks this methylated group [104].

When *V. cholerae* is ingested, it travels to the small intestine and associates with the intestinal villi using a combination of flagella and the pili TCP. Once the vibrios reach the epithelium, they begin to secrete the cholera toxin [105]. This is an AB_5 toxin, with an enzymatically active A unit and a binding B subunit which binds receptor GM1 [106]. The toxin gets taken in by the cell where the A subunit is cleaved and released into the cytosol. It then binds to and activates adenylate cyclase, leading to a large increase in cAMP within the cell [107]. The additional cAMP levels result in activation of Protein kinase A which phosphorylates the cystic fibrosis transmembrane conductance regulator, a chloride channel. Chloride ions flow into the lumen, and water follows the ions down the concentration gradient causing the severe diarrhea seen during infection [108, 109].

It is believed that *V. cholerae* induces diarrhea as a strategy to spread throughout the environment. Following infection, the intestinal microbiota becomes saturated with the bacteria [110, 111]. Due to transcriptional changes, recently shed bacteria are more infectious, leading to higher rates of infection. Infection with *V. cholerae* leads to a loss in the diversity of the microbiota in the first week following infection. However, the microbiota of the infected host usually returns to normal within a few weeks following infection [112].

The standard treatment for cholera consists of rehydration therapy in which the patient receives water mixed with electrolytes to replace the ions lost from the diarrhea. This is typically given orally, or in more severe cases via IV in conjunction with antibiotics. This treatment is very effective, and it is rare for anyone who undergoes treatment to succumb to death.

Unfortunately, in areas where cholera is endemic or in when outbreaks occur there is very little access to the clean water or the hydration fluids.

Immune response to cholera disease

V. cholerae is a noninvasive pathogen and infection does not induce a strong inflammatory response. Infection results in an upregulation of various innate immune factors as well as the accumulation of neutrophils into lamina propria [113]. While they are not able to clear the bacteria, neutrophils are important for preventing systemic spread of the pathogen. The main protective arm of the immune system is the antibody response to the bacteria. While cholera has many antigen targets, including sialidase and TCP, the antibody response primarily targets the two major immunodominant antigens, LPS and CT [114].

Observational and experimental studies have shown that antibody responses which target LPS have the highest correlation with immunity. These responses are typically measured by examining serum vibriocidal titers, a complement dependent assay [115, 116]. In a recent human challenge study by Chen *et al.* only 2 out of the 62 volunteers who developed at least a fourfold increase in vibriocidal titers following CVD-103 HgR vaccination had moderate to severe cholera following challenge [117]. Another CVD-103 HgR study by Tacket *et al.* demonstrated that the vibriocidal titers induced by the vaccine correlated with protection challenge up to 8 days post vaccination [118]. Household contact studies in cholera endemic areas have also established that vibriocidal titers inversely correlate with the incidence of infection [115, 117, 119].

While commonly used, there are several drawbacks to relying on vibriocidal activity as a readout of immunity. Serum titers significantly decline prior to loss of protection, rendering them unable to accurately predict immunity when titers are no longer elevated [120]. There is no titer

at which protection is guaranteed, making it difficult to determine if immunized individuals will be protected from exposure [121, 122]. Finally, vibriocidal titers measure complement activation, which does not reflect the primary mechanism(s) of protection within the intestinal mucosa. IgA is a poor activator of complement, and there is not thought to be a high concentration of complement in the lumen of a healthy person [81, 123]. These facts illustrate that vibriocidal titers are likely a surrogate marker for the actual mechanism of protection. Identifying the target(s) and mechanisms the immune system uses to protect against *V. cholerae* infection is critical for vaccine development efforts.

Infection results in IgM, IgG, and IgA peripheral immune responses which target LPS [44, 124, 125]. While IgM and IgA are common in primary infections, IgG seems to be present only following severe infection or repeat exposures [118]. IgM and IgG antibodies are responsible for the vibriocidal response measured in peripheral serum [126]. LPS specific plasmablasts for all three isotypes can be seen following infection, although the response is largely mediated by IgM in primary and IgG and IgA in secondary responses. These early ASC are likely responsible for clearance of the initial infection. Many of them express gut homing maker CCR9 indicating their potential to home and mediate protection in the mucosal tissue [121]. However, plasmablasts are likely not directly responsible for long term durable immunity seen following infection. The cell types primarily responsible for the duration of long-term immunity have not yet been identified and are an area of active research. The most likely candidates are LPS specific LLPC and/or MBC. Identification of the cell types responsible for immunity will aid in development of vaccines which are able to induce those cell populations [44, 127].

A population of long-lived plasma cells within the gut may be responsible for the immunity seen post infection or vaccination. Intestinal plasma cells would secrete antibody directly into the lumen. This would explain the discrepancy in studies which show a decline in peripheral vibriocidal titers but no corresponding reduction of immunity. In accordance with this idea research should be done to elucidate the longevity of these intestinal plasma cells as well as the antibodies they produce. However, few studies have focused on this area due to the difficulty of obtaining samples in humans from this location.

In a study reported by Uddin *et al.* LPS specific antibodies and plasma cells were measured from small intestinal biopsies obtained approximately 30, 180, and 365 days after *V. cholerae* infection [127]. Both IgG and IgA antigen specific ASC could be detected in peripheral blood. However, only LPS specific IgA antibodies and ASC were detectable within the duodenal the tissue. While antigen specific antibodies within the intestine were elevated at 30 days post infection, levels were undetectable at by day 180. This finding would indicate that these ASC are transient and do not contribute to long term immunity. However, they were still able to detect the presence of LPS specific IgA cells at via ELISPOT one year post infection. This discrepancy indicates that there were limitations in their detection methods that did not allow them to accurately measure the presence of LPS specific antibodies. Another possibility speculated by the authors is that LPS specific ASC primarily produce antibody after antigen exposure. In comparison to IgG plasma cells, IgM and IgA plasma cells can retain their surface immunoglobulin. This surface immunoglobulin is functional and leads to changes in signaling once engaged [128-130]. Taken together, it is conceivable that these antigen specific cells reside in a quiescent state and rapidly secrete protective antibody after BCR stimulation.

Another theory of long-lived cholera immunity is the presence of cholera specific memory B cells. These cells would proliferate and rapidly differentiate into ASC following antigen recognition and result in protection from infection. *V. cholerae* exposure does generate antigen specific IgM, IgG, and IgA MBC [131]. Additionally, LPS specific IgG MBC but not IgA MBC has been correlated with a lower incidence of infection in household contact studies [122, 132]. It remains unclear as to whether to whether the MBC seen in peripheral circulation participate in mucosal immune responses. A recent study by Weisel *et al.* identified a subset of mucosal tissue resident MBC [94]. These cells have phenotypic and transcriptional profiles that are distinct from those in circulation. Additionally, they are more likely to differentiate into IgM ASC compared to their blood counterparts. It remains uncertain the role that these tissue resident B cells play in immunity. However, their presence within the mucosa grants them the ability to rapidly respond to any existing threats. Studies should be undertaken to examine if these tissue resident MBC are generated following cholera exposure and determine how they might contribute to immunity.

While MBC likely play a role in clearing the bacteria, their significance in preventing infection still needs to be further elucidated. Onset of cholera post exposure can occur anywhere between 10 to 72 hours [133]. Whether MBC can mount a protective immune response rapid enough to prevent symptomatic infection within this timeframe is unclear. The presence of LLPC within the intestinal tissue and their relation to immunity is also uncertain. While both MBC and LLPC are important cholera specific immunity, there role and contribution to cholera induced immunity remains uncertain. Identification of the cell types critical for long term durable immunity are needed to guide vaccine development efforts.

In addition to LPS, a significant portion of the infection induced humoral antibody response targets the cholera toxin. These toxin specific antibodies are able to bind to and neutralize the toxin [134]. Surprisingly, given the toxin is the primary virulence factor, antitoxin responses while do not strongly correlate with immunity [114]. This may be due to the potency of the toxin or the amount produced by the bacteria [133]. Cholera toxin is closely related to another diarrheal inducing agent, heat labile (LT) enterotoxin, which is produced by enterotoxigenic *E. coli (ETEC)*. LT, like cholera toxin, is an AB_5 toxin, and binds to GM1 to enter target cells. The cholera toxin B subunit shares 83% homology with the B subunit of heat liable enterotoxin from ETEC [135, 136]. Given the homology, antibodies specific for LT can be cross reactive with CT [40].

In addition to the antibody response many other factors influence the ability of *V. cholerae* to induced disease. People with blood type O are particularly sensitive to cholera disease. While they become infected at the same rates as other blood groups, the disease severity is enhanced in this population [44]. The reasons for this susceptibility are not understood, and areas endemic with cholera typically have low levels of the O blood group population [137, 138]. The composition of the gut microbiota as well as gastric acid levels have also been associated with increased susceptibility [139]. Following infection there is also an increase in active gut homing T cells. The precise role these cells play in the immune response to *V. cholerae* is unclear. It is likely these cells assist in the activation of B cell ASC and MBC responses following exposure [140, 141].

Mechanisms of protection

Due to a lack of complement within the gut lumen it is likely that vibriocidal activity is a surrogate for the main mechanisms of protection. While they do not recapitulate the disease as

seen in humans, animal models and in vitro experiments still provide insight into potential protective mechanisms [108, 142]. Administration of LPS specific antibodies in the rabbit ileal loop model inhibits bacteria mobility, preventing them from entering the gut mucosa [142, 143]. The precise mechanisms behind this effect are unknown, but there are many possible theories as to the cause.

The most common is agglutination, the process by which antibodies bind bacteria to one another and constraint their movement. Another possibility is inhibition of flagellar movement. While anti-flagellar antibodies are produced, their effect on inhibiting motility seems to be limited. The flagella in *V. cholerae* is sheathed in LPS, preventing binding by flagella specific antibodies. However, it does render the flagella susceptible to LPS specific antibodies. These antibodies have been implicated on immobilizing the flagella, although given the speed at which the flagella is able to rotate, it remains unclear if this is a common mechanism [144]. Another possibility is antibodies inducing a stress response in the bacteria. Recent experiments of LPS specific antibodies, however, have demonstrated that this effect is unlikely as antibodies did not induce upregulation of transcripts associated with bacteria stress responses [145]. Bacterial enchaining is a phenomenon where antibodies prevent daughter cells from separating, forcing the bacteria to form long chains that inhibit their movement. Finally, proton motive force has also been speculated to play a role [146, 147]. Understanding exactly how antibodies inhibit *V. cholerae* mobility, identifying antigens or epitopes key important for these functions, and finding ways to improve this response by antibody modifications critical pieces of knowledge needed for effective vaccine design.

Live attenuated vaccine

Observational studies have demonstrated that symptomatic cholera disease elicited long lived protection against secondary exposure [120]. Dr. Myron Levine *et al.* developed several live attenuated vaccines to mimic the protective efficacy seen following infection [148]. The attenuated strain which was most successful was based off the classic Inaba strain 569B. This strain lacked the accessory virulence factors shiga like toxin and hemolysin and was modified to carry a Hg resistance gene. In addition to these modifications, the primary attenuation was the deletion of the A2 subunit and all but the first 11 residues of the A1 subunit from the cholera toxin [149]. The completed vaccine strain was given the designation CVD 103-HgR.

The first studies of this vaccine were done in naïve populations within Switzerland and Maryland. Participants from these early studies showed an increase in peripheral vibriocidal and antitoxin titers following vaccination. The vaccine was also effective in preventing infection with most vaccinated volunteers having no symptoms upon challenge. Even those that were symptomatic had reduced bouts of diarrhea and lower levels of excretion in the stool compared with the untreated group [148]. One dose of this vaccine seemed sufficient, and a secondary dose given 1 – 2 years after the original vaccination was only able to generate a modest increase in vibriocidal titers in 29% of the original group [150].

Most of the above studies were done on naïve populations in western countries where the vaccine elicited strong immune responses. Its effectiveness in endemic areas is not as definitive. The first study done on this population enrolled young Thai adults [151]. The volunteers were given 5×10^8 CFU and peripheral serum titers were measured. All but one of the subjects had a significant rise in vibriocidal titers compared to untreated control. The experiment was repeated using a cohort from another location in Thailand. Unlike the previous study, only 33% of the

responders seroconverted. Increasing the amount given to 10^9 CFU and administering 2 doses the increased the number of volunteers who seroconverted to 58%. Based on this study it was determined that an endemic population required a higher level of organisms to induce an immune response [152, 153]. The reason for this discrepancy is unclear, although it is possible that preexisting immunity within the gut blunted the response [117]. Following the Thailand trial, the vaccine's response in children was examined. Similar to the solider trial, the standard dose used in cholera naïve populations elicited very little response. Increasing the number of bacteria administered by two logs was able to induce seroconversion in 87-91% of subjects. The reasons for the difference in vaccine response of these two populations is unclear but it is likely that preexisting immunity and gut microbiota composition play a role [151, 154].

The duration of immunity the vaccine provided was also examined. Using volunteers in Maryland, they gave the standard dose and challenged with the 569B strain either 8 days or 4-6 months post vaccination. In both case neither vaccine group came down with diarrhea. Interestingly, even though none of the vaccinated group displayed diarrhea, only half of the group had detectable vibriocidal or antitoxin responses following challenge, and some participants did not show an increase in titers post challenge [155, 156]. These results are likely indicative of long-term sterilizing immunity which peripheral titers cannot be accurately measure.

While serological responses have been widely examined, few studies have specifically investigated the ASC response following administration of the vaccine. In a study using a population of naïve volunteers, only 50% of the volunteers had detectable ASC responses towards Inaba LPS following vaccination. The CT response was much improved, with 70-90% of vaccinees showing responses. These vaccinees were challenged 8 days, 1 month, or six

months post vaccination. The closer to vaccination the challenge the fewer ASC responded. This is true for the toxin and the antibacterial response. It also showed no correlation between the ASC response and protection [157, 158].

Another study looked at the ASC response kinetically over 14 months. This study broke the isotype down into IgA, IgG, and IgM. Vibriocidal responses for the vaccine peak at 10 days post administration. This is true for CVD 103-HgR as well as other derivatives such as CVD 110 and CVD 103-HgR2. They were able to show a rise in IgA and particularly IgM ASC following vaccination. This ASC responses peaked on day 9 and had returned to baseline by day 22 [158]. Following a boost on day 418 there was a small rise in IgG and IgM ASC, but nothing in the IgA population. In addition, the booster dose in this study did not elicit a significant rise in two out of the three vaccinees at a year post vaccination. The reason for the blunted response is unknown. It could be driven by the presence of IgA at the mucosa which prevented large activation of ASC. Alternatively, it could indicate delayed activation of high affinity cholera specific MBC. Since the study used lysed cholera as their screen, the antigen(s) responsible for this effect is unclear [158].

Whole cell killed vaccines

Of the available cholera vaccines, the two most widely used are the inactivated oral cholera vaccines Schancol and Dukoral. The primary difference of the two vaccine strains is the addition of the recombinant toxin B subunit in the Dukoral vaccine [102]. The presence of the B subunit slightly increases the protective efficacy of the vaccine in the first few months following administration [114, 159]. Their efficacy and duration of immunity is limited compared to what is generated following natural infection [160]. The reasons for this discrepancy are not well

understood, and ongoing research efforts are being undertaking to identify which aspects are critical for cholera immunity.

Shancol is a whole cell killed cholera vaccine which is composed of formalin or heat killed *V. cholerae* O1 classical Cairo 48, Cairo 50, El Tor Phil 6973, and the O139 strain 4260B. The vaccine is administered in a two-dose regiment given 14 days apart. This vaccine was utilized during outbreak in Haiti following the earthquake. As children are a population that are susceptible to severe cholera disease, trials have focused on examining the vaccines effectiveness in this age group [141].

For children under five the efficacy of this vaccine was quite low, demonstrating only 17% protective efficacy in the first year of surveillance. Protection rapidly increased to 81% on two years post vaccination, but it dropped back down to 37% by year three. The reason for this increase is not known, although it is possible that the vaccine reduced shedding of *V. cholerae* in the overall population during the second year. Cases of *V. cholerae* infection can be asymptomatic, and thus the infected serve as carriers and can disseminate of the bacteria. The ability of Shancol to reduce asymptomatic shedding shortly following vaccination could explain this aberration. The vaccine was more effective in the older children, showing 66-81% efficacy in children 5 years of age and older which remained relatively stable over the three-year observations [161]. It is important to note that this trial only measured cases where hospitalization was required. The cases of moderate/mild diarrhea were not recorded, and the vaccine's ability to prevent these cases is not known.

Dukoral is a whole cell killed cholera vaccine which contains the four O1 strains found in the Shancol vaccine and recombinant CTB. An early study using a rabbit model of infection demonstrated that immunization with the combination of LPS and CTB provided stronger

immunity then either alone [162]. While the effects were not as robust as those seen in mice, when given to human volunteers the combination induced a modest increase in immunity shortly after vaccination compared to LPS alone [163]. Like Shacol, the Dukoral vaccine is administered in multiple doses [117, 164]. Trials also examined the effectiveness of the vaccine in preventing cholera disease in both children and adults.

During the first year the vaccine proved to be moderately effective in preventing infection [124]. The efficacy of the vaccinated group was 62% effective in reducing severe cholera disease in all age groups during the first year. However, the efficacy measured two years post vaccination decreased to 47% and only showed 17% efficacy by year three. Notably, its effective efficacy in children was remarkably poor. When examining the effectiveness in children under 5, the vaccinated group performed 37% worse compared to the untreated population.

The immune response to these two inactivated vaccines is pales when compared to the response observed following infection. The magnitude of the vibriocidal response is approximately 6-fold lower than what is observed from infected patients. Additionally, these responses return to baseline 30 days post vaccination in some volunteers [141]. This contrasts with what is seen in infected donors where levels remain can remain elevated up to a year post infection [160].

Vaccinated young children consistently had weaker anti-toxin immune responses compared to those who had disease. In contrast, the LPS response differed significantly. While IgG titers were modestly raised in both vaccinees and patients, the vaccine failed to induce significant rise in IgM and IgA anti-LPS titers following vaccination [141]. Given the role that anti LPS responses have in cholera immunity, the inability of vaccination to induce these responses likely contributes to its limited protective efficacy.

The whole cell killed vaccines provide many advantages. They provide modest short-term protection, and they are able to be transported and stored without required specialized refrigeration equipment. This allows them to be widely deployed in areas where lack of infrastructure or cost limits the use of other vaccine approaches. However, they unable to generate strong, durable immunity following vaccination. This shortcoming is particularly evident in young children, the population most susceptible to cholera disease. They require multiple doses, a burden for those who are unable to travel to medical facilities for vaccine administration. Finally, the limited protection they offer rapidly wanes within three years, rendering the population susceptible to reinfection. To improve vaccine design efforts must be made to understand the factors necessary for the generation, duration, and mechanisms that drive cholera immunity.

Summary

The humoral system plays a key role in body's capability to protect itself against infection. The B cells which form this system have many important adaptations that aid in their ability to neutralize potential threats. Through extraordinarily complex processes they can generate antibodies which target a diverse array of antigens. It can refine the antibodies, increasing their affinity for the antigen. Furthermore, they can also expand the functionality of the antibodies by changing their isotype and subclass. B cells are comprised of various populations, each specialized for a particular task. Plasmablasts are antibody secreting cells which can aid in early control of the pathogen. Long lived plasma cells consist of mature cells which continually secrete high affinity antibody providing long term immunity. Finally, memory B cells constantly monitor for the recurrence of past threats, ready to rapidly respond to repeat exposures. Combined, this system provides robust protection against disease.

V. cholerae causes a severe diarrheal illness which can be fatal if left untreated. Protection is mediated by the humoral response, and immunity can last for many years following symptomatic exposure. The specificity of protection indicates that LPS specific responses drive this protection. Vaccines have been made to mimic this effect, but their efficacy is moderate and the protection short lived. It remains unclear why infection generates durable immunity and the current vaccines do not. Understanding the factors that are critical for the induction and maintenance of cholera immunity, are necessary for the development of more effective vaccines.

There are still many questions that remain on how certain aspects of humoral immunity regulate cholera disease. What governs the durability of the immune response? Are there factors of the early immune response are predictive of long-term immunity? What are the correlations between peripheral and mucosal immune responses? What are the mechanisms which antibodies

used to neutralize pathogen? The answers to these questions are critical to help understand the induction and maintenance and gut mucosal humoral immunity. Additionally, the insights provided by studies examining the factors can lead to the improvement of vaccine design for *V. cholerae* and other mucosal pathogens.

This dissertation aims to address some of the questions regarding the development of mucosal humoral immunity and how it relates to cholera disease. We studied a cohort of cholera naïve volunteers who received a live attenuated cholera vaccine to model the effect of cholera exposure in humans. This allowed us to examine aspects of the early immune response which potentially correlate with both long term and mucosal immunity (Chapter 2). Next, we used single cell analysis techniques to examine the plasmablast population generated by the vaccine. This allowed us to examine the antibodies produced by gut homing cells, identify gene rearrangements which favor LPS and CTB binding, and discern evidence of affinity maturation in primary immune responses to polysaccharide antigens (Chapter 3). Finally, we examined the impact of isotype, subclass, and epitope on affinity and the role they have in changing the functional capabilities of LPS specific antibodies (Chapter 4). The findings presented in this dissertation provide key insights into human immune systems responses to *V. cholerae* infection and humoral mucosal immunology.

Chapter 2: Longitudinal analysis of human humoral responses after vaccination with a live attenuated *V. cholerae* vaccine

Oluwaseyi Adekunle[a], Robert C. Kauffman[a], Alice Cho[a], Alexandra Dretler[b], Nadine Rouphael[b] and Jens Wrammert[a]

[a] Division of Infectious Disease, Department of Pediatrics, Emory University, School of Medicine, Atlanta, Georgia, USA

[b] The Hope Clinic, Emory Vaccine Center, Division of Infectious Disease, Emory University, School of Medicine, Atlanta, Georgia, USA

This work is currently in review at PLOS Neglected Tropical Disease, 2021

Abstract

Vibrio cholerae is a bacterial pathogen which causes the severe acute diarrheal disease cholera. Given that a symptomatic incident of cholera can lead to long term protection, a thorough understanding of the immune response to this pathogen is needed to identify parameters critical to the generation and durability of immunity. To approach this, we utilized a live attenuated cholera vaccine to model the response to *V. cholerae* infection in 12 naïve subjects. We found that this live attenuated vaccine induced durable vibriocidal antibody titers that were maintained at least one year after vaccination. Similar to what we previously reported in infected patients from Bangladesh, we found that vaccination induced plasmablast responses were primarily specific to the two immunodominant antigens lipopolysaccharide (LPS) and cholera toxin (CT). Interestingly, the magnitude of the early plasmablast response at day 7 predicted the serological outcome of vaccination at day 30. However, this correlation was no longer present at later timepoints. The acute responses displayed preferential immunoglobulin isotype usage, with LPS specific cells being largely IgM or IgA producing, while cholera toxin responses were predominantly IgG. Finally, CCR9 was highly expressed on vaccine induced plasmablasts, especially on IgM and IgA producing cells, suggesting a role in migration to the gastrointestinal tract. Collectively, these findings demonstrate that the use of a live attenuated cholera vaccine is an effective tool to examine the primary and long-term immune response following *V. cholerae* exposure. Additionally, it provides insight into the phenotype and specificity of the cells which likely return to and mediate immunity at the intestinal mucosa. A thorough understanding of these properties both in peripheral blood and in the intestinal mucosae will inform future vaccine development against both cholera and other mucosal pathogens.

Introduction

Vibrio cholerae is the bacterial pathogen responsible for causing cholera, a severe diarrheal illness. There are over three million cases of infection annually resulting in over 95,000 deaths [97]. Cholera is endemic in over 50 countries and, as outbreaks in Yemen highlight, is a persistent global plight, especially where sanitation and clean water supplies fail [98]. The outbreak in Yemen alone was responsible for the doubling of the annual cholera cases reported to the WHO from 2018 to 2019 [165]. Intriguingly, individuals who experience a symptomatic episode of cholera can be protected against subsequent exposure for up to 10 years following the disease [101, 115, 166]. In contrast, inactivated vaccines have shown more limited durability of immunity [102]. In this context, the mechanism(s) contributing to durable immunity are not well understood. Consequently, the focus of current research efforts is aimed at understanding the immune factors responsible for protection, and to aid in the development of vaccines that can provide durable immunity [99, 102, 138, 147].

Humoral responses against *V. cholerae* are thought to be responsible for protective immunity. In endemic areas, the antibodies generated in response to exposure primarily target the two immunodominant antigens of the bacteria, lipopolysaccharide (LPS) and cholera toxin (CT) [104, 113]. The LPS specific antibodies play an important role in vibriocidal activity, which measures the ability of antibodies to bind and induce complement mediated lysis of the bacteria [116]. Serum vibriocidal responses are currently the best-known correlate of immunity to *V. cholerae* infection in humans [114]. However, serum vibriocidal responses do not fully explain cholera protective immunity. Vibriocidal titers wane well before immunity is lost and there is no absolute threshold which ensures sterilizing immunity [167]. The reason for this discrepancy is unclear. One possibility is that the concentration of antibodies in the serum may

not be reflective of the concentration in mucosa where protection is mediated. Moreover, the role of complement mediated lysis as the primary mechanism of immunity within the gut has not been clearly established [123, 168, 169]. While the precise mechanism remain unclear, antibodies targeting the o specific polysaccharide of the LPS molecule are associated with protection [147].

V. cholerae is a non-invasive pathogen and is thus less susceptible to the neutralizing effects of peripherally circulating antibodies. Therefore, protection is likely mediated by antibodies which are secreted into the intestinal lumen by tissue resident plasma cells [90]. Due to the difficulty in examining these tissues in humans, the properties of cholera specific plasma cells at this location are not well understood [127]. Plasmablasts are antibody secreting cells (ASC) that are present transiently in circulation shortly after infection or vaccination [39, 40, 45]. Following circulation these cells may die or migrate to sites such as the bone marrow and mucosal tissues where they transition into long lived plasma cells. Therefore, plasmablasts are a readily accessible population of antigen specific cells that can provide insight into the immunological processes that occur in the mucosa and the properties of cells that may ultimately reside in these tissues.

CVD 103-HgR, currently sold under the trade name Vaxchora, is a live attenuated *V. cholerae* strain that is approved in the United States as a traveler's vaccine [138, 170]. It is modified from the classical Inaba 569B strain [148, 149]. While the primary attenuation is the deletion of 94% of the A_1 toxin subunit, other modifications include the absence of the El tor hemolysin, a shiga like toxin, and the insertion of a mercury resistance marker. The vaccine has proven to be very effective in short term studies, with 80% of human volunteers protected from disease following challenge three months post vaccination [117], and the remaining 20%

showing significantly reduced shedding. The availability of this vaccine provides the opportunity to safely examine the humoral response to an intestinal pathogen in a naïve cohort [148, 154, 171]. Understanding the induction of plasmablasts, memory B cells, antibody isotype, gut homing potential, and antigen binding in a naïve host and determining of how these factors change longitudinally is important not only for our understanding of *V. cholerae* immunity, but can also serve as a model to better understand mucosal immunity. Additionally, the longitudinal aspect of this study provides the opportunity to identify which characteristics of the early immune response are predictive of durable immunity. This information will be helpful in focusing future vaccine improvements. Finally, comparing these responses to natural infection will provide important information regarding key differences between primary immune responses and recall responses in highly endemic areas. In accordance with these goals, we conducted a longitudinal study to examine how components of both the cellular and serological humoral response change in vaccinated individuals and evaluated markers that may reflect the generation and maintenance of mucosal immunity.

Results

Rapid and durable serological responses following primary vaccination.

For the current study 12 healthy volunteers were recruited from the Atlanta, Georgia metropolitan area who had no prior history of *V. cholerae* infection, *V. cholerae* vaccination, or travel to a cholera endemic area within the past five years **(S1 Table)**. Peripheral blood mononuclear cells (PBMC) and plasma were collected on days 0, 7, 10, 15, 30, 90, and 365 following vaccination from whole blood to examine both acute and memory timepoints. The serological analyses were focused on functional assays and binding assays against the immunodominant antigens lipopolysaccharide (LPS) and cholera toxin B subunit (CTB).

The functional responses focused on the vibriocidal and agglutination titers generated following vaccination. Due to previous reports showing that elevated levels of vibriocidal titers are strongly correlated with lower incidence of infection [117], we examined these responses in our cohort. All vaccinees seroconverted (defined by a four-fold increase from baseline in vibriocidal activity) by 10 days post vaccination **(Fig 1A)**. The vibriocidal titers of the majority of our cohort peaked 10 days post vaccination (GMT 4550, range 902-49400), while a smaller subset of donors peaked on day 15 post vaccination (GMT 3610, range 360-47700). Vibriocidal antibodies were also observed as early as day 7 in 83% of the vaccinees, although at an average of threefold less than the peak of the response. Vibriocidal titers then declined an average of 46-fold from peak levels by day 90 post vaccination. Afterwards, the titers remained stable showing no significant difference between the day 90 and 365 time points (day 90 GMT 125 vs day 365 GMT 110; p=0.378).

Agglutination by antibodies specific for proteins and sugars on the bacterial cell surface is another proposed mechanism of immunity. Vibriocidal assays largely measure IgM and IgG responses due to the ability of these isotypes to activate the classical complement pathway. However, agglutination assays can incorporate IgA responses in the measure of bacterial specific antibodies. This could be particularly relevant if a response generated a strong agglutination titer but a comparably weak vibriocidal titers. In our analysis, the agglutination titers largely mimicked the response kinetics of the vibriocidal titers in which the titers rapidly peaked early in the response. In our cohort, 10 vaccinees reached the peak of the response 10 days after vaccination. Interestingly, while the vibriocidal titers remained relatively stable between days 90 and 365 post vaccination, the agglutination responses continued to decline. Only four of the donors examined had detectable agglutination titers at 1-year post vaccination **(Fig 1B)**.

Vibriocidal and agglutination titers correlated positively at every timepoint up to day 30 post vaccination, however, there was not a strong correlation between these two responses after this timepoint.

Next, we examined the serum binding responses to the two immunodominant antigens of *V. cholerae*, LPS and CTB. A significant increase in LPS specific serum antibody responses, as evidenced by a threefold increase in antibody titers after vaccination, was elicited in 11 out of 12 donors. The LPS specific responses were largely dominated by IgM and IgA antibodies **(Fig 1C)**. These titers followed similar kinetics to the early vibriocidal responses. The IgM and IgA anti LPS titers peaked on days 10 (mean 85 mOD/min, range 9-272) and 15 post vaccination (mean 76 mOD/min, range 17-234) respectively. Eight of the vaccinees (66%) had a three-fold increase over baseline IgM anti LPS titers following vaccination. However, in the majority of these donors, the LPS specific IgM antibody titers returned to levels less than threefold above baseline levels by day 90. In two of the vaccinees, LPS specific antibodies 3-fold above baseline were still present in plasma at day 90; however, by one year, these titers were equivalent to baseline levels. In contrast to the IgM titers, only 4 out of the 12 volunteers had an elevated LPS specific IgA titer following vaccination. The LPS specific IgA titers were more transient than the IgM response, returning to baseline levels in all donors by day 30 post vaccination. In contrast to the vaccine's ability to induce an IgM and IgA response, its ability to generate LPS specific IgG antibodies was poor in contrast to what is observed following infection [44]. Relative to baseline levels, only one donor had a threefold increase in LPS specific IgG titers following vaccination.

The vaccine strain CVD-103 HgR only produces the cholera toxin B subunit (CTB) as a result of an attenuating deletion of the CTA1 subunit [148, 149]. Therefore, we focused our toxin specific serological analyses on responses to CTB **(Fig 1D)**; however, as shown in the **(S1 Fig)**,

similar analysis using the cholera holotoxin found no statistical difference in the kinetics or magnitude to either protein. Following vaccination, 75% of our cohort had an increase in plasma antibody titers towards CTB defined as a threefold increase over baseline levels. IgG titers increased above baseline levels in 7 of the volunteers. These responses peaked 15 days post vaccination (mean 155 mOD/min, range 10-400) and remained elevated above baseline in 5 donors 90 days following vaccination (mean 28 mOD/min vs 89 mOD/min; p=0.0025). IgG titers in all but one donor returned to baseline by one-year post vaccination. An analysis of CTB specific IgA serum titers demonstrated that half of the donors had a significant increase following vaccination. These titers peaked on day 10 (mean 168 mOD/min, range 5-174) and returned to baseline 30 days post vaccination in all but one donor, who maintained these elevated for at least a year post vaccination **(Fig 1D)**. Unlike LPS which generated a robust IgM response, there was no significant increase in CTB specific IgM titers at any timepoint following vaccination.

Vaccination induces a potent LPS and CTB specific plasmablast response.

Following vaccination, there was a significant increase in circulating total plasmablasts ($CD3^{-}CD19^{+}CD27^{hi}CD38^{hi}$ lymphocytes) on day 7 compared to day 0 post vaccination (mean 1.9% vs 6.3%; p=0.04) **(Fig 2A)**. Seven of the volunteers (58%) showed an increase in the total plasmablast compartment. Of the vaccinees who mounted an increase, five peaked 7 days post vaccination while two peaked 10 days post vaccination **(Fig 2B)**. As expected, given the transient nature of plasmablasts in circulation, their frequency returned to baseline levels in all donors by 30 days post vaccination. This increase in the vaccine induced plasmablast population is consistent to our prior studies examining the plasmablast responses in patients infected with *V. cholerae* [40].

To define the kinetics and magnitude of antigen specific plasmablast responses following vaccination we also used the enzyme linked immunospot assay (ELISPOT) **(Fig 2C)**. Nine of the vaccinees had detectable LPS specific IgM ASC following vaccination. Of these nine donors, seven had a peak response at day 7 while two peaked at day 10 **(S2 Fig)**. The peak response had an average of 80 LPS specific IgM ASC/million PBMC (range 0 to 294 ASC/million PBMC). Similar to the LPS specific IgM secreting ASC kinetics, a majority of our study cohort (8 of 12) also had detectable LPS specific IgA ASC. Of these eight donors, five had a peak response at day 7 while three peaked at day 10. In comparison to the LPS specific peak IgM response, the peak IgA response was similar (mean 166 LPS specific IgA ASC/million PBMC; range 0 to 1550). Interestingly, only two donors had detectable LPS specific IgG ASC responses. These two donors also had the highest levels of LPS specific IgM ASC in our cohort. Finally, we determined that the antibodies released by the ASC were also cross reactive with LPS from the Ogawa serotype **(S4 Fig)**.

We next examined the CTB specific ASC responses following vaccination. Similar to the LPS responses, a majority of our cohort mounted CTB specific ASC. However, in contrast to the LPS specific responses, only two donors had detectable CTB specific IgM ASC following vaccination (27 CTB specific IgM/million PBMC). The IgG response was much more robust with 8 donors having detectable CTB specific IgG ASC. The CTB specific IgG ASC also peaked 7 days post vaccination (mean 67 IgG/million PBMC; range 0 to 324) in 6 participants and with an additional 2 vaccines who reached their peak on day 10. Eight of the donors also had a CTB specific IgA ASC response which also peaked on day 7 post vaccination (mean 67 CTB specific IgG ASC/million PBMC; range 0 to 417).

Intriguingly, while in sum all donors responded to the vaccine, we observed that only half of the vaccinees had an ASC response to both the CTB and LPS antigens, while the other half mounted a detectable response directed against only CTB (25%) or only LPS (25%), respectively **(Fig 2E)**. The isotype specificity of the LPS and CTB specific ASCs followed a similar trend to what was seen in the serological analyses. Specifically, the LPS responses were primarily derived from IgM and IgA ASC while the CTB responses were largely derived from IgG and IgA ASC **(Fig 2E)**.

Vaccine induced plasmablasts express the gut homing receptor CCR9 in an isotype dependent manner

As plasmablasts circulate following vaccine exposure, we were interested in the potential of the cells to travel to the mucosa where they may release antibodies into the intestinal tract and/or become long lived plasma cells. CCR9 is a chemokine receptor that binds to C-C motif chemokine ligand 25 (CCL25) secreted by intestinal epithelial cells and helps cells traffic to the small intestine [90, 121]. Therefore, using a flow cytometry driven approach we examined the change in CCR9 expression on plasmablasts following vaccination **(Fig 3A)**. This analysis demonstrated a substantial increase in the percentage of CCR9 expressing plasmablasts on day 7 in which an average of 42% percent of the cells expressed the marker, relative to the pre-vaccination expression of 9% **(Fig 3B)**. In some donors, the percentage of CCR9 expressing plasmablasts exceeded 80% (range 8%-82%). As IgA is the principal antibody in mucosal secretions, we also examined CCR9 expression by isotype. On day 7, 59% total IgM+ plasmablasts (range 29% to 89%) had increased expression of CCR9. In contrast, only around 30% of the IgA+ plasmablasts (range 7.4% to 71%) and 22% of the IgG+ plasmablasts (range 4.7% to 48%) plasmablasts expressed CCR9 **(Fig 3D)**.

Memory B cell responses to vaccination are dominated by IgA isotype

Previous household contact studies have shown a correlation between antigen specific memory and a reduced incidence of infection [132, 141]. Therefore, we used an ELISPOT based assay to examine the IgG and IgA MBC responses to LPS and CTB at days 30 and 90 post vaccination. For the LPS specific IgG MBC, only two donors had detectable antigen specific responses following vaccination. Intriguingly, we observed that one of the donors had LPS specific IgG MBC prior to vaccination, however, these cells were not detected on day 30 post vaccination **(S3 Fig)**. Similar to the LPS specific MBC response, only 4 of the volunteers had CTB specific IgG MBC following vaccination. Two of the donors first had detectable responses on day 30, while 4 were detectable on day 90. The relatively low cholera specific IgG MBC, particularly when compared to the robust IgA response, could be indicative of poor MBC generation. Alternatively, it may also indicate that the IgG MBC responses do not circulate systemically but preferentially home and reside in the intestinal or other lymphoid organs. Tissue resident memory B cells are known to occur in humans, however the factors that determine the generation and frequency of these cells following *V. cholerae* exposure have yet to be determined [94].

In contrast to the IgG responses, there were a larger number of donors who had detectable IgA MBC for both antigens. By measuring the LPS specific IgA MBC at days 30 and 90, we observed that the vaccine induced an antigen specific MBC response in eleven of the donors. Six of the responders had detectable MBC on both day 30 and 90. The other five donors had responses on day 30 (2), or day 90 (3), respectively. Additionally, two of the donors had LPS specific MBC prior to vaccination and maintained detectable antigen specific MBCs throughout all timepoints tested.

CTB specific IgA MBC were also increased with ten donors displaying specific MBC on both day 30 and day 90 post vaccination. While we detected CTB specific IgA MBC in six donors on both days, the remaining four vaccinees had specific cells only on either day 30 (2) or day 90 (2). The two donors that had detectable CTB specific MBC on day 0 maintained these responses through day 90. Finally, for those individuals that developed an antigen specific MBC response post vaccination, we observed that the magnitude of the LPS and CTB IgA MBC response was similar. Specifically, the LPS specific IgA accounted for approximately 0.2% (range 0 to 0.65) of the total MBC population while the CTB specific IgA MBC accounted for 0.16% (range 0 to 0.72) of the MBC population.

LPS specific IgM ASC and gut homing IgM plasmablasts correlate with early vibriocidal activity

The main factor which drives humoral immunity to *V. cholerae* in humans has not yet been determined. Although it is not absolute, serum vibriocidal activity strongly correlates with protection [114]. Furthermore, little is known about the dynamics and durability of immune responses to a live attenuated cholera vaccine in an immunologically naïve setting, and how early responses may predict the outcome of immune parameters long term. As such, we attempted to correlate different early humoral responses measured at day 7 with the day 30, 90 and 365 vibriocidal titers to assess which parameters were predicative of persistent vibriocidal responses and thus potential long-term immunity. The antigen specific plasmablast responses at day 7 were predictive of the serological responses up to day 30 (**Figs 4A and B**), similar to what we have previously shown for influenza specific responses [43]. Of these responses, the amount of IgG CTB specific ASC on day 7 positively correlated with IgG anti CTB titers up to one year post vaccination. Additionally, we also observed that the percentage of IgM CCR9 expressing

plasmablasts on day 7 as well as the amount of LPS specific IgM ASC showed the best correlation with early vibriocidal activity. Both the CCR9+ IgM plasmablast (r^2=0.46 P=0.05) and the LPS specific IgM ASC on day 7 (r^2=0.54 P=0.006) responses strongly predicted the vibriocidal activity at day 30 post vaccination **(Figs 4C and D)**. However, these correlations were no longer significant at the later day 90 and day 365 time points. In addition to these measures, we assessed additional parameters including but not limited to LPS specific and CTB specific serum titers, CTB specific IgM, IgG, and IgA ASC, MBC, total plasmablast magnitude, and agglutination. None of the aforementioned responses significantly predicted the long-term vibriocidal activity at day 90 or 365.

Discussion

A thorough examination of the humoral immune response to *V. cholerae* infection is crucial to better understand protection against cholera. The live attenuated vaccine strain used in this study, Vaxchora or CVD-103 HgR, has been primarily used to protect individuals traveling to cholera endemic countries [138, 148, 170, 172]. Thus many previous studies have primarily focused on clinical outcomes such as immunogenicity [154, 173], safety [171], and protective efficacy [118]. In contrast, the current study focused on a detailed examination of the early immune response and how these early events correlate with long term-immunity. In addition, the study aimed to define the durability of immunity induced by this vaccine. With an obligate mucosal pathogen, homing to the intestinal mucosa is essential, and thus we also characterized the vaccine induced expression of the gut homing marker CCR9. Finally, as most cholera vaccine studies have been performed in highly endemic areas, much less is known about the primary immune responses against live bacteria. Taken together, this comprehensive analysis of

the primary immune response after exposure to live bacteria in terms of the induction and durability of immunity after vaccination provides important insights into the induction of immunity against *V. cholerae* and should be valuable for ongoing and future vaccine development efforts.

Vibriocidal titers are a critical immune correlate of protection for cholera. Household contact studies in cholera endemic areas have reported that elevated vibriocidal titers inversely correlate with the incidence of infection [115, 117, 119]. Additionally, human challenge studies illustrate a positive correlation between vibriocidal titers and protection against severe disease [118]. The peripheral vibriocidal titers reported in the present study are consistent with historical data of the humoral response to *V. cholerae* exposure. Studies of *V. cholerae* infection [122], and vaccination with CVD-103 HgR [155] or whole cell killed cholera vaccines [160] have all described the rapid increase and early peak of vibriocidal titers around day 10 post exposure. Similar to those results, all participants in our study seroconverted by day 10 post vaccination. Given previously published findings [117], the magnitude of seroconversion observed in this study indicates that all participants would likely be protected against *V. cholerae* challenge for at least three months post vaccination. The vibriocidal titers declined from their peak at day 10 until they stabilized around 90 days post vaccination. Given the duration of these elevated titers, it is likely that many of our subjects would have some level of protection against challenge at later timepoints. Infection with *V. cholerae* is known to generate robust, durable immunity. When infected individuals were rechallenged 3 years following exposure, none of the subjects developed diarrhea, and only 50% had detectable increase in vibriocidal titers. The vaccinated response follows a similar trend, to a perhaps less robust degree. In another study which examined CVD-103 HgR, when vaccinees were challenged 6 months post exposure, none

developed diarrhea, and approximately 50% - 73% of the participants had an increase in vibriocidal titers [118]. The vibriocidal titers measured prior to challenge were (GMT: 202 ~ 276) which is similar to what we observed in our cohort at one year post vaccination (GMT: 200) [118]. Given the similarity in titers, it is possible that our cohort would also remain protected against challenge. More research should be undertaken to determine the long-term efficacy of this vaccine in both naïve and endemic populations.

Vibriocidal titers measure the ability of antibodies to bind to and induce complement mediated lysis of the bacteria. In the case of *V. cholerae*, this effect is primarily thought to be driven by LPS specific antibodies [40, 126]. In concordance with prior infection [174] and CVD-103 HgR vaccine studies [171], we also saw a rapid increase in these titers following vaccination. In our vaccinees, the LPS specific serum titers and ASC responses primarily consisted of IgM and IgA antibodies. While LPS specific IgG antibodies have been detected in *V. cholerae* infected patients in endemic areas, the induction of these isotype switched antibodies appear to require either repeated exposure to the pathogen or a more severe infection to generate them [44, 124, 125]. Additionally, while IgG responses to LPS can occur, their contribution to the overall vibriocidal activity, particularly in primary exposure is uncertain. A study which depleted either IgM, IgG, or IgA from serum collected from subjects immunized with *V. cholerae* showed that vibriocidal activity was lost following depletion of IgM [126]. Similar to our study, that study also showed a strong correlation between vibriocidal titers and LPS specific IgM responses. Due to the low amount of LPS specific IgG and the reduced ability of IgA antibodies to activate complement, the vibriocidal response in our cohort is likely predominantly mediated by LPS specific IgM antibodies.

In addition to LPS, a significant portion of the infection induced humoral antibody response targets the cholera toxin where it plays an important role in toxin neutralization [133, 134, 175]. In this study, most of the participants experienced a significant increase in antitoxin titers one-month post vaccination. However, in contrast to the LPS response, which was predominantly comprised of IgM and IgA antibodies, the cholera toxin response was largely derived from IgG and to a lesser extent IgA antibodies. As our cohort is primarily cholera naïve, it is surprising to see such a strong IgG response to the toxin antigen, given that isotype switched responses are generally associated with a secondary immune response. Cholera toxin is closely related to another diarrheal inducing agent, heat labile (LT) enterotoxin, which is produced by enterotoxigenic *E. coli (ETEC)*. LT, like cholera toxin, is an AB_5 toxin, and binds to GM1 to enter target cells. The cholera toxin B subunit shares 83% homology with the B subunit of heat liable enterotoxin from ETEC [135, 136]. Therefore, given the homology, it should be considered that the IgG class switched response observed in this study represents an anamnestic response driven by cells originally induced by prior exposure to LT. Indeed, a prior study from our lab has demonstrated that many of the cholera toxin binding antibodies generated from infected patients are selective for LT [40]. Additionally, ETEC infections do occur in the US, both from cases of traveler's diarrhea as well as domestic outbreaks. There were over 300 outbreaks of ETEC in the US alone between 2003-2012, with an estimated 35,000 cases annually, although this number is likely underreported [176, 177].

V. cholerae is a noninvasive pathogen and is thus not directly subjected to peripheral humoral responses. As the bacteria colonizes the small intestine it would primarily be subjected to antibodies that are secreted into the lumen. Therefore, examining the ASC which are responsible for producing the secreted antibodies is of particular interest. Plasmablasts are ASC

that transiently circulate shortly after infection or vaccination [178]. As these cells represent an induced response, they are generally enriched for vaccine or pathogen specific ASCs. It has previously been demonstrated that plasmablasts are induced both by *V. cholerae* infection and vaccination [40, 121]. Similar to those efforts, this study found that the plasmablast population peaked shortly after vaccination between days 7 and 10. In addition to the serological analysis, we found that many of the ASC in circulation were specific to the two major immunodominant antigens of cholera, LPS and cholera toxin. As *V. cholerae* is a mucosal pathogen, it is likely that a portion of the plasmablasts originate from mucosa associated lymphoid tissue (MALT) such as Peyers patches.

CCR9 is well described as a gut homing marker that promotes migration of cells to the small intestine by binding to CCL25 released from small intestinal epithelial cells [90, 179]. Phenotypic characterization of the plasmablast population in our donors showed a significant increase in CCR9 expression following vaccination. Thus, it is likely that these ASC originated in the gut and have the potential to return there following systemic circulation. This increase in CCR9 expression was predominantly found on the IgM plasmablasts which were almost exclusively LPS specific by ELISPOT analysis. In addition to IgM, approximately 30% of the IgA plasmablasts also expressed CCR9. These two isotypes incorporate the J chain protein, which allows them to bind to the poly Ig receptor for transcytosis into the lumen by epithelial cells. Once in the lumen, the antibodies can mediate their effector functions through a variety of mechanisms.

In contrast to IgM, there was far less of an increase in CCR9 expression on the IgG secreting plasmablasts. As the IgG ASC response was almost exclusively CTB specific, it is possible that CTB does not result in the robust generation of CCR9 expressing IgG plasmablasts.

The reason for this discrepancy is unclear, although the location of antigen uptake could play a role given that CTB is secreted and could potentially end up in different anatomical sites as compared to the whole cell bacteria. This is particularly important given the role that location has in influencing the expression of homing receptors. For example, CCR9 expression on immune cells is induced by the retinoic acid produced by the dendritic cells of gut associated lymphoid tissues (GALT) [87]. Studies using mouse models have demonstrated that CCR9 expression on gut immune cells is heavily influenced by the draining lymph node the cell is activated in [180, 181]. While the site of induction of immunity against cholera toxin in humans is not clear, a similar mechanism could explain the lack of CCR9+ IgG cells in our study.

The ability to predict the long-term effectiveness of cholera immunity using early makers of immunity is of particular interest. As vibriocidal activity is the main correlate of protection, we compared early makers of immunity such as plasma titers, ASC levels, and the magnitude and phenotype of responding plasmablasts to vibriocidal titers. Of the parameters examined, only the early LPS specific IgM titers, LPS specific IgM ASC, and CCR9 expressing IgM plasmablasts were all predictive of the with vibriocidal activity later in the immune response (day 30). However, the predictive value of these measure was no longer present systemically at day 90 or 365 post vaccination. Thus, the generation of long-lived antibody mediated immunity against cholera is regulated differently than the early responses, or the effector cells induced early in the response home to mucosal sites and are no longer detectable in circulation. Thus, it is conceivable that the early IgM ASC and CCR9+ plasmablast responses correlate better with long term immunity in the mucosa [179, 182, 183]. This is of particular interest given the high level of CCR9+ expression found on the IgM population, which was largely LPS specific. These issues

are currently being investigated using small intestinal biopsies but are beyond the scope of the current study.

This also raises the question of what is responsible for driving the long-lived peripheral responses we detected in our study. Long-term protection immunity to *V. cholerae* is driven by LPS and CT specific antibodies. These long term antibody responses are thought to be maintained by long lived mucosal plasma cells [127], memory B cells [132], or a combination of the two. The CCR9+ plasmablasts seen in our cohort indicate the potential for long term mucosal plasma cell responses. There is also the possibility that the titers seen at 1 year are generated by bone marrow derived plasma cells. Future studies will direct efforts to understand the contribution of bone marrow and mucosal plasma cell compartments to peripheral titers. The degree to which peripheral immunity reflects mucosal immunity is the subject of many ongoing studies. Understanding the link between the two locations will be critical for a better understanding of cholera immunity and guide ongoing vaccine development efforts.

The current study illustrates the value of the live attenuated *V. cholerae* vaccine as a model system to understand immunity against this pathogen in a setting of a primary exposure. Longer term studies using this system that incorporate repeated vaccination or challenge with virulent *V. cholerae* will provide the opportunity to better assess markers that are predictive of long-term immunity and identify the immunological mechanisms that result in the generation and maintenance of long-term protection. To address these questions, we are currently examining how the systemic response studied here correlates with mucosal responses measured in small intestinal biopsies. These efforts, in conjunction with comparative studies to recall responses in cholera endemic areas will provide additional insight into immunity against this pathogen. In conclusion, this study highlights key factors which may play an important role in the generation

of immunity, such as the correlation between CCR9 and vibriocidal activity. Mediators of durable protective immunity may be identified through an iterative process of comparing immune response in both naïve and immune patients, which can lead to a better understanding of the mucosal immune response to both this disease and other mucosal infections as well as empower ongoing vaccine development strategies.

Materials and Methods

Study design: This study was approved by the Emory institutional review board. Vaccination and blood collections were performed at the Emry Hope Clinic. Written informed consent was obtained from 12 heathy adults aged 18-49 years old from the metro Atlanta, Georgia area. Subjects were given a description of the study prior to enrollment. Participants were screened for good health as determined by medical history and targeted physical examination. Exclusion criteria included any acute or chronic medical condition, medication, or disorder what would make vaccination unsafe, prior history of cholera vaccination or cholera disease. Each subject made a total of 7 visit to Emroy's Hope Clinic over the course of a year. During each visit participants underwent physical examination and vital signs were measured. Following this screening approximately 64 mL of blood was collected. During the first visit subjects were given a single dose of the oral live cholera vaccine (Vaxchora) according to the manufacturer's instructions and remained in the clinic for observation for an additional 20 minutes. In addition, subjects fasted at least one hour prior to and after vaccination. No severe adverse events were reported within study participants. Further details on this clinical trial have been registered under NCT03251495.

Blood collection and processing: Blood was collected by venipuncture immediately following vaccination, and on days 7, 10, 15, 30, 90 and 365. Approximately 64 mLs of blood were drawn into CPT tubes at each timepoint. Additionally, approximately 3 mLs of blood were drawn into serum tubes. Blood was centrifuged at 1600 rcf for 30 min. The serum fraction was removed and aliquoted for further studies. The cell layer was harvested and lysed with 5 mLs of ACK lysis buffer (Quality biological #118-156-101) for 5 minutes. After which cells were washed with PBS

+ 2% FBS three times after spinning at 1200 rpm for 8 minutes. Cells were then resuspended in the appropriate buffer for counting and further experiments.

Flow cytometry and single-cell sorting: Immunophenotyping of the B cell subsets was performed on PBMC after staining with the following antibodies: CD27-APC (O323), CD3-AF700 (HIT3a), CD71-FITC (CY1G4), IgD-PerCPCy5.5 (IA6-2), CCR9-PE (BBC3M4), CD19-PECF594 (HIB19), CD38-PECy7 (HIT2), CD20-V450 (L27), IgA-APC (ISs11-8E10), CD14-AF700 (61D3), CD16-AF700 (CB16), IgG-PECy7 (G18-145), IgM-BV650 (MHM-88), and CD27-BV711 (O323). For each panel, a total of 2 million PBMC were stained. A minimum of 100,000 events were acquired on a BD LSR II Flow Cytometer and data was analyzed using FlowJo software.

ELISPOT assay: ELISPOT was performed to enumerate cholera toxin and LPS specific plasmablast present in the PBMC samples. 96-well ELISPOT assay filter plates (Millipore) were coated overnight at 4^{o}C with CTB (List Labs #104), LPS (generously provided by Dr. Edward Ryan's Laboratory), or polyvalent goat anti-human Ig (10 µµg/mL, Jackson ImmunoResearch) in PBS. Plates were washed with PBS Tween 0.05% and blocked with R10 (RPMI 1640 + 10% FBS +1% P/S +1% L-glutamine) at 37^{o}C for 2 hours. Freshly isolated PBMC were added to the plates in a dilution series starting at 5 x 10^5 cells and incubated overnight at 37^{o}C. The following day plates were washed with PBS, followed by PBS Tween 0.05% and incubated with biotinylated anti-human IgG, IgA, or IgM antibody (Invitrogen) at room temperature for 90 minutes. After washing plates were incubated with avidin D-horseradish peroxidase conjugate (Vector laboratories) and developed using 3-amino-9-ethyl-carbazole substrate (Sigma-Aldrich).

Plates were scanned and analyzed suing an automated ELISPOT counter (CTL, Cellular Technologies).

Memory B cell assay: Antigen-specific memory B cells (MBC) were detected essentially as previously described [184]. Briefly, PBMC were cultured at $1x10^6$ cells per ml of R10 supplemented with 50 uM B-mercaptoethanol (Sigma-Aldrich) and polyclonally stimulated with pokeweed mitogen extract (1 µg/mL, Sigma-Aldrich), phosphothiolated CpG ODN-2006 (6 µg/mL, Invivogen), and Staphylococcus aureus Cowan (1:10,000, Sigma-Aldrich) for 6 days. After *in vitro* stimulation, total and *V. cholerae* specific IgM, IgG, and IgA cells were quantified by ELISPOT assay, as described above.

ELISA Assay: MaxiSorp plates were coated with CTB (List labs #104) at 1µg/mL diluted in 50 mM carbonate buffer overnight at 4^{o}C. The following day plates were washed with PBS Tween 0.5% then blocked with PBS 1% BSA for 90 minutes. Plates were washed then incubated with serum diluted in PBS Tween 0.5% 1% BSA for 90 minutes. Plates were washed then incubated with peroxidase conjugated goat anti human IgM (109-036-011), IgG (109-036-098), or IgA (109-036-129) diluted in PBS Tween 0.5% 1% BSA for 90 minutes. Plates were washed with PBS Tween 0.5% 1% BSA followed by PBS. Wells were developed with OPD substrate solution: 0.4 mg/ml of O-phenylenediamine (Sigma #P8787) dissolved into 50 mM citrate buffer (Sigma #P4560) with 30% H_2O_2. Plates were incubated with OPD substrate solution for 5 minutes. 100 ul of 1M HCl was added to stop the reaction and O.D. was recorded at 490 nm using the Bio-Rad IMark microplate reader. Seroconversion was defined by responses 4-fold higher than day samples.

Vibriocidal Assay: Vibriocidal titers were detected essentially as previously described[40]. *V. cholerae* O1 (strain 19479 El Tor Inaba) was cultured to mid log phase for 2 ½ hours in bovine heart infusion media at 37^{o}C. Bacteria were pelleted at 3,000xg for 10 min and washed twice with PBS. Prior to use bacteria were normalized to an O.D. of 0.3. Guinea pig complement (Sigma S1639), bacteria, and heat inactivated serum (56^{o}C for 30 minutes) were mixed and added to each well for a total volume of 50 ul per well in a flat bottom 96 well plate. Plates were incubated on shaker (50 RPM) at 37^{o}C for one hour. 150 ul of BHI media was added to each well and plates were incubated at 37^{o}C for approximately 3 hours without shaking until the O.D. at 595 nm of untreated control wells was between 0.20-0.28. Plates were read with Bio-Rad IMark microplate reader. Seroconversion is defined as titers which were 4-fold higher than day 0 samples.

Agglutination Assay: Agglutination titers were detected essentially as previously described [40]. *V. cholerae* O1 (strain 19479 El Tor Inaba) was cultured to mid log phase for 2½ hours in bovine heart infusion media at 37^{o}C. Bacteria were pelleted at 3,000 x g for 10 min and washed twice with PBS. Prior to use bacteria were normalized to an O.D. of 0.3. Equal amounts of heat inactivated serum (56^{o}C for 30 minutes) and bacteria were mixed and added to a V-bottom microtiter plate for a total of 50 ul per well. Each plate was sealed with an adhesive film, centrifuged for 10 seconds, then incubated for 20 hours at 4^{o}C. Plates were imaged using a UV imaging system (ChemiDoc, BioRad). Agglutination titers were recorded as the last dilution where bacteria were agglutinated.

Statistical test: Graphs and statistical test were performed using GraphPad Prism software version 8.0. One-way or two-way ANOVA was used to determined statistical significance. Information about the statistics used for each experiment including sample size, experimental methods, and specific statistical test employed can be found in the relevant results section or figure legend.

Acknowledgements

We thank J. Harris and E. Ryan for helpful discussions in putting the manuscript together. We thank C. Kelley, D. Raheja, M. Mulligan and the hope clinic for technical support in organizing the recruitment, blood collection, and follow up healthcare evaluations of study volunteers. We thank all 12 participants who generously donated their time and blood for this study. We thank R. Karaffa and A. Rae of the Emory School of Medicine flow cytometry core and the Emory pediatric flow cytometry core for their assistance in the cell sorting experiments. *V. cholerae* LPS from serotype Inaba and Ogawa were generously provided by E. Ryan and colleagues.

Figures and legend

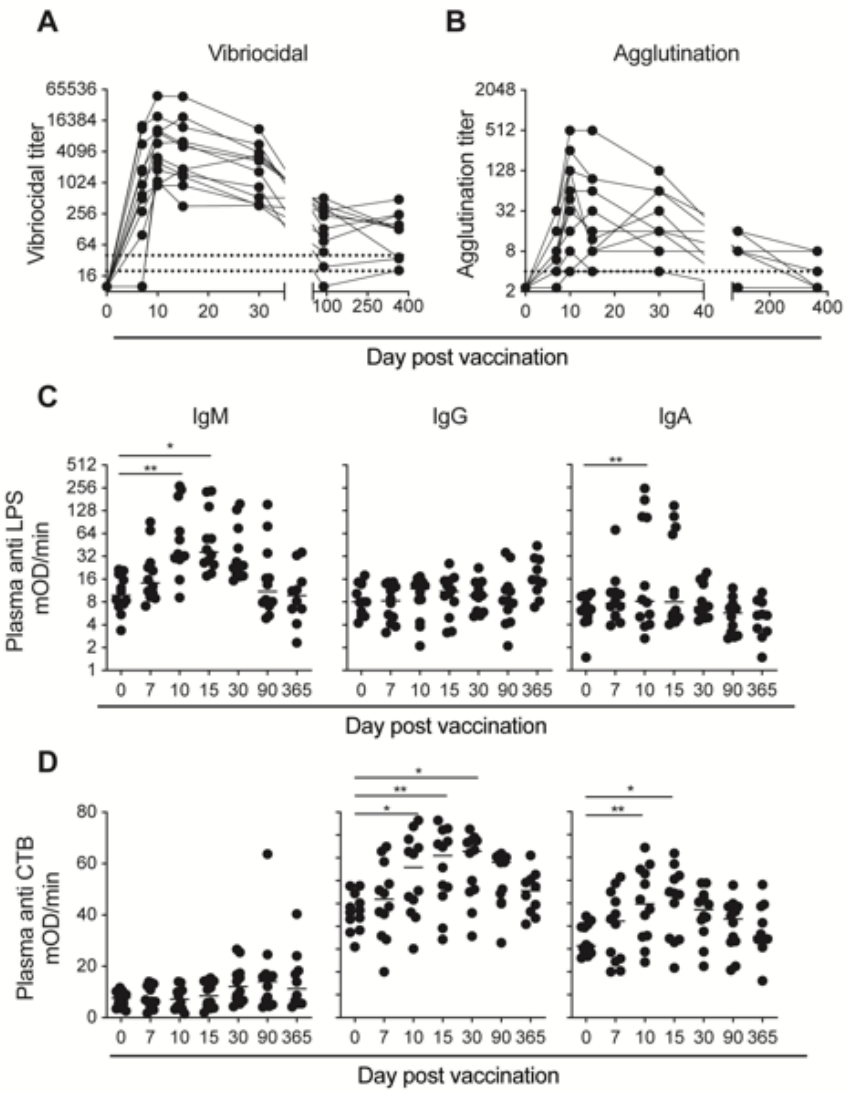

Figure 1: *V. cholerae* specific plasma antibody titers rise rapidly following vaccination and are maintained at least for one year post vaccination. (A) Vibriocidal and (B) Agglutination titers on day 0, 7, 10, 15, 30, 90 and 365 for each of the 12 subjects following vaccination. Dotted line in the vibriocidal and agglutination figures indicate the lowest dilution of serum tested in the assay. (C) Anti lipopolysaccharide and (D) anti cholera toxin B subunit titers for IgM, IgG, and IgA plasma antibodies on days 0, 7, 10, 15, 30, 90, and 365 for each of the 12 subjects following vaccination. Statistical significance between bracketed samples was determined using a one-way ANOVA. Significance values are indicated by asterisk ($P < 0.05$ (*); $P < 0.005$ (**); $P < 0.0005$ (***); P <000.1 (****)).

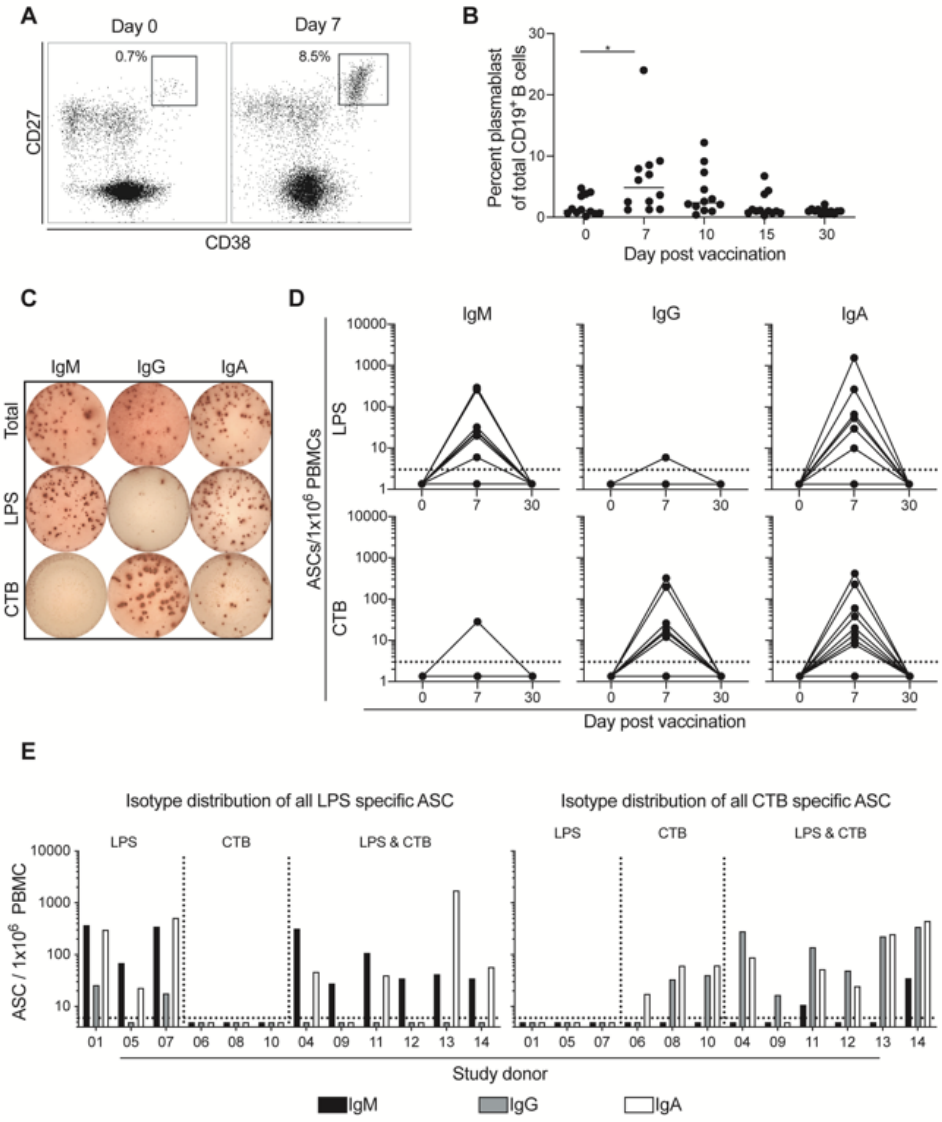
A
Day 0
Day 7
0.7%
8.5%
CD27
CD38
B
Percent plasmablast of total CD19+ B cells
Day post vaccination
C
IgM
IgG
IgA
Total
LPS
CTB
D
IgM
IgG
IgA
LPS
CTB
ASCs/1x10^6 PBMCs
Day post vaccination
E
Isotype distribution of all LPS specific ASC
Isotype distribution of all CTB specific ASC
LPS
CTB
LPS & CTB
ASC / 1x10^6 PBMC
Study donor
IgM
IgG
IgA

Figure 2: Antigen specific plasmablasts increase following vaccination. (A) Representative flow cytometry plot of the plasmablast population from one donor on day 0 and 7 post vacation. (B) summary flow cytometry analysis of the plasmablast population following vaccination for each of the 12 participants on day 0, 7, 10, 15, and 30 post vaccination. Statistical significance between bracketed samples was determined using a one-way ANOVA. Significance values are indicated by asterisks ($P < 0.05$ (*); $P < 0.005$ (**); $P < 0.0005$ (***); $P < 0.0001$ (****)). (C) Representative ELISPOT of the total, LPS, and CTB specific IgM, IgG, and IgA ASC from one subject on day 7 post vaccination. (D) Summary ELISPOT analysis of lipopolysaccharide (LPS) and cholera toxin B subunit specific IgM, IgG, and IgA antibody secreting cells following vaccination from each of the 12 subjects on day 0, 7, and 30 post vaccination. Dotted line indicates limit of detection for the ELISPOT assay. (E) Isotype distribution of IgM (black) IgG (grey), and IgA (white) of all ASC for each of the 12 subjects. Dotted line indicates limit of detection for the ELISPOT assay.

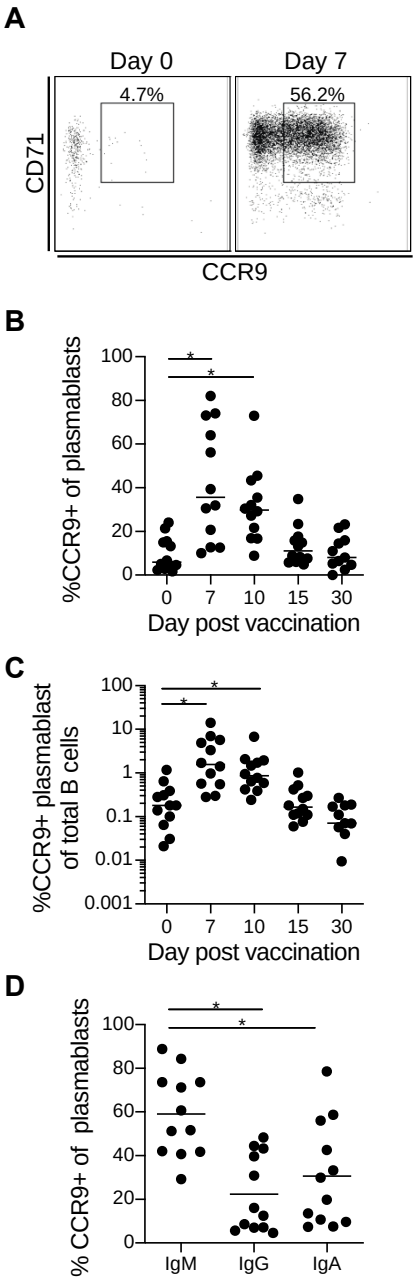
A
Day 0
Day 7
4.7%
56.2%
CD71
CCR9
B
%CCR9+ of plasmablasts
100
80
60
40
20
0
0 7 10 15 30
Day post vaccination
C
%CCR9+ plasmablast of total B cells
100
10
1
0.1
0.01
0.001
0 7 10 15 30
Day post vaccination
D
% CCR9+ of plasmablasts
100
80
60
40
20
0
IgM
IgG
IgA

Figure 3: Induction of CCR9 expression on plasmablasts after vaccination. (A) Representative flow cytometry analysis of the percent of CCR9+ plasmablasts from one donor and (B) summary analysis of the percent of CCR9+ plasmablasts from all 12 subjects. (C) Summary analysis from all 12 donors of the percent of CCR9+ plasmablasts of the total B cell population. (D) Percentage of the IgM, IgG, and IgA expressing plasmablasts which were also CCR9+ on day 7 for each of the 12 subjects. Statistical significance between bracketed samples was determined using a one-way ANOVA. Significance values are indicated by asterisks ($P < 0.05$ (*); $P < 0.005$ (**); $P < 0.0005$ (***); $P < 0.0001$ (****)).

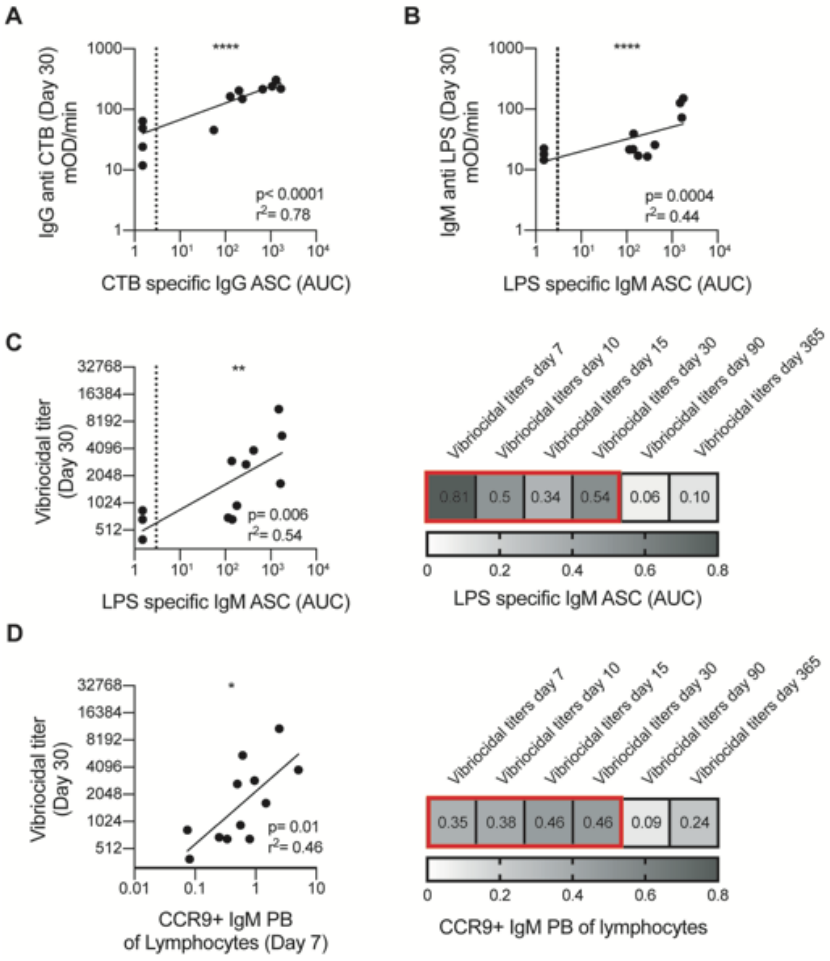
A
IgG anti CTB (Day 30) mOD/min
****
p< 0.0001
r²= 0.78
CTB specific IgG ASC (AUC)
B
IgM anti LPS (Day 30) mOD/min
****
p= 0.0004
r²= 0.44
LPS specific IgM ASC (AUC)
C
Vibriocidal titer (Day 30)
**
p= 0.006
r²= 0.54
LPS specific IgM ASC (AUC)
Vibriocidal titers day 7
Vibriocidal titers day 10
Vibriocidal titers day 15
Vibriocidal titers day 30
Vibriocidal titers day 90
Vibriocidal titers day 365
0.81
0.5
0.34
0.54
0.06
0.10
LPS specific IgM ASC (AUC)
D
Vibriocidal titer (Day 30)
*
p= 0.01
r²= 0.46
CCR9+ IgM PB of Lymphocytes (Day 7)
0.35
0.38
0.46
0.46
0.09
0.24
CCR9+ IgM PB of lymphocytes

Fig. 4: Correlations between early and late humoral responses. Linear regression analysis between (A) cholera toxin b subunit (CTB) specific IgG ASC and IgG CTB plasma titers at day 30 post vaccination for all 12 subjects. (B) Linear regression analysis between lipopolysaccharide (LPS) specific IgM ASC and IgM LPS plasma titers on day 30 post vaccination for all 12 subjects. Representative (left panel) and summary (right panel) of linear regression analysis between LPS specific IgM ASC and vibriocidal plasma titers on day 30 for all 12 subjects. Number in box is the r^2 value and red outline indicates $p<0.05$. (D) Representative (left panel) and summary (right panel) linear regression analysis between CCR9+ IgM plasmablast of total lymphocytes and vibriocidal plasma titers. Number in box is the r^2 value and red outline indicates $p<0.05$. ASC response for (C) and (D) is depicted as area under the curve (AUC) covering days 0, 7, 10, 15, and 30. Correlation analysis performed by log transformation of plasma titers and AUC followed by linear regression analysis. Dotted line indicates lowest number of spots counted for ELISPOT analysis.

Table 1: Characteristics of subjects at time of enrollment	
Age in years, median (range)	35 (22-49)
Sex (M/F/O)	6/5/1
Race	
Black	3
White	8
AI/AN	1
Ethnicity	
White Non-Hispanic	11
Hispanic	1

Supplemental Table 1: Demographics of study participants

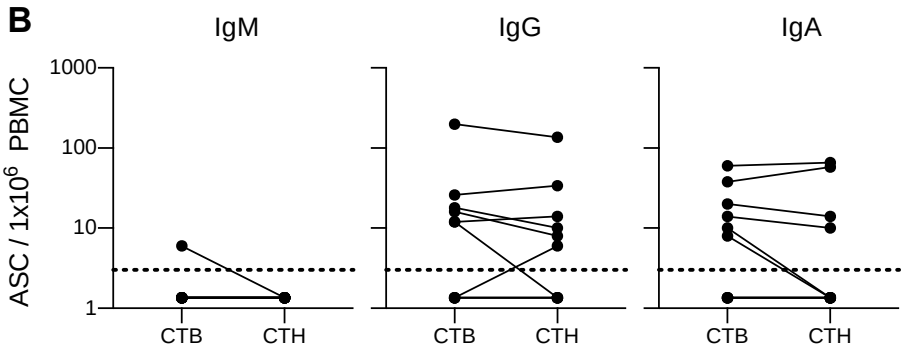

Supplemental Figure 1: Antibodies from vaccinated donors are able to bind to the cholera holotoxin. Summary ELISPOT analysis of CTB and CTH specific IgM, IgG, and IgA ASC measured on day 7 post vaccination for each of the 12 participants. Dotted line indicates limit of detection of the ELISPOT assay.

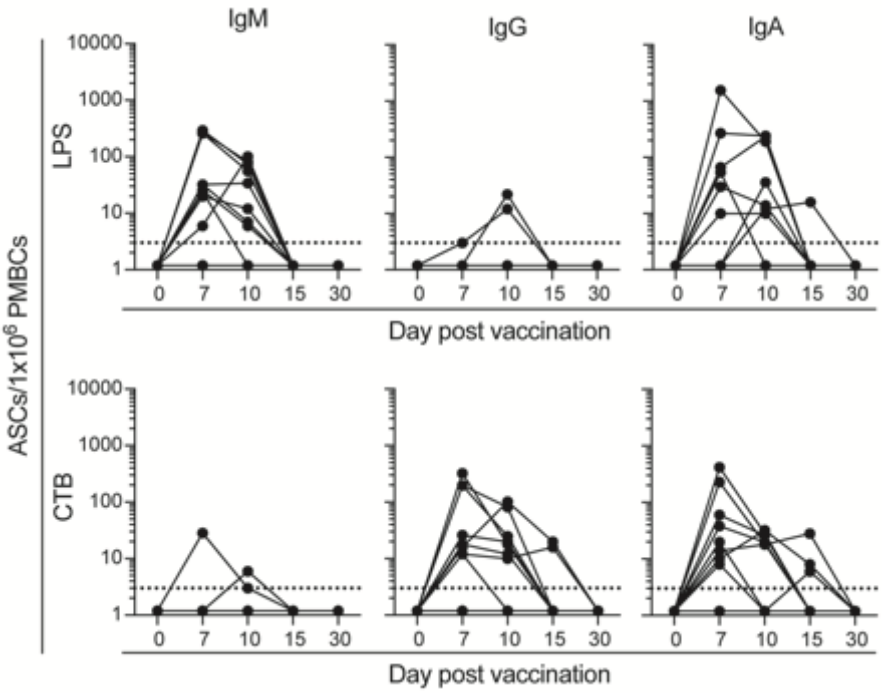

Supplemental Figure 2: Kinetic analysis of antigen specific ASC following vaccination. Summary ELISPOT analysis of lipopolysaccharide (LPS) and cholera toxin B subunit (CTB) specific IgM, IgG, and IgA antibody secreting cells following vaccination from each of the 12 subjects on day 0, 7, 10, 15 and 30 post vaccination. Dotted line indicates limit of detection of the ELISPOT assay.

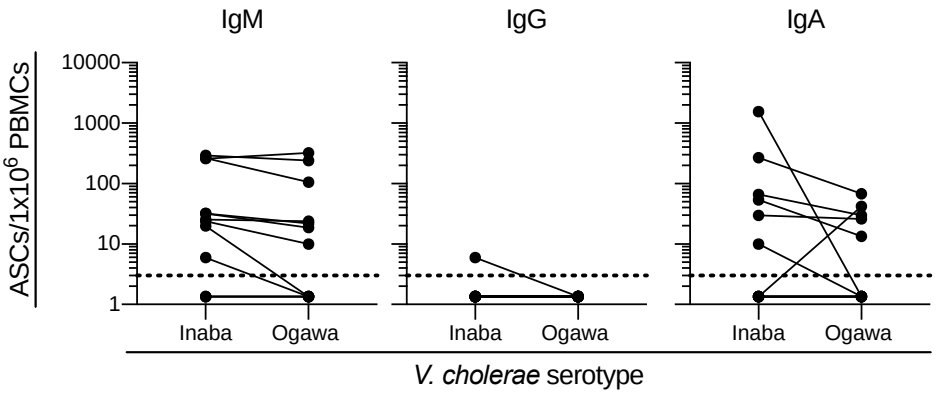

Supplemental Figure 3: ASC responses are cross reactive with LPS from *V. cholerae* serotype Ogawa. Summary ELISPOT analysis of Inaba and Ogawa LPS specific IgM, IgG, and IgA antibody secreting cells following vaccination from each of the 12 subjects on day 7 post vaccination. Dashed line indicates limit of detection of the ELISPOT assay.

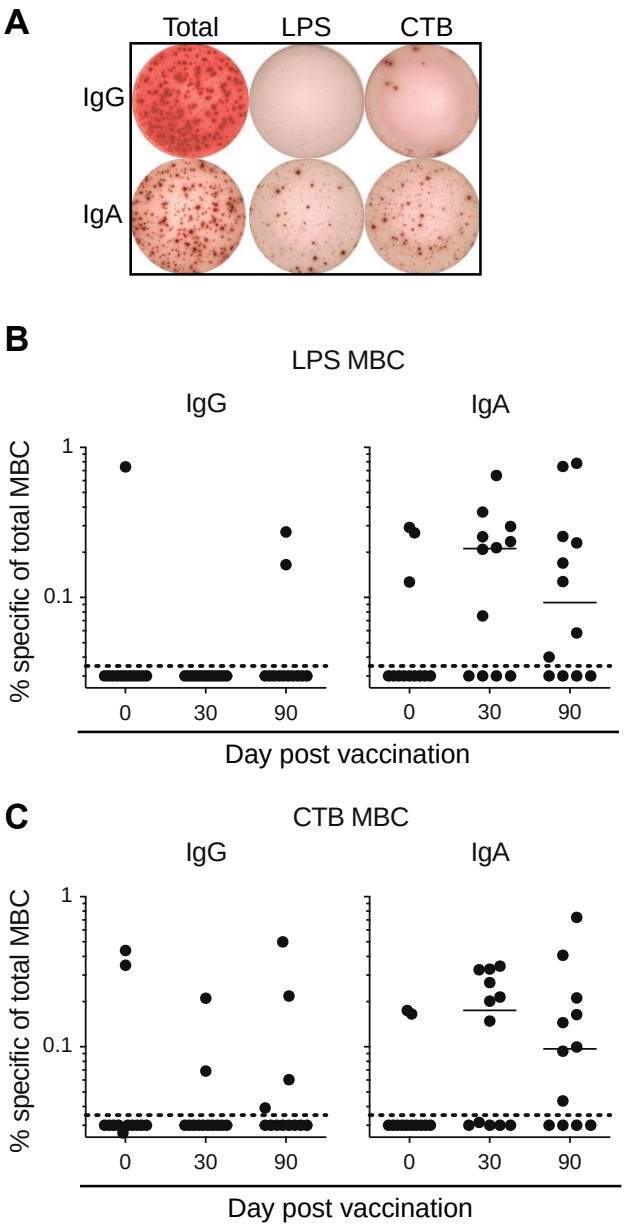

Supplemental Figure 4: Memory B cell responses are modestly elevated post vaccination. (A) Representative ELISPOT and summary analysis of (B) LPS and (C) CTB specific IgG and IgA memory B cells on days 0, 30, and 90 post vacation for each of the 12 participants. Dashed line indicates limit of detection for the memory B cell assay.

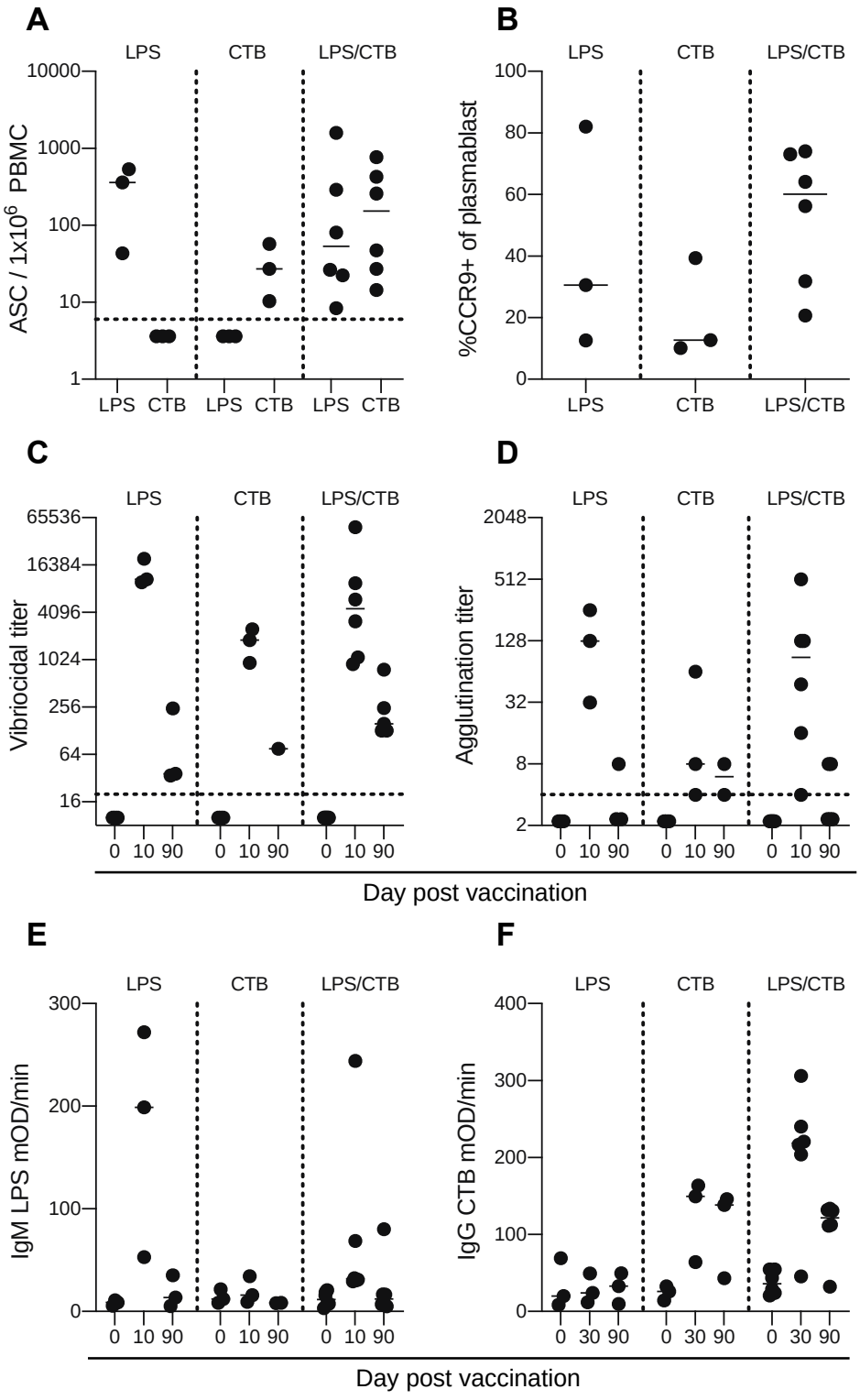
A
LPS
CTB
LPS/CTB
ASC / 1x10^6 PBMC
10000
1000
100
10
1
LPS CTB LPS CTB LPS CTB
B
%CCR9+ of plasmablast
100
80
60
40
20
0
C
Vibriocidal titer
65536
16384
4096
1024
256
64
16
0 10 90
D
Agglutination titer
2048
512
128
32
8
2
Day post vaccination
E
IgM LPS mOD/min
300
200
100
0
F
IgG CTB mOD/min
400
0 30 90

Supplemental Figure 5: Antigen specific donor responses. Donors divided into LPS only, CTB only, and LPS/CTB double responders based on ASC response. (A) day 7 ELISPOT responses, (B) percent positive CCR9 plasmablasts, (C) vibriocidal titers, (D) agglutination titers, (E) LPS anti IgM titers, and (F) CTB anti IgG titers.

Chapter 3: Gut homing plasmablasts induced by *Vibrio cholerae* vaccination exhibit hallmarks of affinity maturation

Oluwaseyi Adekunle[a], Robert C. Kauffman[a], Lindsay E. Nyhoff[a], Carson Norwood[a], Juton Winston [b], Nadine Rouphael[b] and Jens Wrammert[a]

[a] Division of Infectious Disease, Department of Pediatrics, Emory University, School of Medicine, Atlanta, Georgia, USA

[b] The Hope Clinic, Emory Vaccine Center, Division of Infectious Disease, Emory University, School of Medicine, Atlanta, Georgia, USA

Abstract

Vibrio cholerae is the causative agent of the severe acute diarrheal disease cholera. *V. cholerae* is a noninvasive pathogen, therefore immunity to cholera is likely mediated by intestinal B cells at the mucosal surface. Previous studies have shown that the plasmablasts induced in response to *V. cholerae* immunization express gut homing markers. To gain insight into the cells which play an important role in mucosal protection to *V. cholerae*, we used single cell analysis techniques to characterize and analyze the plasmablasts and antibodies induced following administration of a live attenuated cholera vaccine to a naïve population. We observed that the plasmablasts were largely specific for the immunodominant antigens of *V. cholerae*, lipopolysaccharide (LPS) and cholera toxin B subunit (CTB). The CTB specific cells had levels of somatic hypermutation, affinity, and cross reactivity to heat liable toxin B subunit (LTB) that were comparable to what has been previously described from infection derived CTB specific antibodies. The LPS specific antibodies preferentially bound to Inaba LPS, were cross reactive to Ogawa LPS, but largely non-reactive to the LPS of other bacterial species, indicating OSP specificity. A majority of the LPS specific antibodies were generated from plasmablasts that highly expressed the gut homing receptor CCR9. Finally, we observed that many of the LPS specific plasmablasts produced antibodies which had relatively high numbers of mutations. The number of mutations, localization of mutations to the complementary determining regions, and affinity of the antibodies to LPS had a strong positive correlation, which is likely indicative of ongoing affinity maturation. These findings provide key insight in the cells which provide immunity to *V. cholerae* at the mucosal surface.

Introduction

Vibrio cholerae is the pathogenic bacteria responsible for cholera, a severe diarrheal illness. This pathogen affects up to 3 million people annually, resulting in over 100,000 deaths each year [97]. Inactivated oral cholera vaccines have been developed for use in locations where cholera is endemic to help reduce the disease burden in the local populations. Unfortunately, limitations including the requirement of multiple doses, low efficacy, and limited duration of protection impede their use in these areas [185]. The relatively weak immunity observed from the inactivated vaccines stands in stark contrast to the response seen in natural infection, where individuals remain protected long after symptom onset [166]. The factors that lead to the robust, durable immunity seen following symptomatic infection is unclear. Research has sought to identify the aspects of the immune response that have a critical role in directing the duration and effectiveness of long-term cholera immunity [40].

V. cholerae is a noninvasive pathogen, therefore immunity is likely mediated and maintained within the intestinal mucosa. Previous studies have described the importance of gut homing B cells in clearing and preventing infection of intestinal tissues [93]. However, examining intestinal immune cells in human subjects requires invasive surgical procedures which has limited investigative research in this critical tissue. We have previously investigated responses to *V. cholerae* in a naïve cohort using the live attenuated vaccine, Vaxchora, as a model of immunization. Plasmablasts are a population of recently proliferated antibody secreting cells (ASC) that are seen transiently in circulation following infection or vaccination. Because they represent an induced response, these cells are largely specific for the immunizing agent [39, 186]. We observed an expansion of both the overall plasmablasts population as well as *V. cholerae* specific antigen responses following vaccination. The two major immunodominant

antigens of cholera are the cholera toxin and lipopolysaccharide, and each antigen drove a unique isotype response. Responses to cholera toxin B subunit (CTB) were largely mediated by IgG antibodies. The robust anti-lipopolysaccharide (LPS) response, in contrast, was primarily derived from IgM and IgA antibody secreting cells (ASC). Importantly, we also noted there was a significant increase in the expression of the gut homing marker CCR9 on the overall plasmablasts population, primarily on the IgM and IgA secreting cells. Due to their gut homing expression and antigen specificity, these plasmablasts represent a readily accessible population of antigen specific B cells which likely play a role in both acute and potentially long-lived, intestinal immune responses.

To further examine these responses and gain better insight on human mucosal cholera immunity, we generated and examined a panel of monoclonal antibodies from plasmablasts sorted from vaccinated volunteers using single cell analysis techniques. This approach allowed us to perform an in-depth analysis of the repertoire, affinity, and antigen selection on a single cell level of these *V. cholerae* induced plasmablasts. These analyses provide exceptional insight on the nature of the intestinal homing plasmablast response following *V. cholerae* exposure.

Results

Robust peripheral LPS and CTB antigen specific plasmablasts responses are detectable one-week post vaccination

From our cohort of vaccinated subjects, we selected six individuals for further single cell analysis. The vaccinees chosen for advanced analysis had a significant expansion in the percentage of circulating plasmablasts following vaccination (**Figure 1A and 1B**). Although all vaccinees had significant increase in this population, ranging in upwards of 20% of the total B cell compartment in one donor, there was significant variation between subjects (mean=9 range

2.6 - 20.8). In addition to the expansion of the total plasmablasts population, many of the cells were largely specific for *V. cholerae* antigens. As determined by ELISpot analysis, each subject had a significant percentage of ASC that were specific for the immunodominant antigens of *V. cholerae*, LPS and CTB (**Figure 2C and 2D**). The antibody response to the antigens were largely isotype restricted; LPS was mainly derived by IgM and IgA ASC while antibodies to CTB were generated from IgG and IgA ASC. While all donors had antigen specific ASC responses to the vaccine, there was individual variation in the magnitude and antigen specificity of the response to the vaccine in our cohort.

Single cells from the overall plasmablast population were sorted 7 days post vaccination. Using single cell PCR techniques 193 heavy and light chain amplicons were obtained, sequenced, and analyzed for V gene usage, somatic hyper mutation, clonality, and isotype. From these transcripts a total of 149 antibodies were generated with average of 24 per donor (range: 19-37) (**Supplemental Table 1**). We measured the affinity of the antibodies we generated against CTB and LPS, the two immunodominant antigens of *V. cholerae*. We observed that all six of our subjects had monoclonal antibodies (mAbs) which bound to one or both of these antigens (**Figure 2**). We were able to generate 13 CTB specific mAbs from four of our six donors as seen in **Figure 2A**. Interestingly, we noted that the affinity of CTB specific antibodies was primarily binary; with each antibody having either very high or very low affinity for the toxin with few intermediate antibodies present. Additionally, the affinity of the response was donor restricted, with two of the donors having very high affinity antibodies while the other two subjects had antibodies with very low affinity. Intriguingly, the high affinity seen in the antibodies generated from our vaccinated subjects was comparable to toxin specific antibodies produced from infected patients (**Figure 2A**).

Given that our cohort was cholera naïve and should not have encountered CTB prior to vaccination, it was surprising to see that some of the subjects had generated high affinity antibodies. CTB shares 83% homology with heat liable toxin B subunit (LTB) which is produced by some strains of *Escherichia coli* [135]. Unlike *V. cholerae*, exposure to *E. coli* is far more common within the United States where the subjects for the trial were recruited [176, 177]. We have also previously demonstrated that the CTB specific antibodies generated from infected patients were also cross reactive to LTB [40]. Therefore, we screened the CTB specific antibodies against LTB (**Figure 2B**). We found that all of the high affinity CTB specific antibodies were cross reactivity to LTB with similar levels of affinity. In contrast, the low affinity CTB specific antibodies had only minor or low cross reactivity to LTB.

We were able to produce 55 LPS specific mAbs from five of the participants (**Figure 2C**). In contrast to the CTB mAbs in which the affinity was either very high or very low, the affinity of the LPS specific mAbs ranged from moderate to low. While some donors had only low affinity antibodies, others such as donors CV3.04 and CV3.13 both had modest and low affinity mAbs. The majority of the LPS specific mAbs that our laboratory had previously derived from *V. cholerae* infected patients were high affinity. There are two serotypes of *V. cholerae* which cause disease, Inaba and Ogawa, which only differ in the presence of the terminal methyl group in LPS of Ogawa [187]. Despite this difference, the LPS specific antibodies generated from Ogawa infected patients were largely cross reactive to Inaba LPS. We hypothesized that the antibodies generated from the vaccine, which is based on an Inaba strain, would also be cross reactive to Ogawa LPS. Therefore, we screened the LPS specific antibodies against LPS from both strains. We found that most of the Inaba specific LPS mAbs also bound to Ogawa LPS, albeit with lower affinity (**Figure 2D**).

LPS is comprised of three components: lipid A, a core saccharide, and the O specific polysaccharide. In humans, LPS specific antibodies primarily target the O specific polysaccharide which is largely unique to each bacterial strain. We screened our mAbs against a small panel of non-cholera LPS from other intestinal bacteria to see if the mAbs were cross reactive to the LPS of other strains of bacteria. We found that most of the antigen specific mAbs were selective for *V. cholerae* LPS and CTB and only a few of the antibodies showed very low level affinity to the LPS of non-vibrio species (**Supplemental Figure 1**).

Vibriocidal titers are the best correlate of immunity to cholera disease. Therefore, we also measured the vibriocidal capacity of the antibodies (**Figure 3A**). The vibriocidal titers largely resembled what we observed in the antibodies binding to LPS. Most of the antibodies had intermediate or low vibriocidal titers, compared to the highly vibriocidal antibodies which we had previously generated from infected patient CF29. We have previously established that most of the vibriocidal antibodies generated from infection were also LPS specific. To determine if this was the case in our naïve cohort, we compared the vibriocidal titer of the mAb to their affinity for LPS (**Figure 3B**). We observed a significant positive correlation between the affinity to LPS and vibriocidal titers in both the vaccine and patient derived antibodies. We also observed that a majority of the vibriocidal antibodies were also LPS specific.

Gut homing is an important aspect of protective intestinal immune responses. We had previously observed that the majority of the plasmablasts induced by vaccination expressed CCR9, a chemokine receptor that traffics cells to the small intestine. We also had noted that CCR9 was primarily expressed on IgM and IgA secreting plasmablasts. We wanted to ascertain if the antigen specific antibodies we had generated originated from gut homing cells. To accomplish this, we examined the CCR9 expression of the LPS and CTB specific plasmablasts

(**Supplemental Figure 2**). We found that the majority of the LPS specific plasmablasts had high expression of CCR9. In contrast, only around half of the CTB specific plasmablasts expressed high levels of CCR9. We also examined how mutation, v gene, clonality, and affinity correlated with CCR9 expression, but none of those responses had significant correlation with CCR9 expression.

LPS specific responses are dominated by VH3 family rearrangements.

Our previous analysis from infected patients revealed that the VH repertoire utilized by LPS specific antibodies was restricted to VH3 family members. In contrast, the response to CT used a more diverse array of IGHV genes. We were interested to ascertain if VH usage shifted due to the selective pressure of consecutive *V. cholerae* exposures or if the certain IGHV genes were more efficient at recognizing cholera antigens. The VH gene usage from all the plasmablasts we examined were represented largely by VH1, VH3, and VH4 members, but of these three VH3 was by far the most dominant (**Supplemental Figure 3**).

Similar to what we had previously observed from infected patients, the VH gene usage of the LPS specific antibodies was largely restricted to members of the VH3 family. However, members of the VH1 and VH4 were also recruited to the anti LPS response. We then examined the individual VH gene used to see if certain rearrangements were shared between multiple patients and/or vaccinees. We found that V3-23, V3-33, and V4-39 rearrangements were common among multiple vaccinees. Interestingly we also discovered that V3-23 and V3-53 gene segments were used by members of both the infected and vaccinated groups (**Figure 4A and 4B**). While many rearrangements were used, the response in both infected patients and vaccinees was dominated by a few rearrangements such as V3-7, and V3-33. These particular rearrangements represent clonal expansions.

In contrast to the limited VH family diversity we observed in the LPS specific antibodies, the CTB repertoire was more varied in our vaccinated subjects (**Figure 4C and 4D**). While still primarily utilizing VH3 family members, VH1 and VH4 combined comprised over 53% of the total CTB specific sequences. The VH family members used in mAbs from infected patients was also diverse, with members of the VH4, VH5, and VH7 also utilized. When we examined the individual VH genes used for the CTB responses, we noted it had a more diverse and balanced representation of the various segments. There were several segments shared between subjects, and V3-23, V3-21, and V4-59 rearrangements were found in both infected patients and vaccinees. V3-21 is particularly interesting, as monoclonal antibodies utilizing this rearrangement from infected patients exclusively bound to the cholera toxin A subunit. The toxin A subunit is absent in vaccine strain, which may explain the lack of this rearrangement in the vaccinated subjects. Additionally, we noted that the V3-23 rearrangement in particular was utilized by LPS and CTB specific antibodies from both vaccinees as was as infected subjects.

Antigen specific responses are highly clonal and contain high levels of mutations.

We used the sequencing analysis to determine clonal relationships of the plasmablasts and the level of somatic hyper mutation (SHM) of the antibodies (**Figure 5**). Each vaccinee had numerous clonal expansions on levels which were similar to our previous findings from infection (**Figure 5A**). The clonal expansions were almost universally antigen specific, and the majority of them were specific to LPS. This is in contrast with what we have previously observed from infected patients, where the antigen specificity of the clonal expansions was more evenly divided between LPS and CTB [40].

The antigen specific responses showed a wide range of mutations within the VH gene region (**Figure 5B**). The LPS specific antibodies had a wide range in of mutation, with some

antibodies having fewer than 10 mutations while others had over 40 (range 8 – 44). Similarly, the CTB specific antibodies also showed a wide range in specificity to the target (range 4-52). The levels of SHM seen in the vaccine LPS and CTB specific responses, particularly in the high affinity mAbs, were nearly equivalent to what we have observed from our infected cohort (**Supplemental Figure 4**). Additionally, we observed that a signification proportion of the LPS specific cells were largely derived from IgM and IgA secreting plasmablasts. In contrast, the CTB specific cells were largely derived from IgG secreting plasmablasts. This matches our previous findings when examining total ASC response following vaccination. Given the high rate of mutations in the antigen specific plasmablast, we were curious to see if we could identify evidence of antigen selection. One method to examine this is examining the number of replacement (R) over silent (S) mutations within the complementary determining region CDR. An R/S ratio greater than 2.9 within the CDR is likely indicative of antigen selection. We observed R/S ratio's exceeding 2.9 within the CDR of the antigen specific plasmablasts from all six of our subjects (**Figure 5C**). This ratio was not observed in the Framework regions, indicating that selective pressure is occurring within the antigen binding regions of the antibodies.

SHM correlate with affinity, suggesting ongoing affinity maturation.

Our group has previously found evidence of affinity maturation toward LPS, a T-independent antigen. In addition, examination of serotype selectivity showed evidence of durable memory which had been generated at the mucosal surface. Given the R/S ratio we observed in the CDR's of the antigen specific antibodies, we were curious to see if we could find more evidence of affinity mature responses within our cholera naïve subjects.

To approach this, we used linear regression analysis to identify correlations between the number of variable region mutations and affinity to all the LPS and CTB antigen specific cells from each of the six vaccinees (**Figure 6**). For both LPS (**Figure 6A**) and CTB (**Figure 6 B**), we observed a strong positive correlation between the affinity of the antibody and the total number of mutations.

While this approach highlighted the general relationship between mutations and correlations, we also wanted to examine the evolutionary relationship between related cells. To approach this, we selected a clone group from which were able to generate 9 LPS specific antibodies. We then used phylogenetic tree analysis to organize the antibodies based on their Vh sequence and then compared them to their affinity for the target. Utilizing this approach, we were able to demonstrate that within the clone group, the more mutations the antibodies accumulated the higher affinity the antibodies had towards LPS. Plasmablasts can be derived from naïve or antigen experienced precursors. We wanted to determine if the antibodies in our panel could have been generated from naïve B cells, based on the relatively high levels of SHM we observed, particularly, in the LPS specific cells. Prior research has described that SHM occurs at a rate of 1.1×10^{-3} mutations/bp/cell division [188]. Using these numbers, we calculated the theoretical mutation rate for the antigen specific and nonspecific antibodies from both our vaccinated and infection induced plasmablasts (**Supplemental Figure 5**). We found that many of the cells with high levels of SHM had a theoretical mutation rate substantially higher than 1.1×10^{-3}, which makes it unlikely that those cells originated from naïve precursors.

Discussion

Understanding the cells which are responsible for maintaining cholera immunity is critical to better understand the way. Plasmablasts represent a population of effector cells

generated by immunization, have a high degree of specificity for the immunizing agent, and have the potential to drive enduring immune responses. Additionally, as our group and others have previously described, plasmablasts induced by the *V. cholerae* exposure express gut homing markers which indicates their potential to mediate immunity at the intestinal mucosa [121]. This is particularly important because cholera immunity is likely driven by local intestinal, rather than peripheral responses. Due to these factors examination of these cells can give critical insight into the mucosal immune response *to V. cholerae* infection.

V. cholerae has many antigens including TcpA, flagellin, and OmpU which people infected with the pathogen do develop responses to [175, 189, 190]. However, the immunodominant response seen at the polyclonal level in both naïve and endemic settings favors LPS and CT. While these responses may not be detectable in large scale, it remains possible that single cell analysis techniques could identify new novel antigens, particularly in primary immunizations where the immunodominance to LPS and CT may not be as dominant [159].

The mAbs generated from our cohort of vaccines, however, also preferentially bound to LPS and CTB at a similar frequency to what we have seen in infected donors [40]. Classically, antibodies generated in response to novel antigens tend to be dominated by relatively low affinity IgM responses [191]. As this is a naïve cohort, we would expect the response to be dominated by relatively low affinity, weak binding antibodies. While the majority of the LPS response was mediated by low affinity mAb, there was a small population of antibodies which had moderately high affinity to the polysaccharide. In addition to the affinity, many of these antibodies had high levels of SHM, and displayed a strong positive correlation when correlated with affinity to LPS. These observations shed insight on several key factors on mucosal immunity.

Foremost, there is clear evidence of somatic hyper mutation and affinity maturation occurring in mucosal tissues in response to the polysaccharide antigens. We have observed a similar effect from our infected cohort where in addition to identifying highly mutated and class switched cells, the antibodies from one donor were more selective to the noncirculating serotype [40]. Those findings are indicative of a long-lived reservoir of antigen specific memory B cells to a polysaccharide antigen. Classically, polysaccharides were thought to be unable generate durable immunity or the germinal center reactions typically associated with high levels of SHM. However, recent research focusing on T-independent antigens, extrafollicular responses, and mucosal tissues demonstrate that this rule is not absolute [21]. In our study, most of the LPS specific antibodies carried levels of SHM which were comparable to what has been reported from infected patients. Additionally, our vaccinees did not develop antibody responses which targeted lipid A, but instead targeted the OSP. These data may indicate that the B cells are likely not reacting to free floating LPS but are encountering whole bacteria or secreted membrane vesicles. This would be extremely important, as the bacterial membrane likely contains embedded proteins which would be capable of driving T-dependent responses and lead to T cell assistance [192].

The live attenuated vaccine used in this study is of the Inaba serotype. Responses in endemic studies show that the antibodies are cross reactive. Therefore, we examined the potential cross reactivity in our cohort as well. Every donor in our cohort had LPS specific antibodies which were cross reactive with Ogawa LPS. Generally, the antibodies showed higher affinity for Inaba then Ogawa LPS. During our previous work exploring the mechanisms of *V. cholerae* based immunity we speculated that epitope plays a key role in determining antibody effectiveness. We showed that antibodies which were more selective tended to have high

functional capacity, possibly due to binding of the terminal stock of the OSP [193]. Examining the potential epitopes of these serotype selective and non-selective antibodies could shed further light on this data.

As plasmablasts represent a transient response, phenotypic characterization can shed insight on their origins and potential destination. Therefore, we examined the gut homing marker CCR9 expression on these individual cells and analyzed them to determine if there are correlations which favor the gut homing phenotype. There did not seem to be any correlation between CCR9 expression, affinity, V gene usage, or V_H mutations. The best correlation of CCR9 expression was antigen specificity to cholera. LPS specific antigen specific cells were significantly more likely to be CCR9 compared to those which were not specific. However, there were a modest number of antigen specific cells which did not express CCR9. Additionally, we observed that CCR9 expression even varied within clone groups. Overall mutation rate was not predictive of CCR9 expression. However, within clone groups who members had different levels of CCR9 expression, clones with higher levels mutations expressed the receptor while clones with lower levels of mutation did not. While the numbers are too small to make any definitive conclusions, it is interesting to speculate that the time spent accumulating mutations may be an important factor in altering homing marker expression.

Studies in mice have shown that gut immunization leads to the production of LLPC that take up residence in both the bone marrow and mucosal compartments. A study examining the response to cholera toxin in mice found that following immunization the bone marrow compartment contained IgG and IgA plasma cells, while only IgA plasma cells were found in the intestinal tissue [95]. Because immunity to *V. cholerae* is likely mediated by tissue resident intestinal cells, it is important to understanding the factors which control mucosal homing.

It is possible that CSR influences the expression of homing receptors. IgM, IgG, and IgA plasma cells produced following influenza infection have unique transcriptomes. Some of the genes differentially expressed between the isotypes include those related to homing [194]. That study showed that only the IgA specific plasma cells upregulated genes associated with homing to mucosal tissues. This effect may be immunogen/site specific, as our own studies have shown that IgM, in contrast to IgA, had the highest expression of CCR9. Another possibility is that the site of induction for each isotype is different. The environment in mucosal lymph nodes like Peyer's patches strongly favors IgA differentiation [90]. It is possible that cholera antigens are taken to distal lymph nodes, whether by diffusion or transported by dendritic cells or macrophages. In these environments class switching to IgG would likely be favored. This theory would explain the isotype preferences for CTB and LPS as well as resolving the disconnect between peripheral and mucosal responses. Studies which examine the link between the acute plasmablasts response with long term plasma cell clones in the mucosa are needed to shed clarity on this issue.

While most people respond to the vaccine, the magnitude of the response and isotype selectivity was heterogeneous among our vaccine cohort. Examination of the repertoire identified several VH rearrangements that bound to LPS and were represented across multiple subjects. In contrast to mice, which are able to generate antibodies targeting the Lipid A portion, the response seen in both human infection and vaccination targets the OSP. IGHV 3-23 seems to be a common V gene that is used to target this epitope. Its usage was seen from multiple individuals in both the infected and vaccinated populations. IGHV 3-23 is known to be polyreactive to many antigens which might explain its preferential recruitment into anti-cholera responses [195]. Given the heterogeneous nature of the response seen among the vaccinees, it is possible that

some donors had higher frequencies of these particularly IGHV genes prior to vaccination [196]. Examining the frequency of these cells prior to vaccination to determine if there is any correlation with immunity magnitude could prove useful. If certain VH rearrangements are favored, it may be possible to predict immunization efficacy by examining the repertoire of IGHV genes of pre vaccinated subjects.

Intriguingly, we noted a relatively high number of mutations within the antigen specific plasmablasts population. Their presence could be suggestive of highly efficient germinal center mediated SHM. Another possibility is that these cells may originate from memory, rather than naïve precursor cells. This is likely the case for the highly mutated, high affinity CTB specific mAb seen from the vaccinated group. These antibodies showed similarly high levels of affinity to *E. coli* heat liable toxin B subunit (LTB). LTB shares approximately 83% homology with CTB, and it is likely that some of our cohort may have been exposed to this pathogen in the past [135]. It is likely, given the homology between the two toxins, that the MBC generated from an LTB encounter would have the ability to activate in response to CTB exposure. Interestingly, the low affinity CTB specific antibodies showed either low or no cross reactivity to LTB. Given their low affinity and correspondingly low number of mutations, it is possible that these cells were generated from naïve B cell precursors. It would be interesting to determine if de novo responses are more selective towards CTB and require additional rounds of maturation to develop high affinity cross reactive antibodies.

The highly mutated LPS specific antibodies we observed, particularly those with moderate affinity to the polysaccharide, may also originate from memory precursors. The gut microbiota contains numerous species and it is conceivable that there are commensal vibrio or other related species which share some commonality with the *V. cholerae* OSP [197]. While the

strains of *V. cholerae* known to cause epidemics are not endemic to the US, infection with non O1 or O139 strains of *V. cholerae* do occur. Additionally, infection with other Vibrios species including *V. parahaemolyticus, V. vulnificus, and V. alginolyticus* also occurs and they are responsible for causing around illness in 80,000 people in the United States annually [177].

Studies have shown the presence of both IgM MBC and plasma cells within the mucosa that secrete antibody in response to antigens from the commensal microbiota [91]. Thus, the body is already "primed" with memory cells that are potentially cross reactive to novel antigens. While their initial affinity to LPS or CTB may be low, they are still antigen experienced cells and thus are able to mount a rapid response towards pathogen. This includes the rapid formation of ASC as well as developing further mutations through germinal center reactions or extra follicular responses [75]. These responses would likely be mediated primarily by IgM MBC, and this could explain both the high level of mutations paired with the unswitched nature of the response.

Screening microbiota samples from cholera naïve donors with cholera specific mAbs could be used to identify the presence of these microbial mimics. The IgM MBC and PC within the gut secrete antibodies which can be polyreactive or strain specific [91]. Another possible approach would be generation of antibodies from memory B cells or plasma cells within the mucosa cholera naïve individuals and screen for cross reactivity to LPS or CTB.

This study provides key insights in the immune response to *V. cholerae* exposure by utilizing techniques to examine plasmablasts at a single cell level generated during primary exposure. We have shown that the response to LPS, while diverse, seems to favor specific V_H region rearrangements. These cells may shape and influence a person's ability to respond effectively to the bacteria, as well has altering the diversity of the antibody pool following subsequent infection. Finally, we illustrate the presences of highly mutated clones following

exposure that are indicative of ongoing affinity maturation and possibly preexisting cross-reactive memory cells. These findings have implications on explaining the heterogeneity of responses seen to mucosal immunizations and inform strategies to improve vaccine development efforts.

Materials and Methods

Study population: Study participants were enrolled from residents of the metro Atlanta, Georgia area. Demographics were 5 female, 6 male, 1 other with an age range of 22- 49. Participants were in good health and had no history of prior cholera vaccination or disease. Medical history from each participant was obtained followed by a physical examination. Subjects were given a description of the study and signed an informed consent form prior enrollment of the study. Individuals were given a single dose of the oral live cholera vaccine (Vaxchora) according to manufacturer's instruction. Subjects fasted at least one hour prior to and after vaccine administration. Vaccination and blood collections were performed at the Emory Hope Clinic.

Blood collection and processing: Blood was collected by venipuncture immediately following vaccination, and on days 7, 10, 15, 30, and 90. Approximately 64 mLs of blood were drawn into CPT tubes at each timepoint. Additionally, approximately 3 mLs of blood were drawn into serum tubes. Blood was centrifuged at 1600 rcf for 30 min. The serum fraction was removed and aliquoted for further studies. The cell layer was harvested and lysed with 5 mLs of ACK lysis buffer (Quality biological #118-156-101) for 5 minutes. After which cells were washed with PBS + 2% FBS three times after spinning at 1200 rpm for 8 minutes. Cells were then resuspended in the appropriate buffer for counting and further experiments.

Flow cytometry and single-cell sorting: Immunophenotyping of the B cell subsets was performed on PBMC after staining with the following antibodies: CD27-APC (O323), CD3-AF700 (HIT3a), CD71-FITC (CY1G4), IgD-PerCPCy5.5 (IA6-2), CCR9-PE (BBC3M4), CD19-PECF594 (HIB19), CD38-PECy7 (HIT2), CD20-V450 (L27), IgA-APC (ISs11-8E10), CD14-AF700 (61D3), CD16-AF700 (CB16), IgG-PECy7 (G18-145), IgM-BV650 (MHM-88), and CD27-BV711 (O323). For each panel, a total of 2 million PBMC were stained. A minimum of 100,000 events were acquired on a BD LSR II Flow Cytometer and data was analyzed using FlowJo software.

ELISPOT assay: ELISPOT was performed to enumerate cholera toxin and LPS specific plasmablast present in the PBMC samples. 96-well ELISPOT assay filter plates (Millipore) were coated overnight at 4^{o}C with CTB (List Labs #104), LPS (generously provided by Dr. Ryan's Laboratory), or polyvalent goat anti-human Ig (10 µµg/mL, Jackson ImmunoResearch) in PBS. Plates were washed with PBS Tween 0.05% and blocked with R10 (RPMI 1640 + 10% FBS +1% P/S +1% L-glutamine) at 37^{o}C for 2 hours. Freshly isolated PBMC were added to the plates in a dilution series starting at 5 x 10^5 cells and incubated overnight at 37^{o}C. The following day plates were washed with PBS, followed by PBS Tween 0.05% and incubated with biotinylated anti-human IgG, IgA, or IgM antibody (Invitrogen) at room temperature for 90 minutes. After washing plates were incubated with avidin D-horseradish peroxidase conjugate (Vector laboratories) and developed using 3-amino-9-ethyl-carbazole substrate (Sigma-Aldrich). Plates were scanned and analyzed suing an automated ELISPOT counter (CTL, Cellular Technologies).

Monoclonal antibody generation: mAbs were generated from single-cell sorted plasmablasts by single-cell expression cloning, essentially as previously described [198]. Briefly, total cDNA was prepared from sorted cells by random hexamer primed reverse transcription (Sensiscript, Qiagen). Ig heavy chain and light chain (kappa/lambda) variable domain sequences were amplified by nested PCR using chain-specific primer cocktails encompassing all variable (V) gene families and the constant domain. Amplification of variable domains derived from IgG, IgA, and IgM ASCs was performed by multiplexing the constant domain specific 3 antisense primers. Sense primers used in the second round of nested PCR were modified by fusing the 5' end of each primer to the M13R sequence (5'-AACAGCTATGACCATG-3'). PCR reactions were performed using Hot Start Taq Plus Master Mix (Qiagen) and primers were used at a final concentration of 200 nM per primer. Purified nested PCR products were sequenced in order to identify the V and J gene rearrangement of the heavy and light chain. Afterwards, a second PCR was performed using a high-fidelity DNA polymerase (Phusion Hot Start II, NEB) and V and J gene family specific primers that incorporated Ig chain specific restriction sites. Variable domains were then directionally cloned into human mAb heavy chain (IgG1) and light chain (kappa/lambda) expression vectors (Genbank accession numbers FJ475055, FJ475056, and FJ517647). Variable domains containing internal restriction sites were amplified by a modified PCR containing 50 µM 5- methyl-dCTP (NEB) and 150 µM dCTP. This modification did not affect PCR fidelity and abrogated the truncation of variable domains after restriction digestion. Following vector construction and sequence confirmation, heavy and light chain vectors were transiently co-transfected into Expi293F cells according to manufacturer's instructions (Life Technologies). Antibodies were purified from cell culture supernatants using protein-A conjugated agarose beads (Pierce).

Sequence analyses: Sequence analysis was performed as previously described [40]. Briefly, Germline variable domain gene usage and somatic hypermutation was analyzed using the international ImMunoGeneTics (IMGT) online information system and the NCBI web-based tool IgBLAST. Somatic hypermutation levels in VH genes represent the number of nucleotide substitutions in FR1 through CDR3 relative to the closest germline sequence match in the IMGT. Plasmablast clonal expansions were determined by multiple sequence alignments of heavy and light chains with matching Ig gene rearrangements. Cells with identical junctional diversity in both the heavy and light chain were grouped as part of a single clonal expansion. Mutation rate was defined as number of mutations divided by the length of the V region multiplied by the number of cell divisions assuming a cell division rate of 1 division per 8 hours [188].

ELISA Assay: MaxiSorp plates were coated with CTB (List labs #104) at 1µg/mL diluted in 50 mM carbonate buffer overnight at 4^{o}C or LPS at 25µg/mL in PBS overnight at 4^{o}C. Inaba and Ogawa LPS was generously provided by Dr. Edward Ryan. LPS from other bacteria obtained from Millipore Sigma; *E. coli* O111:B4 (L2630), O26:B6 (L8274), O128:B12 (L2755), *K. pneumoniae* (L4268), *P. aeruginosa* (L9143), *S. enterica* (L6011). The following day plates were washed with PBS Tween 0.05% then blocked with PBS 1% BSA for 90 minutes. Plates were washed then incubated with serum diluted in PBS Tween 0.05% 1% BSA for 90 minutes. Plates were washed then incubated with peroxidase conjugated goat anti human IgM (109-036-011), IgG (109-036-098), or IgA (109-036-129) diluted in PBS Tween 0.5% 1% BSA for 90 minutes. Plates were washed with PBS Tween 0.5% 1% BSA followed by PBS. Wells were developed with OPD substrate solution: 0.4 mg/ml of O-phenylenediamine (Sigma #P8787)

dissolved into 50 mM citrate buffer (Sigma #P4560) with 30% H_2O_2. Plates were incubated with OPD substrate solution for 5 minutes. 100 ul of 1M HCl was added to stop the reaction and O.D. was recorded at 490 nm using the Bio-Rad IMark microplate reader. Positivity was assed as signaling higher than 3x the signal of a non-cholera specific antibody.

Vibriocidal Assay: Vibriocidal titers were detected essentially as previously described [40]. *V. cholerae* O1 (strain 19479 El Tor Inaba) was cultured to mid log phase for 2 ½ hours in bovine heart infusion media at 37ºC. Bacteria were pelleted at 3,000xg for 10 min and washed twice with PBS. Prior to use bacteria were normalized to an O.D. of 0.3. Guinea pig complement (Sigma S1639), bacteria, and antibodies were mixed and added to each well for a total volume of 50 ul per well in a flat bottom 96 well plate. Plates were incubated on shaker (50 RPM) at 37ºC for one hour. 150 ul of BHI media was added to each well and plates were incubated at 37ºC for approximately 3 hours without shaking until the O.D. at 595 nm of untreated control wells was between 0.20-0.28. Plates were read with Bio-Rad IMark microplate reader. Seroconversion was defined by responses 4-fold higher than day 0 samples.

Agglutination Assay: Agglutination titers were detected essentially as previously described [40]. *V. cholerae* O1 (strain 19479 El Tor Inaba) was cultured to mid log phase for 2½ hours in bovine heart infusion media at 37ºC. Bacteria were pelleted at 3,000 x g for 10 min and washed twice with PBS. Prior to use bacteria were normalized to an O.D. of 0.3. Equal amounts of antibody and bacteria were mixed and added to a V-bottom microtiter plate for a total of 50 ul per well. Each plate was sealed with an adhesive film, centrifuged for 10 seconds, then incubated for 20 hours at 4ºC. Plates were imaged using a UV imaging system (ChemiDoc, BioRad). Agglutination titers were recorded as the last dilution where bacteria were agglutinated.

Acknowledgements

We thank C. Kelley, D. Raheja, M. Mulligan and the hope clinic for technical support in organizing the recruitment, blood collection, and follow up healthcare evaluations of study volunteers. We thank all study participants who generously donated their time and blood for this study. We thank R. Karaffa and A. Rae of the Emory School of Medicine flow cytometry core and the Emory pediatric flow cytometry core for their assistance in the cell sorting experiments. *V. cholerae* LPS from serotype Inaba and Ogawa were generously provided by E. Ryan and colleagues.

Figures

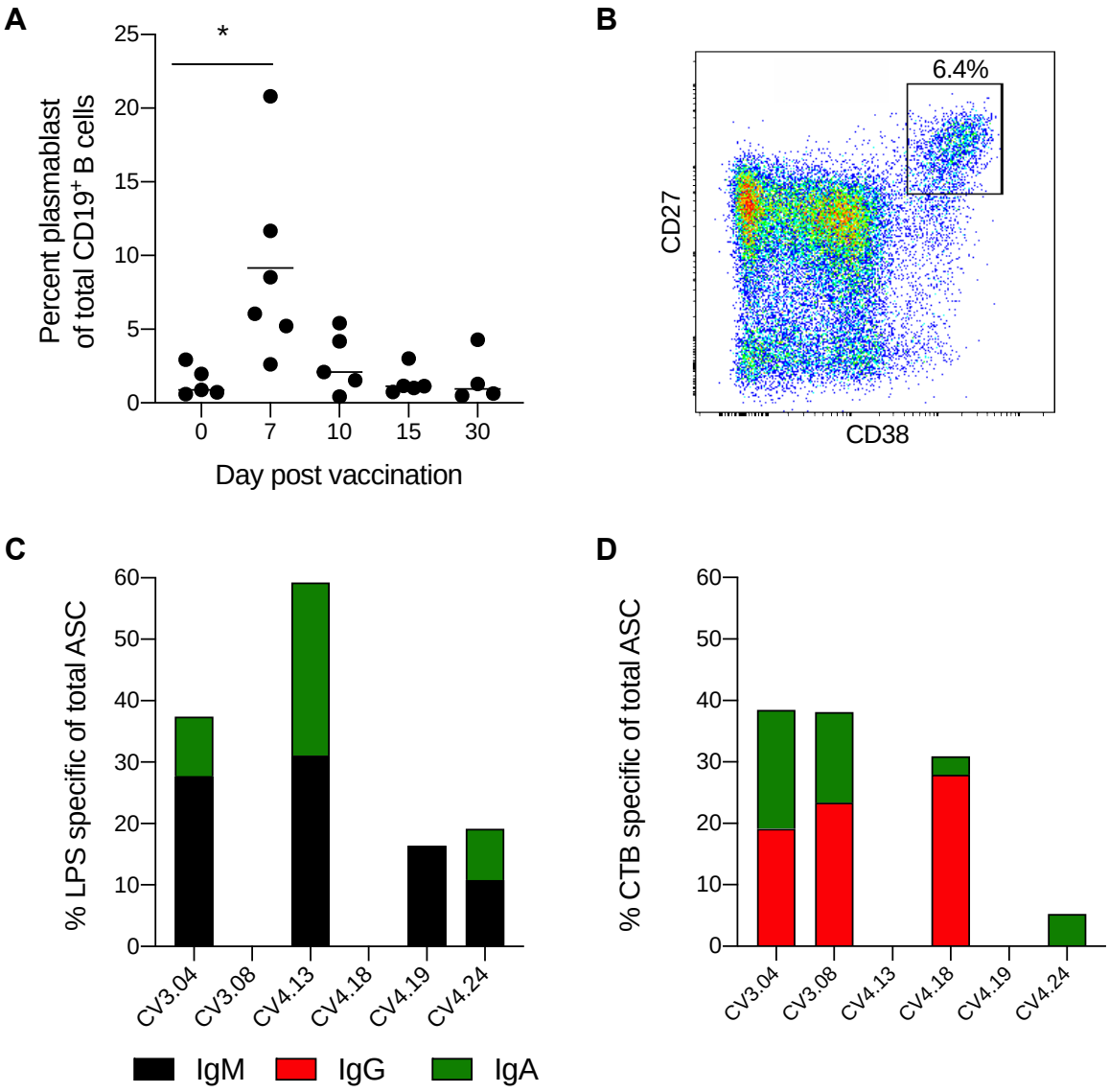
A
*
Percent plasmablast of total CD19+ B cells
25
20
15
10
5
0
0
7
10
15
30
Day post vaccination
B
6.4%
CD27
CD38
C
% LPS specific of total ASC
60
50
40
30
20
10
0
CV3.04
CV3.08
CV4.13
CV4.18
CV4.19
CV4.24
IgM
IgG
IgA
D
% CTB specific of total ASC
60
50
40
30
20
10
0
CV3.04
CV3.08
CV4.13
CV4.18
CV4.19
CV4.24

Figure 1: Vaccination with the live attenuated vaccine leads to robust increase in antigen specific plasmablasts frequencies. (A) Representative and (B) summary analysis of the proportion of the circulating plasmablasts population seen 0, 7-, 10-, 15- and 30-days post vaccination for each of the 6 donors. (C) Percent LPS specific antibody secreting cells of the total IgM (Black), IgG (Red), and IgA (Green) antibody secreting cell population measured 7 days post vaccination as determined by ELISpot assay. (D) Percent CTB specific antibody secreting cells of the total IgM (Black), IgG (Red), and IgA (Green) antibody secreting cell population measured 7 days post vaccination as determined by ELISpot assay. Statistical significance between bracketed samples was determined using a one-way ANOVA. Significance values are indicated by asterisks ($P < 0.05$ (*); $P < 0.005$ (**); $P < 0.0005$ (***); $P < 0.0001$ (****)).

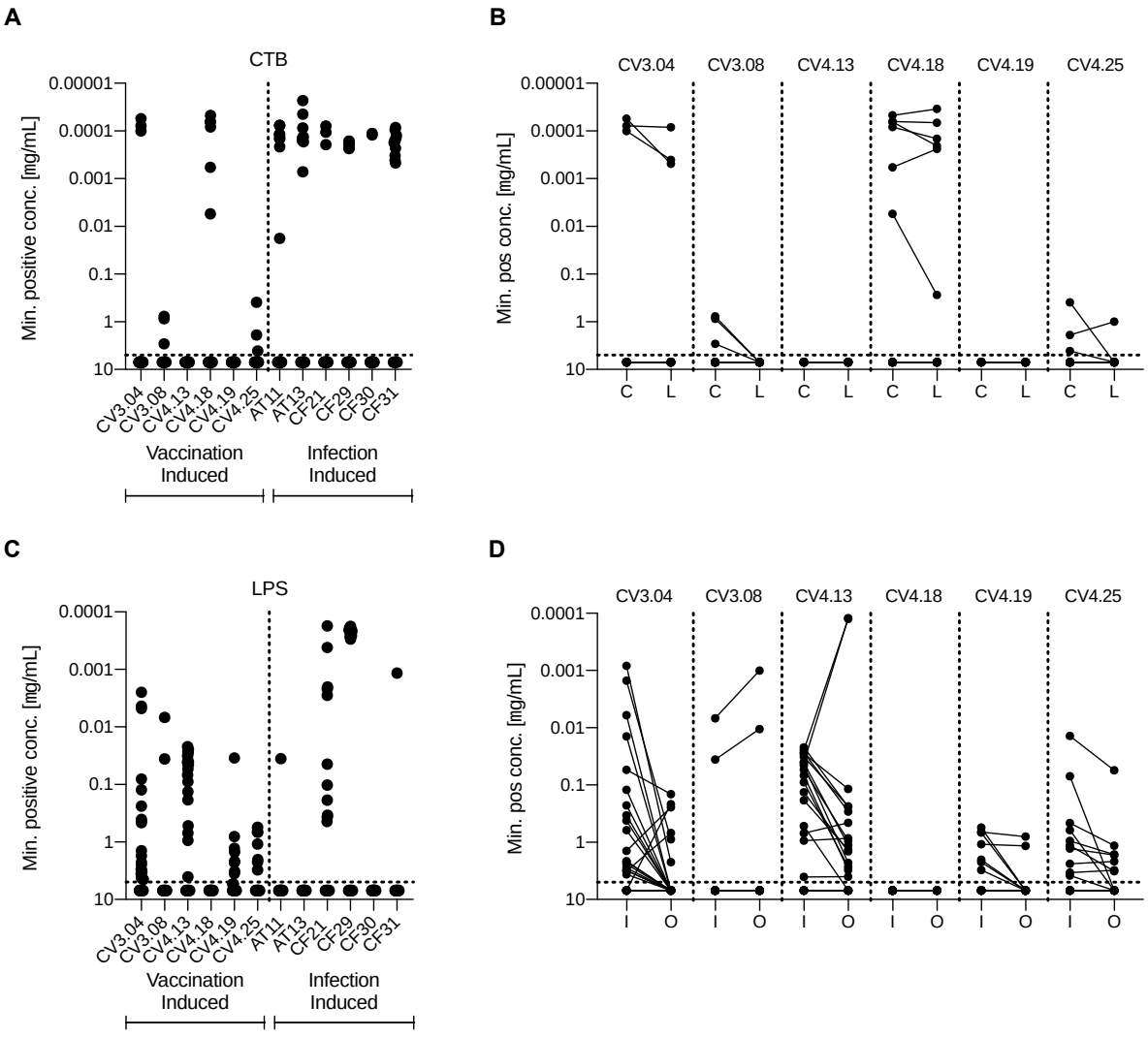
A
CTB
Min. positive conc. [mg/mL]
0.00001
0.0001
0.001
0.01
0.1
1
10
CV3.04
CV3.08
CV4.13
CV4.18
CV4.19
CV4.25
AT11
AT13
CF21
CF29
CF30
CF31
Vaccination Induced
Infection Induced
B
CV3.04
CV3.08
CV4.13
CV4.18
CV4.19
CV4.25
Min. pos conc. [mg/mL]
C
L
C
L
C
L
C
L
C
L
C
L
C
L
C
L
C
L
C
L
C
L
C
L
D
CV3.04
CV3.08
CV4.13
CV4.18
CV4.19
CV4.25
Min. pos conc. [mg/mL]
I
O
I
O
I
O
I
O
I
O
I
O
I
O
I
O
I
O
I
O
I
O
I
O
C
LPS
Min. positive conc. [mg/mL]
0.0001
0.001
0.01
0.1
1
10
CV3.04
CV3.08
CV4.13
CV4.18
CV4.19
CV4.25
AT11
AT13
CF21
CF29
CF30
CF31
Vaccination Induced
Infection Induced

Figure 2: A significant percentage of the monoclonal antibodies generated from the vaccinees show high levels of affinity, and cross reactivity. (A) Monoclonal antibody affinity of vaccine and patient derived antibodies to CTB as determined by ELISA. Dashed line on y-axis divides monoclonal antibodies generated from vaccination (left) from the antibodies generated from infection (right). Dashed line on x axis indicates lowest dilution tested. (B) Cross reactivity of CTB specific antibodies to heat liable toxin B subunit [L] for each of the six vaccinees. (C) Monoclonal antibody affinity of vaccine and patient derived antibodies to LPS as determined by ELISA. Dashed line on y-axis divides monoclonal antibodies generated from vaccination (left) from the antibodies generated from infection (right). Dashed line on x axis indicates lowest dilution tested. (D) Affinity of vaccine derived Inaba LPS specific antibodies to Ogawa LPS for each of the six vaccinees.

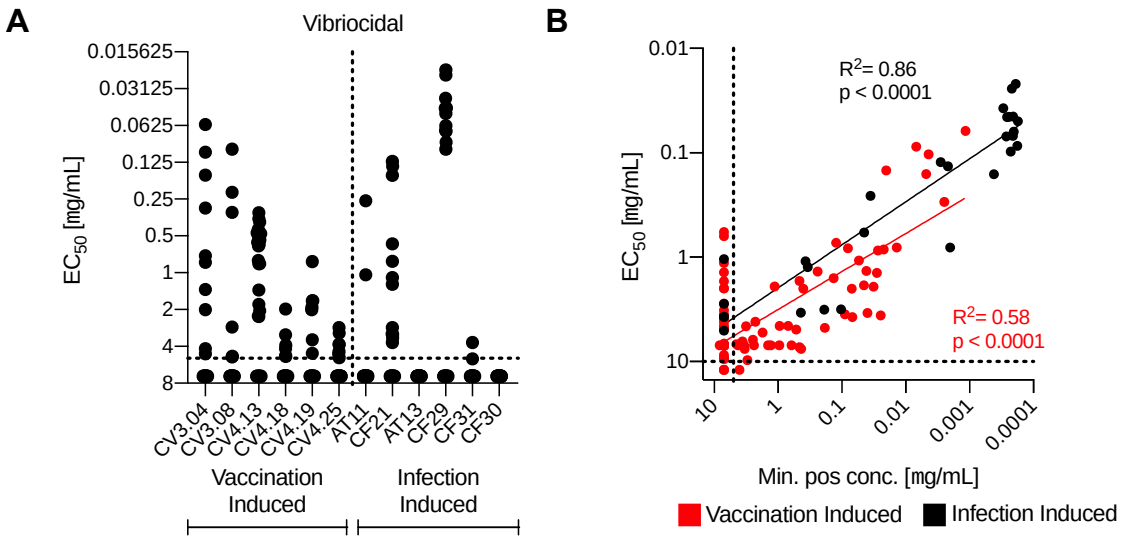

Figure 3: Affinity of LPS specific antibodies correlates with vibriocidal titers.

(A) Vibriocidal potency of monoclonal antibodies derived from the six vaccinated donors or six infected patients. Dashed line on y-axis divides monoclonal antibodies generated from vaccination (left) from the antibodies generated from infection (right). Dashed line on x axis indicates lowest dilution tested. (B) Linear regression analysis comparing the monoclonal antibodies vibriocidal titers and binding affinity to Inaba LPS. Vaccine derived antibodies are colored red, patient derived antibodies are colored black. Dashed line on axis indicates the maximum dilution tested. Statistical analysis was performed on log10 transformed values.

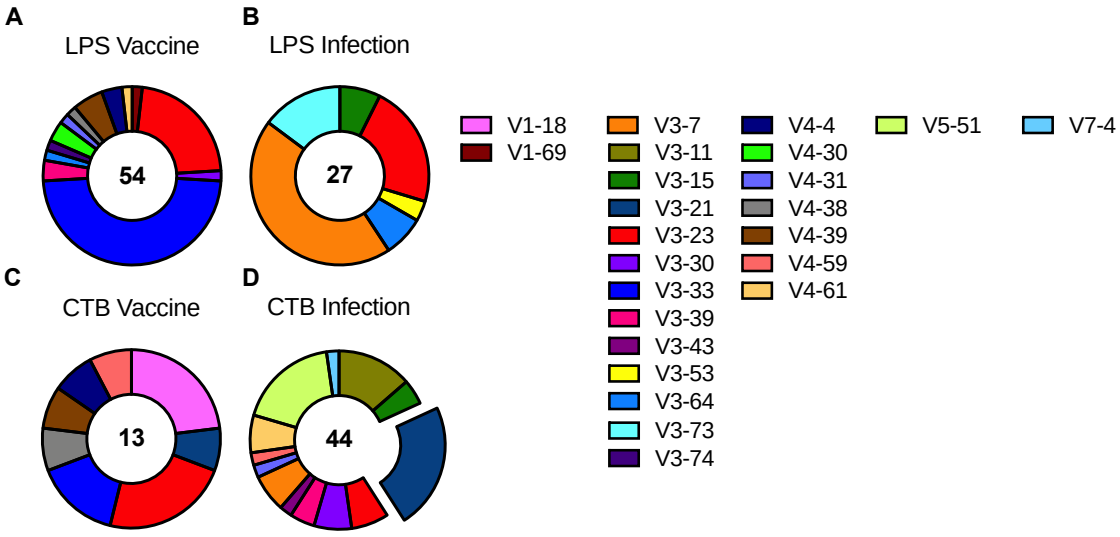

Figure 4: LPS specific response are dominated by members of the VH3 family. Summary of the IGHV gene usage of the (A) LPS specific vaccine derived and (B) LPS patient derived antibodies shown as a percentage from the six vaccinees and the six patients. Summary of IGHV gene usage of the (C) CTB specific vaccine derived and (D) CTB specific patient derived antibodies shown as a percentage from the six vaccinees and the six patients. Size in pie chart indicates the percentage of IGHV usage. Number in the pie chart indicates the total number of sequences used in the analysis. Legend in the right panel shows color scheme of V gene usage. Expanded section indicates sequence used exclusively for CTA specific antibodies.

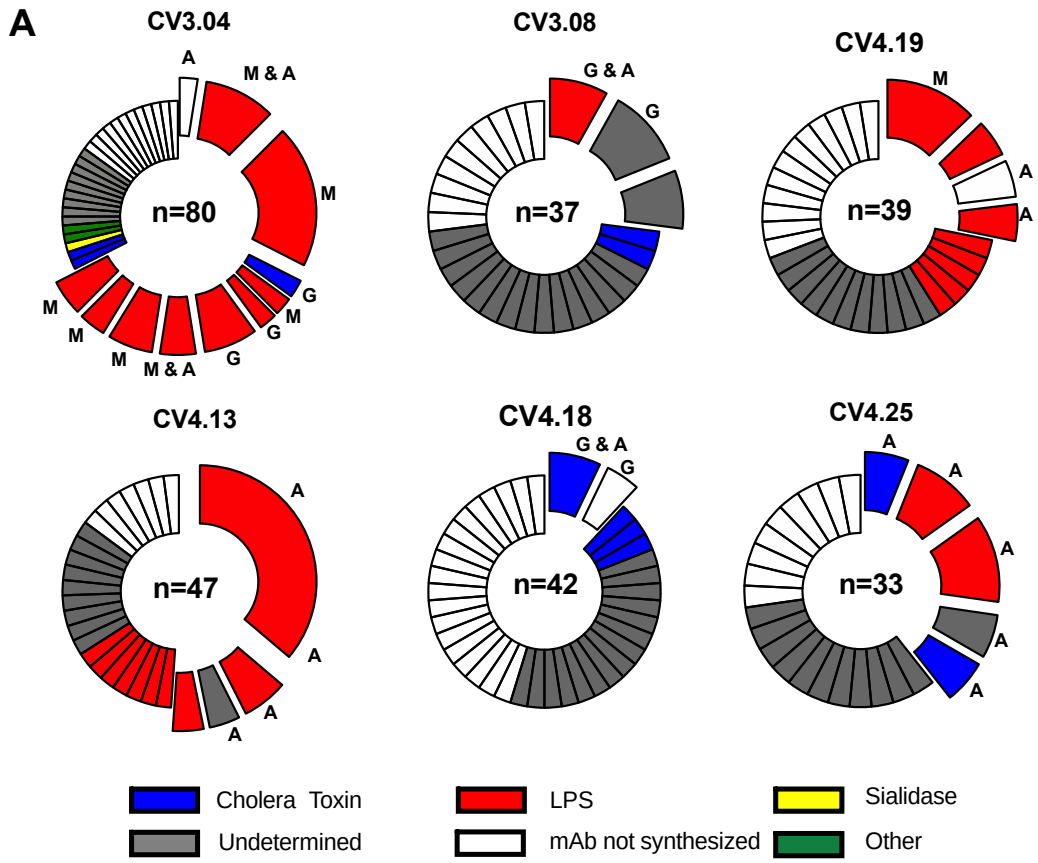
A
CV3.04
n=80
CV3.08
n=37
CV4.19
n=39
CV4.13
n=47
CV4.18
n=42
CV4.25
n=33
Cholera Toxin
LPS
Sialidase
Undetermined
mAb not synthesized
Other

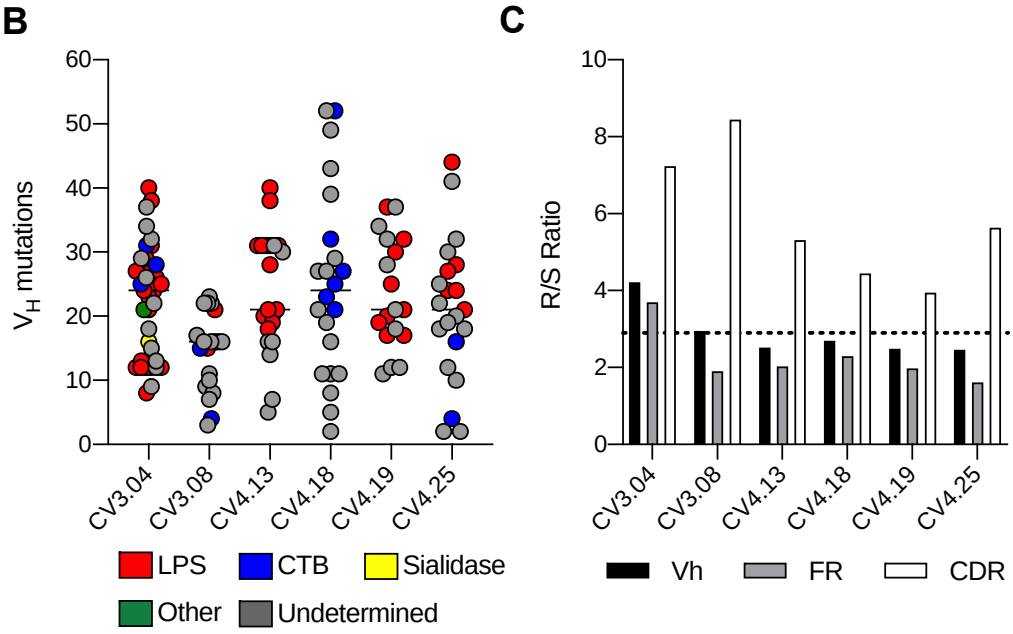
B
V_H mutations
CV3.04
CV3.08
CV4.13
CV4.18
CV4.19
CV4.25
LPS
CTB
Sialidase
Other
Undetermined
C
R/S Ratio
Vh
FR
CDR

Figure 5: Vaccination induces plasmablasts feature robust clonal expansions and a high number of mutations. (A) Clonality of sequenced Ig for each donor with expanded section of the pie chart indicating number and size of clone group. Number in center indicates the number of sequences which were analyzed. Letter next to expanded section indicates the isotype of the cells found in the clone group. Color indicates antigen specificity of the antibodies within the clone group; LPS (red), CTB (blue), sialidase (yellow), other (green), mAb not synthesized (white), and undetermined (grey). Letter next to clone group indicates the isotype of cells within the clone group (M=IgM, G=IgG, A=IgA). Clonality is defined as sequences sharing identical V, D, J, CDR3, and light chain rearrangements. (B) Number of mutations in of the V_H region as compared to the closest germline sequence from the generated monoclonal antibodies. Each individual circle represents an individual monoclonal. Antibodies are color coded based on antigen specificity; LPS (red), CTB (blue), sialidase (yellow), other (green), unknown (grey). (C) R/S ratio of all the entire Vh gene, Framework regions (FR), and complementary determining regions (CDR) of the LPS and CTB specific antibodies from each of the six vaccinated subjects. Ratio above 2.9 (dashed line) indicates antigen selection.

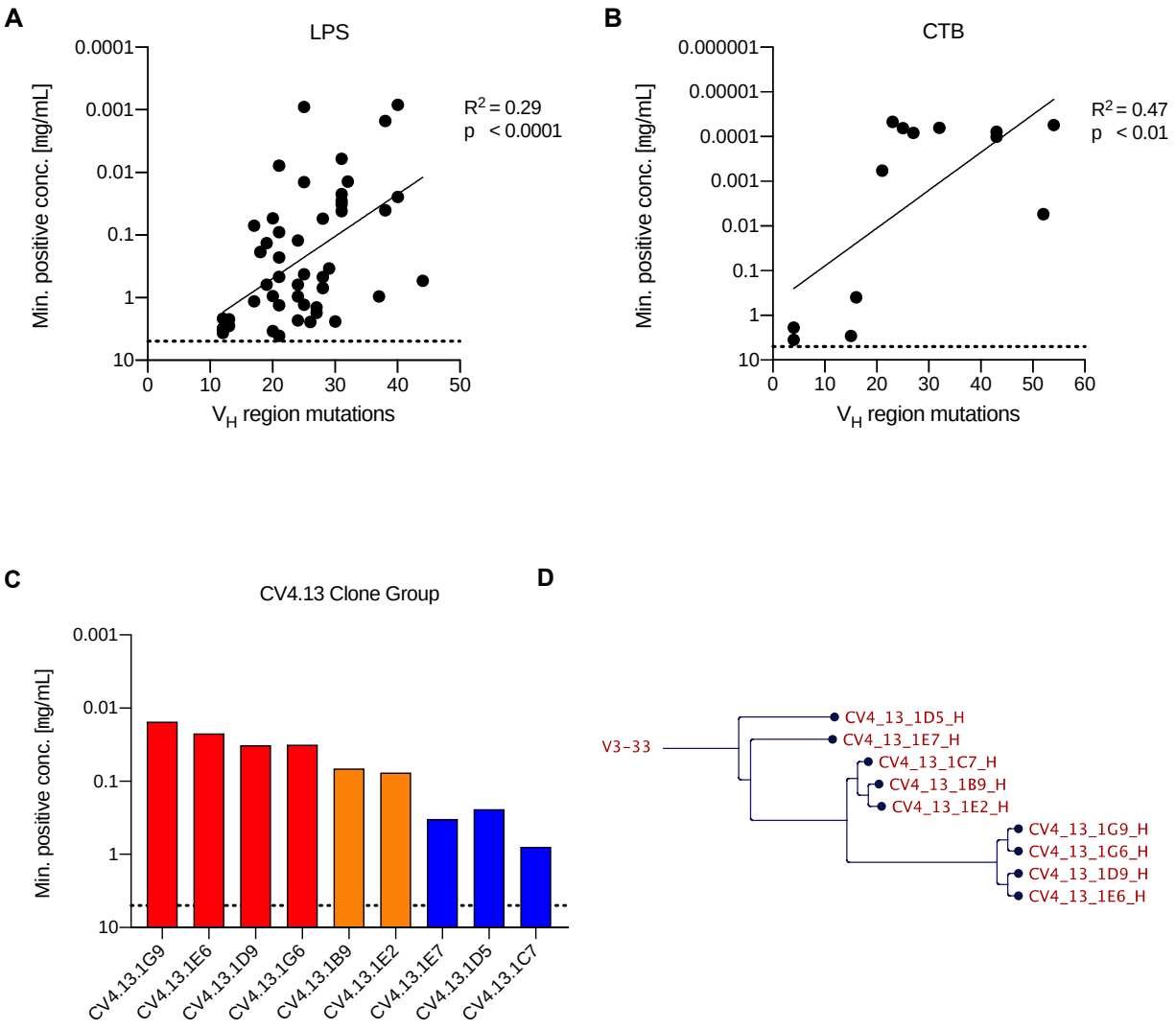
A
LPS
Min. positive conc. [mg/mL]
0.0001
0.001
0.01
0.1
1
10
0
10
20
30
40
50
V_H region mutations
R^2 = 0.29
p < 0.0001
B
CTB
Min. positive conc. [mg/mL]
0.000001
0.00001
0.0001
0.001
0.01
0.1
1
10
0
10
20
30
40
50
60
V_H region mutations
R^2 = 0.47
p < 0.01
C
CV4.13 Clone Group
Min. positive conc. [mg/mL]
0.001
0.01
0.1
1
10
CV4.13.1G9
CV4.13.1E6
CV4.13.1D9
CV4.13.1G6
CV4.13.1B9
CV4.13.1E2
CV4.13.1E7
CV4.13.1D5
CV4.13.1C7
D
V3-33
CV4_13_1D5_H
CV4_13_1E7_H
CV4_13_1C7_H
CV4_13_1B9_H
CV4_13_1E2_H
CV4_13_1G9_H
CV4_13_1G6_H
CV4_13_1D9_H
CV4_13_1E6_H

Figure 6: Evidence of ongoing affinity maturation in LPS specific vaccine induced plasmablasts. Linear regression analysis between the affinity of (A) LPS and (B) CTB specific antibodies and the number of V_H region mutations from all six of the vaccinees. V_H region mutations represent the number of mutations within the heavy chain variable region as compared to the closest germline sequence. Linear regression analysis was performed on the log10 transformed data, and the coefficient of determination (r^2) was identified. (C) Affinity to LPS as determined by ELISA from a clone group comprised of 9 LPS specific antibodies from subject CV4.13. Clonality was determined by sequence analysis of each antibody. Sequences are color coded based on affinity to LPS; high (red), medium (orange), low (blue). (D) Phylogenetic tree analysis of CV4.13 clone group, color coded as in (C). Length and direction of branches indicate sequence similarity. Relationship determined by maximum likelihood phylogeny using the CLC main workbench v21 software.

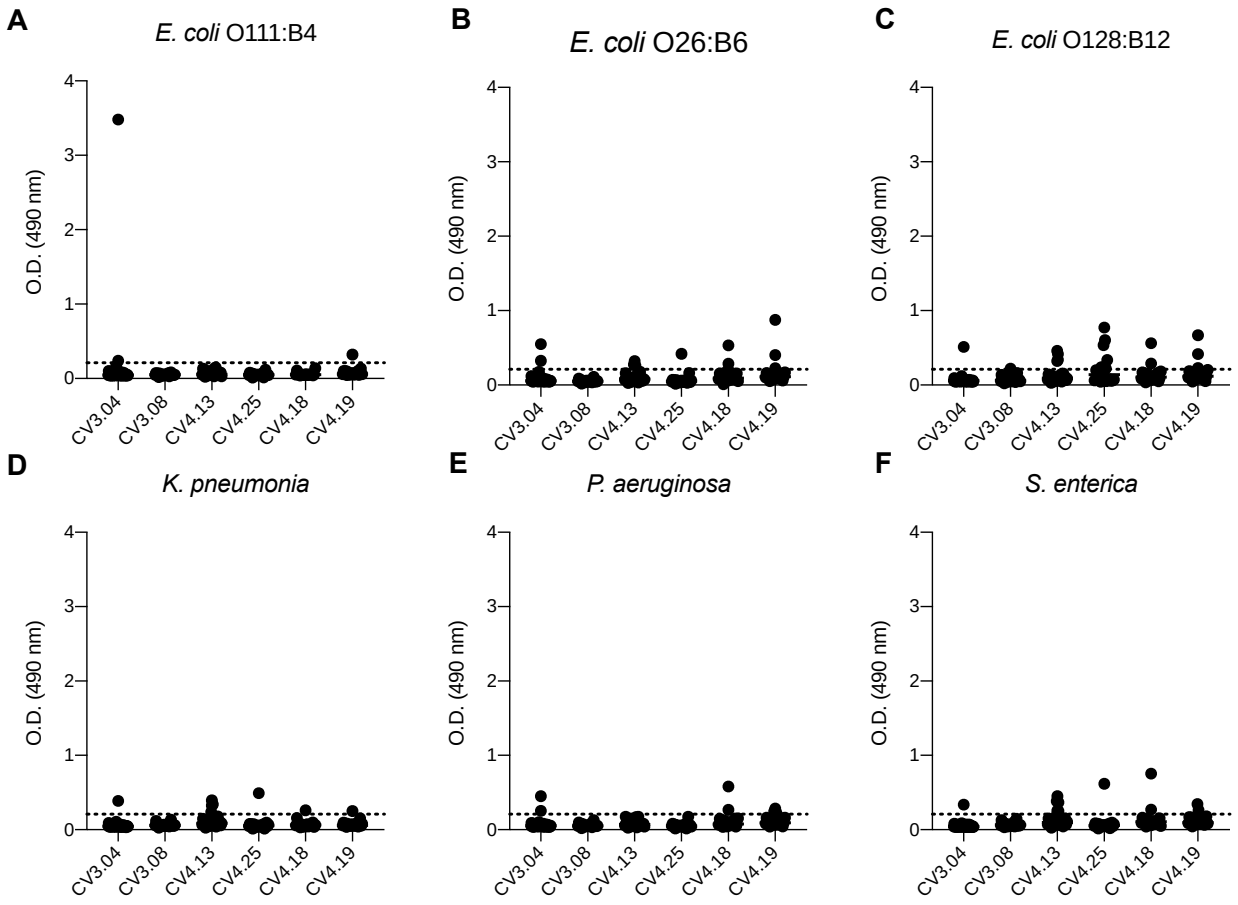

Supplemental Figure 1: Antibodies generated from vaccinees show little evidence of cross reactivity to other strains of LPS. Reactivity of monoclonals generated from each of the six vaccinees to a panel of LPS from (A) *E. coli* O111:B4, (B) *E. coli* O26:B6, (C) *E. coli* O128:B12, (D) *K. pneumoniae*, (E) *P. aeruginosa*, and (F) *S. enterica* as measured by an ELISA. Antibodies were screened at a concentration of 5 ug/mL. Dashed line indicates 3x the background of background of EMC04 (flu specific control antibody).

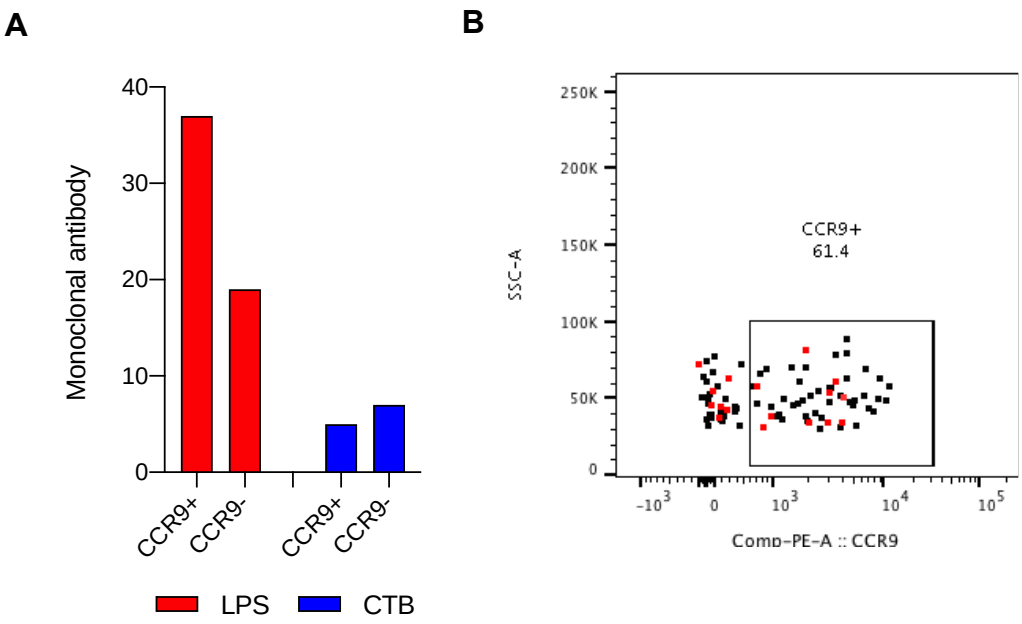

Supplemental Figure 2: Most of the antigen specific monoclonal antibodies originated from gut homing cells. (A) LPS (red) and CTB (blue) specific antibodies were divided based on the CCR9 expression of their originating cell. Specificity of the antibodies was determined by ELISA. (B) Representative example from one subject of the gating strategy used to determine the CCR9 expression of each plasmablasts. CCR9 expression for each individual cell was determined using the IndexSort plugin v 2.7 in Flowjo. Data shown includes LPS and CTB specific antibodies from all six vaccinees included in the study.

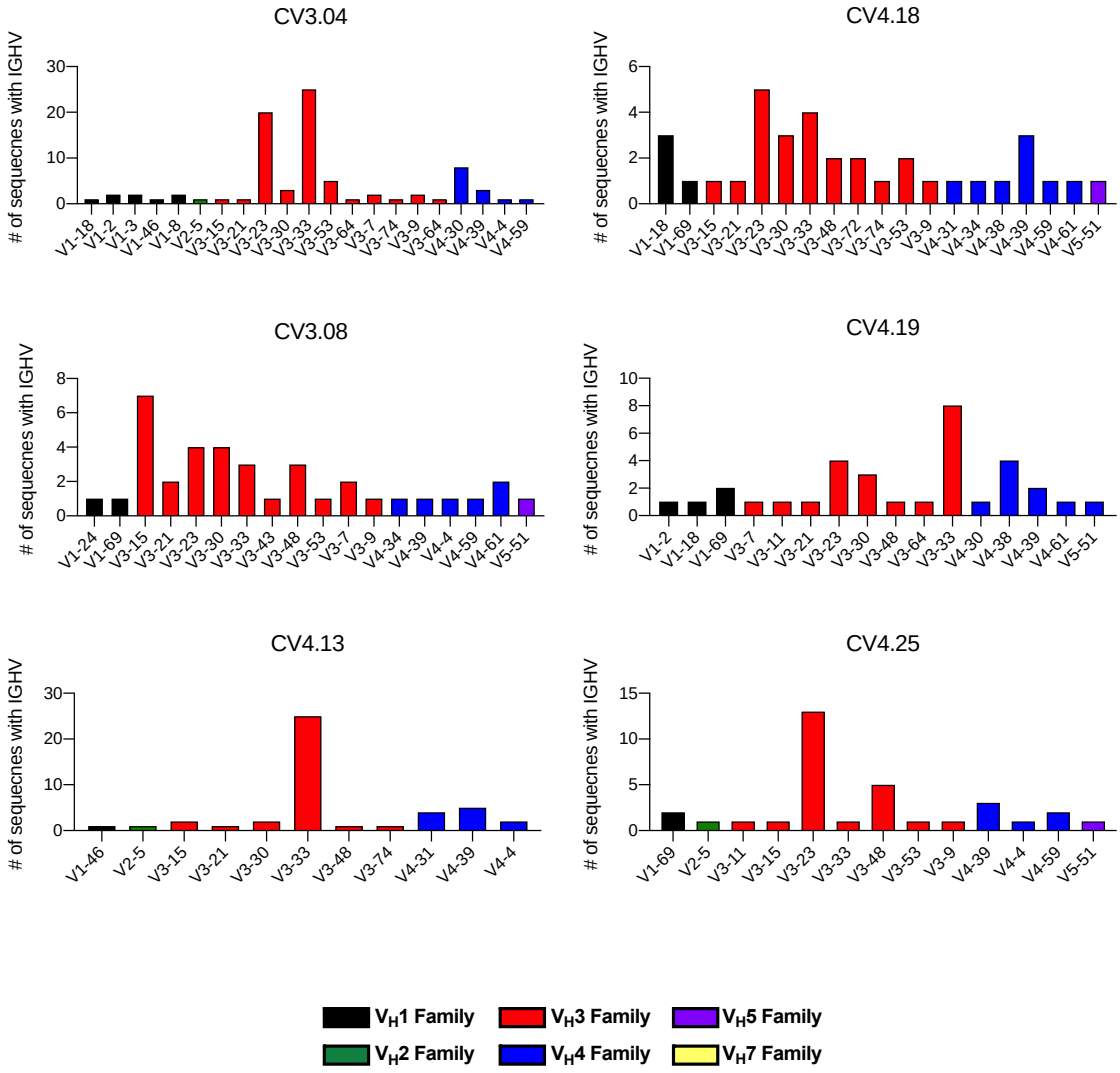

Supplemental Figure 3: V gene usage of plasmablasts induced by a live attenuated cholera vaccine. IGHV gene usage of all plasmablast that were sequenced following vaccination for each of the six vaccinees. Each graph represents a separate donor. Bars are color coded based on the VH family which was used; black (VH1), green (VH2), red (VH3), blue (VH4), purple (VH5). The specific V_H used is indicated on the x-axis and the number of sequences which used a particular V gene is labeled on the y-axis.

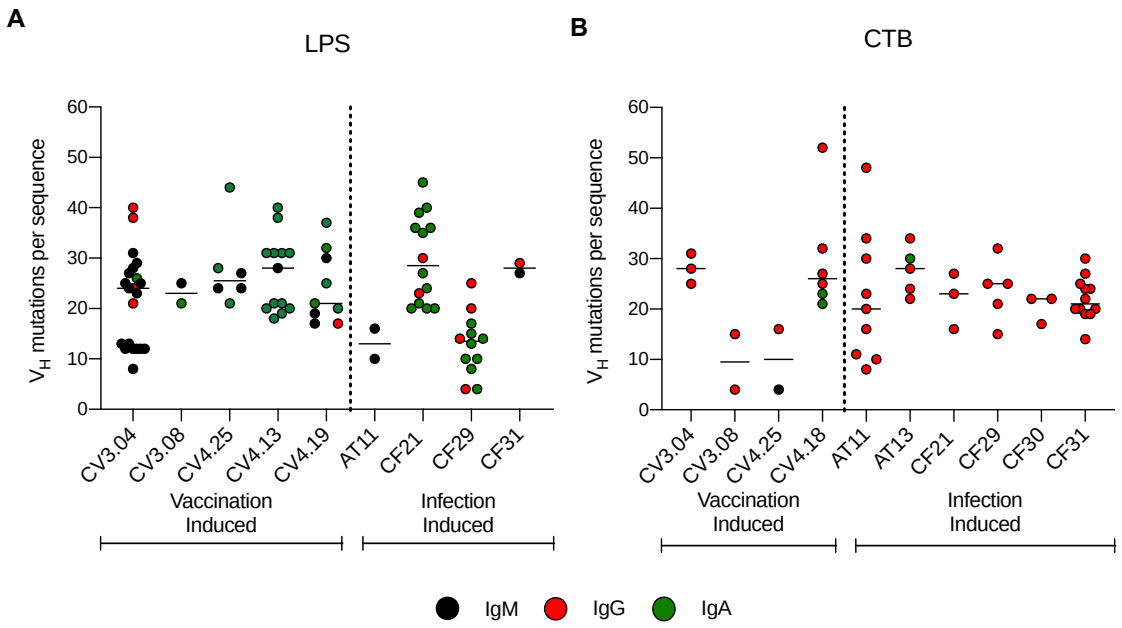

Supplemental Figure 4: Isotype of LPS and CTB specific plasmablasts for vaccinated and infected subjects. (A) LPS and (B) CTB specific vaccine and infection induced plasmablasts. Each dot represents a single plasmablast. Color indicates original isotype of the plasmablasts; IgM = black, IgG = red, IgA = green. Y axis indicates the number of total mutations within the heavy variable region as determined by closest germline sequence.

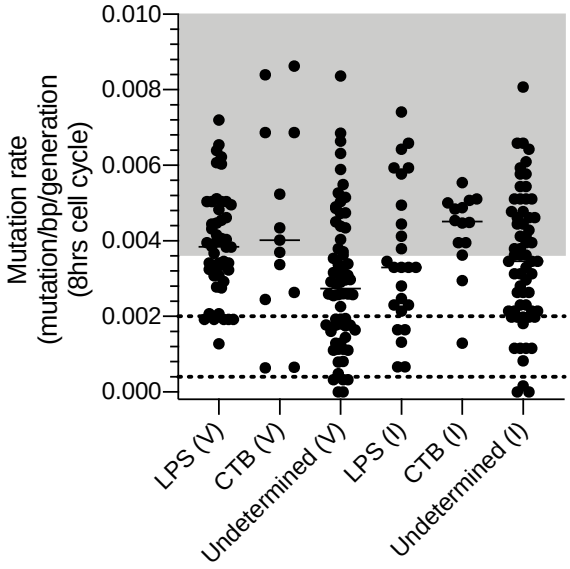

Supplemental Figure 5: Theoretical somatic hypermutation rate of cholera induced plasmablasts. Calculated hypothetical mutation rates from LPS specific, CTB specific, and non LPS/CTB (undetermined) from the cholera induced plasmablasts of the six vaccinated (V) and six infected (I) subjects. Rate was determined from the number of mutations within the Vh variable region to the length of the V segment with an assumed cell cycle duration of 8 hours. As reference, prior mutations rates are indicated. Upper dashed line indicates mutation rate of 1.1×10^{-3} mutations/bp/division. Lower dashed line indicates mutation rate of 4×10^{-4} mutations/bp/division. Shaded area indicates theoretical mutation rate significantly higher than 10^{-3}.

Donor mAbs				
Donor	LPS	CTB	Other	Total
CV3.04	21	3	13	37
CV3.08	2	2	17	21
CV4.13	17	0	10	27
CV4.25	6	2	16	24
CV4.18	0	6	15	21
CV4.19	9	0	10	19
Total	**55**	**13**	**81**	**149**

Supplemental Table 1: List of antibodies generated from vaccinated subject. List of the cholera specific (LPS, CTB) and cholera nonspecific antibodies generated from the plasmablasts of each of the six subjects.

Chapter 4: Immunoglobulin isotype and epitope potently influence the functional properties of Vibrio cholerae O-specific polysaccharide antibodies

Robert C. Kauffman[1†], Oluwaseyi Adekunle[1†], Hanyi Yu[2], Alice Cho[1], Lindsay E. Nyhoff[1], Meagan Kelly Bufano[3], Jason B. Harris[4], Firdausi Qadri[5], Stephen B. Calderwood[6], Edward T. Ryan[7,8], Jun Kong[2,8] and Jens Wrammert[1*]

[1]Division of Infectious Disease, Department of Pediatrics, Emory University, School of Medicine, Atlanta, Georgia, USA

[2]Department of Computer Science, Emory University, School of Medicine, Atlanta, Georgia, USA

[3]Division of Infectious Diseases, Massachusetts General Hospital, Boston, Massachusetts, USA

[4]Department of Pediatrics, Harvard Medical School, Boston, Massachusetts, USA

[5]Infectious Diseases Division, International Centre for Diarrhoeal Disease Research, Bangladesh (icddr,b), Dhaka, Bangladesh

[6]Department of Medicine, Harvard Medical School, Boston, Massachusetts, USA

[7]Department of Immunology and Infectious Diseases, Harvard T. H. Chan School of Public Health, Boston, Massachusetts, USA

[8]Department of Mathematics and Statistics, Georgia State University, Atlanta, Georgia

[†]Contributed equally

The work of this chapter was published in 2021 in *mBio*

Article citation: Kauffman RC, Adekunle O *et al*. Impact of Immunoglobulin Isotype and Epitope on the Functional Properties of *Vibrio cholerae* O-Specific Polysaccharide-Specific Monoclonal Antibodies. *mBio*. 2021 PMID: 33879588; PMCID: PMC8092325.

Abstract

Vibrio cholerae causes the severe diarrheal disease cholera. Clinical disease and current oral cholera vaccines generate antibody responses associated with protection. Immunity is thought to be largely mediated by lipopolysaccharide (LPS)-specific antibodies, primarily targeting the O-antigen. However, the properties and protective mechanism of functionally relevant antibodies have not been well defined. We previously reported on the early B cell response to cholera in a cohort of Bangladeshi patients, from which we characterized a panel of human monoclonal antibodies isolated from acutely induced plasmablasts. All antibodies in that previous study were expressed in an IgG1 backbone irrespective of their original isotype. To clearly determine the impact of affinity, immunoglobulin isotype and subclass on the functional properties of these monoclonal antibodies, we have re-engineered a subset of low and high-affinity antibodies in different isotype and subclass immunoglobulin backbones and characterized the impact of these changes on binding, vibriocidal, agglutination, and motility inhibition activity. While the high-affinity antibodies bound similarly to O-antigen, irrespective of isotype, the low-affinity antibodies displayed significant avidity differences. Interestingly, despite exhibiting lower binding properties, variants derived from the low-affinity mAbs had comparable agglutination and motility inhibition properties to the potently binding antibodies, suggesting that how the mAb binds to the O-antigen may be critical to function. In addition, not only pentameric IgM and dimeric IgA, but also monomeric IgA, was remarkably more potent than their IgG counterparts at inhibiting motility. Finally, analyzing highly purified F(ab) versions of these antibodies, we show that LPS crosslinking is essential for motility inhibition.

Importance

Immunity to the severe diarrheal disease cholera is largely mediated by lipopolysaccharide specific antibodies. However, the properties and protective mechanism of functionally relevant antibodies have not been well defined. Here, we have engineered low and high-affinity LPS-specific antibodies in different immunoglobulin backbones in order to assess the impact of affinity, immunoglobulin isotype and subclass on binding, vibriocidal, agglutination, and motility inhibition functional properties. Importantly, we found that affinity did not directly dictate functional potency as variants derived from the low affinity mAbs had comparable agglutination and motility inhibition properties to the potently binding antibodies. This suggests that how the antibody binds sterically may be critical to function. In addition, not only pentameric IgM and dimeric IgA, but also monomeric IgA, was remarkably more potent than their IgG counterparts at inhibiting motility. Finally, analyzing highly purified F(ab) versions of these antibodies, we show that LPS crosslinking is essential for motility inhibition.

Introduction

Protective immunity to cholera is thought to be predominantly antibody-mediated [199]. Both clinical disease and current oral cholera vaccines (OCVs) generate responses in the serum and gastrointestinal tract that are associated with protection [115, 200]. Clinical disease is thought to result in long-term, durable immunity that lasts 3 to 10 years [96, 201] and provides nearly 100% protection. In contrast, OCVs have an average two-dose efficacy of only 58% after 60 months [202]. Protection is thought to be primarily mediated by lipopolysaccharide (LPS)-specific antibodies [124]. Of the approximately 200 serogroups in circulation, pathogenic *V. cholerae* isolates are comprised of just two different serogroups, O1 and O139, which differ based upon their LPS structure [203]. Importantly, protection is strictly serogroup specific, underscoring the importance of LPS-specific antibodies in conferring protective immunity [114, 120]. The O1 serogroup is currently responsible for most of the 2.9 million cholera related infections and more than 100,000 deaths that occur each year [97]. This serogroup is further subdivided into the Ogawa and Inaba serotypes. Although their LPS structures are nearly identical, they differ by the presence of a single methyl group on the terminal sugar moiety of the 12-16 subunit long O-antigen that extends from core-oligosaccharide [187].

In mice, immunization with soluble *V. cholerae* O1 derived LPS has been shown to generate antibody responses that recognize the O-antigen, the core-sugar, and the lipid-A components of the LPS molecule [204]. In contrast, *V. cholerae* infected humans generate LPS-specific antibody responses that almost exclusively target the O-antigen [40, 124]. A significant body of evidence demonstrates that these O-antigen-specific antibody responses are strongly associated with immunity following infection [115, 205]. Through a process termed immune exclusion, *V. cholerae* LPS-specific antibodies are thought to inhibit successful colonization of

the small intestine, thus preventing the production and release of cholera toxin, the protein exotoxin responsible for the severe diarrheal symptoms associated with cholera [206, 207]. The exact mechanisms that allow antibody-mediated inhibition of bacterial colonization have not been fully elucidated, but likely occur through a multifactorial series of mechanisms including bacterial agglutination [208], enchaining dividing cells [209], and inhibiting bacterial motility [210, 211].

Serum vibriocidal antibodies are associated with protective immunity and are a critical component in vaccine evaluation [212]. Early serum depletion studies have suggested that vibriocidal titers are primarily derived from LPS O-antigen-specific IgM and to a lesser extent IgG1 and IgG3 antibodies [124, 213]. Despite this, complement mediated protection is unlikely to be a critical component of mucosal immunity to a non-invasive bacterial pathogen given the low amount of complement in the intestinal tract [169, 214]. Moreover, vibriocidal titers decline to baseline levels before protective immunity wanes [167]. Thus, vibriocidal antibody titers are likely an indirect marker of protection, which presumably occurs at the site of infection in the small intestine. In contrast to vibriocidal IgG and IgM serum antibodies, LPS-specific IgA in the intestinal mucosa likely plays a critical role in long-term disease protection [127]. IgA is the predominant immunoglobulin isotype in the intestine, where it persists in a J-chain stabilized, dimeric form [81]. IgA is also actively transported from the lamina propia, through the epithelial cell layer into the lumen, where it interacts with the mucus layer (reviewed in [215]). Importantly, cholera infection and vaccination have been shown to induce significant increases in LPS-specific duodenal IgA [127, 216]. Moreover, infection induces a significant number of LPS-specific IgA secreting lamina propria plasma cells. These responses peak 30 days after infection and can persist through at least day 180 [127]. However, mucosal LPS-specific IgA

titers wane before protection is lost [127], suggesting that not only mucosal plasma cells but perhaps also memory B cells are a key component of long-term cholera immunity. The importance of memory B cells (MBCs) is supported by studies showing that circulating LPS-specifc MBCs are associated with a decreased risk of infection in household contacts of cholera patients [132], and that LPS-specific MBCs remain elevated for at least one-year post infection, which is longer than traditional measures of antibody-mediated immunity by ELISA and vibriocidal titers [122]. Together, these findings suggest that a combination of pre-existing LPS-specific antibody secreting plasma cells and rapid anamnestic responses derived from MBCs are critical to protection in the gut mucosa.

To better understand how cholera induces immunity, we recently reported the use of single-cell monoclonal antibody (mAb) expression cloning to generate and characterize the properties of infection-induced plasmablast responses in patients from Dhaka, Bangladesh, a cholera endemic area [40]. Plasmablasts emerging shortly after human infection or vaccination are enriched for antigen-specific antibody-secreting cells [186]. Therefore, they represent a valuable source of antibodies that reflect the properties and natural history of both pre-existing and novel responses. Repertoire analysis of cholera-induced plasmablasts demonstrated that clonally expanded populations were often enriched for LPS-specific cells [40]. In addition, many of the antibodies were highly mutated and bound more potently to the O1-Inaba serotype that had not been in circulation for the last five years suggesting that these cells derived from recall responses to a previously encountered polysaccharide antigen. These monoclonals also demonstrated a wide range of binding potency toward the LPS molecule [40]. The antibodies in the aforementioned study bound with equal affinity to purified LPS and OSP-core conjugated to BSA, indicating that they do not target the lipid A component of LPS [40]. In addition, their

binding, vibriocidal, and agglutination properties were determined for both the Ogawa and Inaba O1 serotypes. It is possible that the binding site of some mAbs may overlap with the core-domain; however, the four mAbs analyzed in this study demonstrated serotype selectivity these assays. Given that the serotypes are distinguished by the structure of the O-antigen we hypothesize that they are primarily specific for the O-specific polysaccharide moiety of LPS. Finally, our analysis of Ig isotype demonstrated that the majority of LPS-specific antibodies were primarily derived from IgM and IgA secreting plasmablasts [40]; however, to facilitate their examination, the initial characterizations of these antibodies were executed in a human IgG1 background regardless of the original isotype [40].

Despite the importance of LPS-specific antibodies in mediating protective immunity, the impact of Ig isotype and subclass on the functional qualities of these antibodies has not been rigorously characterized. Moreover, the exact mechanisms by which LPS-specific antibodies confer protection remain to be fully elucidated. Given the difference in Ig distribution in blood and mucosal tissue, we sought in this study to assess the impact of Ig isotype and subclass on the functional properties of O-antigen-specific antibodies in the context of an identical antigen binding site over a range of different binding potencies. To that end, we determined that modifications to the immunoglobulin isotype and subclass, which presumably increase antibody avidity, markedly enhanced the agglutination and motility inhibition functional properties of the antibodies. This demonstrates a critical role of O-antigen crosslinking in mediating these processes, a finding that was further supported by analyses of F(ab) fragments generated from this panel. Intriguingly, we also observed that mAbs with lower binding strength generally had comparable or modestly superior motility inhibition properties to the high-binding mAbs, suggesting that the unique steric interaction between an antibody and the O-antigen can strongly

influence functional potency. Therefore, the findings presented herein inform future rational vaccine and therapeutic mAb development approaches, by providing insight into the impact of Ig isotype, subclass, and epitope on the functional potency of LPS O-antigen-specific antibodies.

Results

Generation of a panel of immunoglobulin isotype and subclass variants of LPS O-antigen binding monoclonal antibodies with a range of binding potencies.

To define the impact of isotype and subclass on the functional qualities of LPS O-antigen-specific antibodies, over a range of binding potencies, we selected a subset of antibodies identified in a previous study of Bangladeshi cholera patients [40]. This study included 138 monoclonal antibodies generated from single-cell expression cloning of infection-induced plasmablasts. Of these, 24 mAbs were LPS-specific, and presumably recognized the O-specific polysaccharide (OSP) moiety of LPS. For the initial analysis of these cells, mAbs were expressed in an IgG1 backbone as previously described [186, 198]. To further understand the impact of isotype and subclass on the binding and functional qualities of these LPS-specific antibodies, we selected two mAbs that bound the O-antigen with apparent high-affinity and two that bound with low-affinity. **Figure 1A** shows the binding qualities by ELISA of these four antibodies expressed as human IgG1, demonstrating a 100 to 1000-fold range in binding activity against *V. cholerae* O1-Ogawa-O-antigen, which had been conjugated to bovine serum albumin (BSA).

The heavy chain binding sites (VDJ fragment) from these four mAbs were sub-cloned into a panel of vectors with different constant regions, and then expressed as monomeric human IgG1, IgG2, IgG3, IgG4, IgA1 (mIgA1), dimeric IgA1 (dIgA1), and pentameric IgM. For simplicity, the mAbs are named in this report based on their binding potency, with the original

nomenclature, and plasmablast antibody isotype shown in **Figure 1B**. As summarized in the flow chart in **Figure 1C**, after variable domain sub-cloning, monomeric mAbs were produced by transient transfection of heavy and light chains. For expression of dIgA and pentameric IgM, transfections were performed using a third J-chain expression vector. IgA transfections containing the J chain generated a mixed population of monomeric and dimeric mAbs, which were separated by size exclusion chromatography after initial affinity column purification **(Figure 1D; left)**. IgM was purified by size exclusion chromatography (**Figure 1D, right**), yielding preparations with approximately 90% purity. **Figure 1E** shows a representative gel where mAb variants have the same size light chain (bottom band) but differently sized heavy chains (top band). Using this type of analysis, the protein content of these preparations was normalized based on densitometry analysis of the light chain band following reducing SDS-PAGE. Throughout the course of functional studies, mAbs were evaluated by non-reducing SDS-PAGE to confirm structural integrity. A representative non-reducing gel showing mAbs of the expected size is shown in **Figure 1F.**

Isotype variants of high-binding mAbs have comparable binding properties but different functional characteristics

We focused our initial efforts on the two high-affinity antibodies because changing the isotype and valency of the mAb did not markedly impact their antigen binding properties. As shown in **Figure 2** changing the constant domain did not affect the binding properties of the mAb High-1. However, increasing the avidity of mAb High-2 by expression as dimeric IgA1 or pentameric IgM did appear to modestly enhance binding potency. As changing the constant domain had minimal affect on binding, we could directly evaluate the effect of immunoglobulin

isotype and subclass on the functional properties of these mAbs. To evaluate function, we tested this panel of antibodies in vibriocidal, agglutination, and motility inhibition assays. Representative experimental data from these functional assays are shown in S**upplemental Figure 1**.

Vibriocidal titers have been strongly correlated with protective immunity. Our analyses of the two high-binding mAbs demonstrated that the IgM variant was the most potent isotype. In fact, relative to IgG1, IgM derived from mAbs High-1 and mAb High-2 was 20 and 150 times more potent, respectively. Among the IgG subclass variants, IgG1 and IgG3 had the most vibriocidal activity. This is in agreement with their ability to activate the classical complement pathway [77]. While IgG4 does not activate the classical complement pathway [77], we found that this variant had modest vibriocidal activity. This may reflect high epitope density enhancement of the alternative pathway [217]. For these vibriocidal analyses, data were background subtracted from experiments performed in parallel with heat-inactivated complement. This is important since, for each mAb, we observed apparent low-level complement-independent inhibition of bacterial outgrowth in the vibriocidal assay possibly due to antibody mediated agglutination or enchaining of dividing cells. This effect was strongest for dimeric IgA1 and IgM antibodies. A representative example of data collected from mAb High-1 is shown in **Supplementary Figure S2** illustrating the magnitude of vibriocidal EC_{50} values derived from assays using either fresh or heat-inactivated complement**.**

Next we investigated the effect of isotype and subclass on bacterial agglutination. After ingesting *V. cholerae*, agglutination may enhance immune exclusion, and through enchaining, inhibit bacterial growth. As seen in **Figure 2**, changing the IgG subclass had minimal effect on the agglutination properties. In contrast, dimeric IgA1 and IgM, resulted in a 10 to 30-fold

increase in agglutination potency. Surprisingly, despite having comparable binding properties, monomeric IgA also displayed dramatically enhanced agglutination activity with potencies more than 10 times greater than observed for the monomeric IgG1 variant for each mAb **(Figure 2)**.

Inhibition of bacterial motility is thought to be a major mechanism of antibody mediated protection [192, 211]. Thus, as shown in **Figure 2,** we used a soft-agar migration assay to quantify the effect of our antibody variant panel on motility**.** We found that changing the IgG subclass of mAb High-1 had a minimal effect on motility inhibition, which is similar to our findings with agglutination. In contrast, IgM and dimeric IgA1 variants were 5-10-fold more potent than IgG1. Surprisingly, monomeric IgA1 was eightfold more potent than IgG1; however, this difference was less pronounced for mAb High-2 whose baseline IgG1 motility inhibition titer was higher than mAb High-1. Taken together, these data demonstrate that while the immunologlobulin isotype and subclass has a minimal impact on the binding strength of these two mAbs, their functional potency can be dramatically impacted by changes in their respective antibody constant region and antigen binding site valency.

Binding potency and avidity do not directly dictate effectiveness

Following our initial binding and functional analyses of the high-affinity antibody isoforms, we next examined a comparable panel generated from two antibodies that displayed poor O-antigen binding strength when expressed as IgG1. Binding analyses demonstrated a profound effect of immunoglobulin isotype, subclass, and valency on the binding strength of these two antibodies, which is in stark contrast to what we observed for the two high-binding antibodies **(Figure 3A)**. Despite having an identical antigen binding domain, antibodies expressed as IgG3 had a 10 to 100-fold increase in binding potency relative to the IgG1 variant.

The monomeric and dimeric IgA versions of these mAbs also displayed enhanced binding strength, at levels comparable to IgG3; the dimeric version of each IgA1 mAb exhibited approximately four-fold higher potency than its monomeric IgA1 counterpart, presumably due its higher avidity **(Figure 3A)**. IgM variants had the highest binding potency displaying a striking 1,000 to 10,000-fold increase in the minimal effective binding concentration relative to IgG1. Interestingly, both low and high affinity antibodies had equally strong binding potencies when expressed as IgM despite their dramatically different binding potencies when expressed as IgG1.

The vibriocidal activity of an antibody is highly dependent on both its capacity to bind antigen and the ability of its constant domain to activate specific complement proteins. Consequently, for the two low-binding strength antibodies, assessing the direct contribution of the constant domain to vibriocidal activity is confounded by the fact that changing the isotype and subclass also markedly affected the binding properties **(Figure 3A).** Given that context, while the vibriocidal capacity of the IgG1 variants was lower than that of the high-binding antibodies, the IgM and IgG3 variants were similar **(Figure 3B).** Lastly, we found IgM to be the most potent isoform displaying up to 10,000 times higher vibriocidal activity than IgG1 **(Supplemental Figure S3)**, further underscoring the importance of this isotype to the overall vibriocidal titer.

Despite the significant differences in binding potency, the agglutination activity of both low-binding mAb Ig variants **(Figure 3C, black symbols)** was surprisingly similar to that of the two high-binding mAbs **(Figure 3C, red symbols).** For example, the IgG3 variant of mAb Low-1 has a binding titer that is 1000-fold lower than mAb High-1 (IgG3) and 300-fold lower than mAb High-2 (IgG3). Nevertheless, we observed that, relative to mAb High-1, it was more effective at agglutinating bacteria. Analyses of mIgA1 were more similar, with the high-binding

mAbs displaying 2 to 4-fold enhanced agglutinating potential; however, even this modest enhancement is of note given the differences in IgA binding strength. In addition, our analysis of low-binding mAb variants demonstrated that dimeric IgA1 variants were seven to ten times more effective at agglutinating bacteria relative to monomeric IgA1 **(Figure 3C)**. Together, these data demonstrate a critical role of avidity in enhancing agglutination activity, and, more importantly, suggest that how the antibody interacts sterically with the O-antigen may also be important to function.

As previously noted, motility inhibition is a critical property of *V. cholerae* neutralizing antibodies. Using a soft-agar motility assay, our analysis of antibody mediated motility inhibition indicated that dimeric IgA1 variants of the low-binding mAbs were seven to ten times more potent than monomeric IgA1 **(Figure 3D)**. This demonstrates an important role for avidity driven enhanced crosslinking in mediating this function. Moreover, pentameric IgM and dIgA1 had comparable potencies, indicating that further enhancement of antibody mediated antigen crosslinking does not markedly enhance motility inhibition **(Figure 3D)**. In addition to these findings, we observed that isoforms derived from the two low-affinity mAbs had inhibitory potencies that were generally equivalent, and in some cases, modestly exceeded (2 to 4-fold) the immunoglobulin variants derived from both high-affinity antibodies **(Figure 3D)**. This is particularly notable in the context of the disparate binding potencies for all isoforms except for IgM **(Figure 3A)**, which incidentally, was modestly more effective in the context of variants derived from the two low-binding strength mAbs **(Figure 3D)**. The non-correlative pattern (r^2 = 0.03) of binding and motility inhibition between the high and low-affinity mAbs is highlighted in **Supplemental Figure S4,** which depicts a linear regression analyses of the binding and motility inhibition titers described in **Figure 3A and 3D**. These findings are similar in many respects to

the agglutination analyses. Thus, this surprising result further underscores the hypothesis that the epitope and steric properties of the antigen-antibody interaction are critical to function.

IgA2 variants have comparable functional potency to IgA1 antibodies.

IgA1 is the dominant IgA subclass in the small intestine where antibody mediated immunity to cholera is likely to occur. Therefore, our study initially focused on the generation and characterization of antibodies in an IgA1 backbone. Nevertheless, IgA2 is inherently more resistant to IgA proteases in the gut that readily degrade IgA1 antibodies [215]. Given the unique differences in tissue distribution and subclass specific biochemical properties, we expanded our analyses to evaluate the binding, agglutination, and motility inhibitory properties of these mAbs expressed in a human IgA2 backbone (**Supplemental Figure S5**). We observed that IgA2 antibodies had comparable O-antigen binding properties, though there was a suggestion that some may exhibit a two to threefold lower binding potency relative to IgA1 **(Supplemental Figure S5A).** Agglutination analyses suggested that antibodies expressed as dimeric IgA2 were modestly more potent (2 to 4-fold) than IgA1. However, this difference was not observed when expressed as IgA2 monomers (**Supplemental Figure S5B).** Lastly, IgA1 and IgA2 variants were not different in regard to bacterial motility inhibition potency (**Supplemental Figure S5C).** Because we observed no difference in the functional capacity of IgA1 and IgA2, the enhanced resistance to proteolytic degradation seen in IgA2 antibodies may be a consideration in the development of strategies that aim to induce IgA subclass specific immune responses or deliver monoclonal antibody therapies or prophylactics.

O-antigen-specific mAbs inhibit motility in a binary fashion, without affecting the speed of non-neutralized vibrios.

Soft-agar motility inhibition assays do not discern the relative effect of bacterial agglutination from direct antibody-mediated inhibition of flagellar motion. They are also unable to determine if motility inhibition is a binary process whereby some bacteria are rendered immotile while others are unaffected, or if it is a continuous process, in which antibodies are able to reduce the speed of individual vibrios. To investigate these questions, we used confocal microscopy to observe the effect of antibody treatment on the motility of a GFP expressing *V. cholerae* O1-Ogawa strain (RT4273). Initial observations with mAb High-1 confirmed previous soft-agar migration analyses **(Figure 2)** demonstrating that the IgG1 variant of this antibody is relatively ineffective. This was indicated by the presence of extended fluorescent tracks made by motile bacteria even in the presence of 20 nM antibody (~3 μg/mL) **(Figure 4A; left).** In contrast, changing the isotype to monomeric IgA1 resulted in a significant gain of function, in which complete arrest was observed five minutes post treatment at the same concentration **(Figure 4A; center).** An equivalent phenotype was observed for the dimeric IgA1 variant of this antibody **(Figure 4A; right).** Incidents of micro-agglutination consisting of 3-5 cells were observed in all samples, though this was more pronounced for the IgA treated samples. Observing the arrest of an individual bacterium is challenging due to their speed and movement in and out of the plane of viewing. However, shortly after adding the antibody, we observed incidents of motility arrest in which the bacterium was isolated at the time motility ceased (data not shown). This is similar to observations made by other investigators [146, 147] indicating that antibody induced motility arrest can occur at the level of the individual bacterium in the absence of agglutination.

Next, we assessed if motility inhibition was primarily a binary process or a continuous one. This was accomplished using a novel image enhancement, segmentation, and tracking algorithm, which quantified the number of moving bacteria and determined their average speed using a series of time-lapse two-dimensional (2D) fluorescent images. An example of the tracking system image output is shown in **Figure 4B.** In this panel, individual tracked objects are colored and their positions at 100 millisecond intervals are connected by a line. Using this analysis, we found that the mean speed of motile bacteria in negative mAb isotype control samples was 62 μm/s **(Figure 4C, red bars; right y-axis)**. This is similar to the previously reported *V. cholerae* mean speed measured at 60 μm/s [218], thereby validating this approach. To assess the effect of antibody treatment on bacterial speed, we combined a mid-log phase culture with a titrated amount of antibody to achieve a 20-80% reduction in the number of motile bacteria **(Figure 4C, black bars; left y-axis)** relative to treatment with a negative isotype control mAb. This was necessary as adding too much mAb rapidly halted all bacterial motion, whereas adding too little resulted in no effect. Each experiment counted at least 25 motile bacteria in antibody treated samples (Mean=137, Range=26-437, SD=103) and 100 motile bacteria in control samples (Mean= 290, Range 103-741, SD =200). This analysis indicated that the mAb concentration necessary to render a portion of the sample immotile approximated the minimal effective concentration in soft-agar motility inhibition assays (**Figure 3)**. Importantly, using this quantitative live-cell tracking approach, we observed that the mean speed of the remaining motile bacteria was not significantly different from that of paired negative controls ($p>0.1$; one-way ANOVA). This suggests that antibodies primarily inhibit *V. cholerae* motility in a binary manner.

Evaluation of F(ab) fragments demonstrates that antigen crosslinking is important to binding potency and essential to motility inhibition.

Lastly, we generated highly purified F(ab) fragments to investigate if O-antigen crosslinking is essential to antibody mediated motility inhibition. In addition, we used monovalent F(ab)s to assess the impact of avidity on binding potency given our observations that modifying the isotype, subclass, and valency could affect binding (**Figure 3)**. F(ab)s were prepared from the IgG1 variant of each mAb by conventional papain digestion and purification (**Figure 5A)**. In addition to F(ab) fragments, this procedure generated a rare 100 kDa product, which was resistant to sequential protein A purification treatments and evident using high contrast imaging in coomasie stained gels **(Figure 5A)**. Size-exclusion chromatography (SEC) was used to resolve the two products and obtain highly pure F(ab) reagents **(Figure 5B).** We were then able to conduct binding and motility inhibition studies using these highly pure reagents.

ELISA based assays used to assess the contribution of engaging both IgG arms demonstrated that F(ab)s from mAbs High-2, Low-1, and Low-2, had a greater than 100-fold reduction in binding potency relative to the parent IgG1 mAb (**Figure 5C, solid black line**). These data demonstrate that multivalent binding is critical to the overall binding characteristics of these three antibodies. This is in stark contrast to mAb High-1 where F(ab)s had equivalent binding potency to the parent IgG1 **(Figure 5C)**. Next, after completing the previously described binding studies demonstrating that F(ab)s retain antigen binding, though at reduced levels relative to IgG1, we evaluated if the highly pure F(ab) preparations would inhibit motility in the absence of crosslinking. This was performed using the soft-agar motility inhibition assay in which the semi-solid agar was infused with F(ab)s at a high concentration (500 nM). Motility

inhibition was assessed relative to 500 nM of a negative IgG1 isotype control and the bivalent IgG1 version of each antibody at 100 nM **(Figure 5D)**. Importantly, for all four antibodies, F(ab)s did not significantly ($p > 0.5$) inhibit bacterial motility as evidenced by the equivalent diameter of the bacterial growth ring in F(ab) treated and isotype control wells **(Figure 5D).** This result is consistent with a critical role of O-antigen crosslinking in motility inhibition and suggests that epitope specificity determines if an IgG molecule can engage both arms simultaneously when binding to LPS.

Discussion

While we anticipated that multimeric IgA and IgM would have enhanced binding properties due to their higher avidity, we were surprised by the extent to which antibody isotype and subclass affected binding and function. With regard to binding, we found that the low-binding mAbs, but not the high-binding mAbs, were exceedingly sensitive to changes in isotype and subclass. Increased binding potency of the IgG subclasses was generally associated with larger mean F(ab)-F(ab) binding angles [219]. Of the four IgG subclasses, maximal binding of both low-binding mAbs was observed when they were expressed in an IgG3 background. In addition to having the largest mean F(ab)-F(ab) binding angle, IgG3 also has the greatest hinge-fold flexibility [219]. Together, this likely facilitates antigen binding by both F(ab) arms. This is supported by our observation that monovalent F(ab) fragments derived from low-binding mAbs had a greater than 100 fold reduction in binding potency relative to bivalent IgG1, indicating that avidity is indeed critical to their binding strength.

Another important finding from this study is the observation that changing the isotype and subclass could enhance the functional properties of all four mAbs. Moreover, we made the

intriguing observation that variants derived from both low-binding mAbs generally had equivalent or moderately enhanced functional potency relative to variants derived from the two high-binding antibodies. This finding could have implications for rational vaccine design, as it suggests that the functional relevance of *V. cholerae* O-antigen specific antibodies may be dependent on the epitope and steric interaction between the antibody and the bacterium and not only the binding potency. Thus, when evaluating the immunological response to disease and vaccination, agglutination and motility inhibition assays should be considered in addition to binding driven measurements such as ELISA. The ability of the vibriocidal assay to reflect both binding and antibody functionality, including agglutinating and anti-motility activity, should be further explored. This study did not utilize x-ray crystallography to definitively determine the binding configuration of the complex formed between the antibody and the O-antigen; however, we previously reported that the low-binding mAbs possessed a higher degree of O1 serotype selectivity than the high-binding mAbs [40]. Since the O-antigen structure of the Ogawa and Inaba serotypes differs solely by the structure of the terminal sugar moiety, it is intriguing to speculate that the low-binding mAbs primarily interact with the terminal sugar moiety and that the steric nature of this interaction is critical to their binding and remarkably strong functional properties. The structure of an O-antigen-antibody complex has been solved for at least one Ogawa selective, mouse derived, monoclonal antibody termed S-20-4 [220]. The crystal structure revealed that the antigen binding site formed a pocket that accommodated the terminal sugar. This positioned the antibody at the surface of the LPS layer orthogonal to the bacterial outer membrane. If similar interactions occur with the low-binding mAbs described here, then their enhanced activity may be due to the fact that their perpendicular position on the surface of outer membrane facilitates the crosslinking of LPS terminal sugar residues. In conjunction with

our F(ab) fragment analyses demonstrating that antigen crosslinking is essential to motility inhibition, this would further help to explain why antibodies with greater F(ab)-F(ab) binding angles and avidity have enhanced binding and motility inhibiting properties.

A panel of antibodies with similar properties was described by Roche *et al*. in which the binding and agglutination characteristics of *Francisella tularensis* LPS O-antigen-specific mAbs were described [221]. Importantly, mAbs that bound to internal, O-antigen side chain epitopes had very high affinities but poorly agglutinated bacteria. In contrast, antibody FB11, which bound to the terminal sugar moiety, had a much lower binding affinity, yet strongly agglutinated bacteria. Their study also demonstrated that internal epitope binding antibodies were markedly less dependent on avidity [221]. Another study by the same group identified additional mAbs similar to FB11. The x-ray crystal structure of one of these mAbs (N62) showed that the F(ab) formed a pocket accommodating the terminal sugar similar to that of *V. cholerae* O-antigen-specific mAb S-20-4. Consequently, the antibody was well positioned to crosslink proximal antigens [222]. We were unable to segregate our panel of antibodies into distinct terminal sugar and internal sugar O-antigen epitopes by competition ELISA (data not shown). Nevertheless, we observed that while mAbs High-1 and High-2 had similar binding affinities, mAb High-2 was indeed more potent in agglutination and motility inhibition assays. Thus, it is conceivable that the two high-binding mAbs interact differently with the O-antigen, which ultimately influences their ability to crosslink LPS molecules. While we did not experimentally demonstrate that mAb High-1 does not easily crosslink LPS, our F(ab) binding analyses showed that it retains high binding activity even without crosslinking. In contrast, mAb High-2 derives much of its high-binding strength from crosslinking. Ongoing biochemical and structural analyses aim to elucidate

specifically how these mAbs interact with the O-antigen and reveal the mechanisms by which these antibodies function.

IgM is more effective than IgG in its ability to activate the classical complement pathway. Without knowing the relative contribution of each isotype to the overall vibriocidal titer, a relatively low titer dominated by IgG antibodies may reflect a more mature, isotype switched, response. Such a response could reflect a higher degree of protection than a response with a higher IgM dominant vibriocidal titer and may be better reflected in mucosal IgA responses not assessed by the vibriocidal assay. Our data support this possibility given the finding that monoclonal IgM was the most vibriocidal immunoglobulin isoform demonstrating a potency that was at least 20-200-fold more potent than IgG for the two high-binding mAbs while having similar binding strength. Given our findings demonstrating the exceptional potency of the IgM isotype, coupling vibriocidal analyses to measures of total and specific serum IgG and IgM vibriocidal antibodies may be useful in dissecting the maturation of the immune response and its correlation to protection.

Antibody-mediated motility arrest at the level of the individual *V. cholerae* bacterium has been shown to occur independently of agglutination by multiple investigators using LPS-specific antibodies [146, 147, 211]. This effect seems to be a key feature of LPS-specific antibodies. Other antigen targets, such as flagellin and OmpU, have not been demonstrated to effectively inhibit cholera motility or provide protection *in vivo* [223]. Multiple models have been proposed to describe how these antibodies inhibit motility. For example, it has been suggested that antibody binding to the O-antigen may induce a stress response and subsequent signal cascade that arrests motility [146, 224]. Motility could also be inhibited by cross-linking the flagella to the bacterial body; however, overcoming the force of the rotating flagella may be an obstacle to

this model [146]. Alternatively, while the flagella might not ultimately be crosslinked to the bacterium, these shear forces could cause significant damage to the flagella, flagellar sheath, or outer membrane. In addition to these models, it has been proposed that crosslinking LPS on the sheathed flagella could deform its structure and inhibit its function [147]. Finally, analyses of O-antigen specific antibodies that bound the enteric pathogen *Cronobacter turicensis,* indicated that mAbs could generate micropores in the outer membrane resulting in the neutralization of the membrane potential necessary for flagellar rotation *[225]*. While our study does not conclusively ascertain the mechanisms by which our panel of antibodies affect motility, we made several observations that are instructive.

Our live-cell tracking analyses indicated that, at partially neutralizing conditions, the speed of the remaining motile vibrios was not significantly affected. This signifies that motility inhibition is not a continuous process but rather a binary one whereby once a critical threshold of antibody binding is met, the bacteria are rapidly rendered immotile. Candidate models for a binary mechanism include crosslinking of the flagella to the main body, loss of the flagella, a stress response, and the neutralization of the sodium motive force following a disruption in outer membrane integrity by flagellar binding shear forces. In support of a stress response model induced by direct binding, previous studies have indicated that motility can be inhibited by non-crosslinking F(ab) fragments generated from LPS specific mAbs ZAC-3 and 2D6 [146, 226]. However, these findings were not supported in a subsequent study utilizing LPS-binding F(ab)s derived from polyclonal serum isolated from mice immunized with *V. cholerae* outer membrane vesicles (OMVs) [147] or convalescent cholera patients [211].

Importantly, F(ab)s purified by size-exclusion chromatography in this study did not significantly affect motility at a concentration of 500 nM (25 µg/mL), which is comparable to the

15 µg/mL F(ab) concentration previously reported [146, 226]. In contrast, motility was inhibited in assays using non-SEC purified F(ab)s from mAb High-2 **(Supplemental Figure 6)**. The high molecular weight protein component of the F(ab) preparation comprised approximately 3% of the total protein, had binding properties similar to bivalent IgG1, and may primarily have a structure similar to a bivalent F(ab)'2 **(Supplemental Figure 7)**. Therefore, assays performed at 500 nM of total protein would contain approximately 7.5 nM of this species, which is above the minimum effective motility inhibition concentration of High-2 IgG1. Taken together, this raises questions in regard to previous observations of F(ab) induced motility inhibition and its support of a stress response model of motility inhibition. In contrast, our findings demonstrate that O-antigen crosslinking is essential to a binary mechanism of motility inhibition.

In conclusion, understanding the impact of isotype and subclass on the functional properties of human-derived O-antigen specific antibodies will significantly improve our understanding of what types of adaptive immune responses are the most beneficial. This will ultimately inform the development of more effective vaccines and therapies. To that end, findings from this study support the importance of antibodies directed against the O-antigen component of LPS. Our observation that variants derived from the low-affinity antibodies generally had equivalent or enhanced functional activity relative to variants derived from the high-affinity antibodies, also suggests that how an antibody binds the O-antigen may strongly influence functional potency. Given the serotype selective properties of the low-affinity antibodies, it is intriguing to speculate that antibodies targeting the terminal sugar moiety may have superior functional activity. Future studies utilizing high-resolution imaging, component labeling techniques, and structural analyses will help elucidate the mechanisms that mediate their enhanced agglutination and motility inhibition properties. In addition to our surprising findings

regarding the low-affinity antibodies, we found that monomeric IgA was exceedingly potent in regard to bacterial agglutination and motility inhibition for all four antibodies relative to IgG1. Studies have reported that glycans in the IgA hinge region may augment non-specific binding and agglutination and can induce a T-shaped conformation [227]. In the current context, this would enhance the binding of widely spaced antigens and facilitate interactions between the flagella and the main body [228, 229]. Thus, in addition to the steric nature of the O-antigen-F(ab) interaction, the inherent properties of IgA may also make a significant contribution to functional potency. Given the enhanced functional properties of IgA variants and the fact that IgA is readily transported into the intestinal lumen, our data suggest that future vaccine designs should promote the generation and maintenance of intestinal B cells that secrete IgA as well as IgM that interacts with the O-antigen in a manner similar to the low-binding mAbs described herein.

Materials and Methods

Subcloning variable domains into isotype and subclass expression vectors

The heavy chain variable domain was amplified by PCR using 1 ng of a previously generated IgG1 expression vector [40] and subcloned into the heavy chain expression vectors IgG2, IgG3, IgG4 (gift of Hedda Wadermann, Max Plank Institute), IgA1, IgA2 [230] (gift of Hugo Mouquet, Institut Pasteur, and IgM [231] (gift of Lynn Dustin, University of Oxford). Amplification of the variable domain was performed using a high fidelity DNA polymerase Phusion (NEB) in HF Buffer according to the manufacturer's recommendations. The forward primer "AgeI-Ig Forward" (5'-CCTTTTTCTAGTAGCAACTGCAACCGGTGTAC-3') and reverse primer "XhoI/SalI-Ig Reverse" (5'-CTTGGTCGACGCgctcGAGACGGTGACC-3') were used at a final concentration of 500 nM. Underlined sequences denote restriction sites AgeI,

SalI, and XhoI respectively. To allow for sequences to be cloned into the IgM expression vector, the terminal four nucleotides of the J chain "CTCA" were mutated by primer induced mutagenesis to "GAGC" generating an XhoI restriction site without modifying the antibody amino acid sequence. The mutagenesis site is denoted by lowercase letters in the reverse primer. Reaction conditions were 98ºC for 1 min, 25 cycles (72ºC for 30 sec, 98ºC for 10 seconds), final extension 72ºC for 5 minutes.

Following PCR, amplicons were purified using QIAquick PCR purification columns. For subcloning into IgG and IgA expression vectors, 10 ng of each amplicon was digested with AgeI-HF, SalI-HF, and DpnI in CutSmart Buffer (NEB). To generate IgM vectors, amplicons were digested with XhoI instead of SalI-HF. Restriction digests were performed in a volume of 10 µL at 37ºC for 30 minutes, followed by heat inactivation at 70ºC for 20 minutes. Digested amplicons were ligated to heavy chain vectors that had been appropriately cut and dephosphorylated. Ligations were performed overnight at 16ºC with 10 ng vector, 2 units T4-DNA ligase (NEB), 1 mM ATP (NEB) and 1X CutSmart buffer in a 15 µL final reaction volume.

Ligations were chemically transformed into XL-10 gold ultracompetent *E. coli* (Agilent) according to the manufacturer's recommendations. Transformants were selected on LB-ampicillin (100 µg/mL) agar plates. Individual colonies were grown overnight in LB-ampicillin broth and plasmids were isolated using a QIAprep Spin Miniprep Kit. Inserts were sequenced using the SP6 sequencing primer to confirm the identity of the cloned variable domain and the isotype and subclass of the vector.

Monoclonal antibody expression and purification

All mAbs were expressed by transient transfection using suspension expi293F cells (Thermo Fisher) cultured in expi293 expression media according to the manufacturer's recommendations. Monomeric IgG and IgA transfections were performed using a 1:2 molar ratio of heavy and light chain expression vectors. For expression of dimeric IgA and pentameric IgM, transfections were performed using a 1:1:1 molar ratio of the heavy chain, light chain, and a third J-chain expression vector (gift of Hugo Mouquet). Supernatants were harvested 5-6 days after transfection. Supernatants were clarified by centrifugation at 3,000 x g for 5 minutes followed by syringe filtration using 0.45 µm PES filters. IgG antibodies were purified by affinity chromatography using Protein-G sepharose beads (Thermo Fisher). IgA antibodies were purified by affinity chromatography using IgA mAb select beads (Thermo Fisher). Monomeric IgG and IgA were purified by incubating supernatants and purification beads overnight at 4ºC in a slowly rotating inversion mixer. Beads were sequentially washed in 2 mL protein centrifuge columns (Pierce) with 4 mL DPBS, 4 mL 1 M NaCl, and 4 mL DPBS. Antibodies were eluted with 4 mL 0.1 M glycine pH 2.7 (IgG) or pH 3.0 (IgA) into 30 kDa protein centrifugation concentrators containing 260 µL (IgG) or 300 µL (IgA) 1 M Tris-Cl pH 9.0. Two buffer exchanges were performed with DPBS and antibodies were suspended at a concentration between 0.5 and 2 mg/mL.

IgA transfections containing the J chain generated a mixed population of monomeric and dimeric antibodies with each species comprising between 40-60% of the total antibody population. Following initial binding chromatography purification of IgA, dimeric IgA was separated from monomeric IgA by gel filtration. Gel filtration was performed using a HiLoad 16/600 Superdex 200 pg column (GE Healthcare) on an AKTA purifier 10 running Unicorn Software version 5.1 according to the manufacturer's recommendations. Samples were eluted in

PBS at a flow rate of 1 mL/minute. Fractions with a retention volume between 50 and 55 mL, corresponding to dimeric IgA, were pooled and concentrated using a 30 kDa protein centrifugation concentrator to a concentration of 1-2 mg/mL.

Pentameric IgM was purified from supernatants by first concentrating the sample using a 100 kDa centrifugal filter. IgM was further purified by size exclusion chromatography using a HiLoad 16/600 Superdex 200 pg column. Approximately 4 mL of IgM containing supernatant was injected onto the column and eluted in PBS at a flow rate of 1 mL/minute. The first 5 mL fraction eluted after the column void volume (~40 mL) was collected. This fraction corresponds to proteins >600 kDa, and predominately contained pentameric IgM. The IgM containing fraction was concentrated using a 30 kDa protein centrifugation concentrator to a protein concentration of 1-3 mg/mL. For all antibodies, sodium azide was added as a preservative at a final concentration of 0.05%.

Antibody concentration was determined by measuring the absorbance value at OD 280 nm using a Thermo Scientific NanoDrop 2000 spectrophotometer. Previously reported extinction coefficients for each isotype were used to determine protein concentrations [77]. Finally, we used the average molecular weight of each isotype and subclass to calculate the molarity of each antibody stock solution [232, 233].

Antibodies were evaluated for purity and integrity by SDS-PAGE analysis. Reducing SDS-PAGE analysis was performed by combining 3 µg of antibody diluted in PBS with an equal volume of 2X Laemmli Sample Buffer (BioRad) containing 5% 2-mercaptoethanol. Samples were heated at 95ºC for 10 minutes and resolved on a 10% Mini-PROTEAN TGX gel (BioRad) in Tris/Glycine/SDS running buffer. Non-reducing SDS PAGE analysis of IgG antibodies was performed as described for reducing SDS-PAGE analysis with the exception that 2-

mercaptoethanol was omitted from the loading dye and samples were heated at 70ºC for 10 minutes. For monomeric and dimeric IgA antibodies, samples were mixed with NuPAGE 4X LDS Sample Buffer and resolved on a NuPAGE 4-12% Bis-Tris Gel (Invitrogen) with MOPS-SDS running buffer. IgM samples were combined with NuPAGE 4X LDS Sample Buffer and resolved on a Native PAGE 3-12% Bis-Tris gel (Invitrogen) with Tris-Acetate SDS running buffer. Gels were stained in Coomassie blue staining solution (50% methanol, 10% acetic acid, 0.1% w/v coomassie blue R-250) by microwaving the gel in the 50 mL staining solution for 1-2 minutes. Gels were destained by 2-3 rounds of boiling in 1 L deionized water for 10-15 minutes per cycle. Imaging was performed using the BioRad Gel Doc™ XR+ System. Densitometry analysis was performed with Image Lab version 6.0 (BioRad). SDS-PAGE and size exclusion chromatography were used to confirm that multivalent structure of dimeric IgA and IgM antibodies were stable during the course of experimental analyses and that monomeric IgA mAbs did not spontaneously form dimeric isoforms.

Enzyme-linked immunosorbent assays

V. cholerae O1-Ogawa O-specific polysaccharide-core (OSP) was purified and conjugated to bovine serum albumin (BSA) as previously described [234, 235] from LPS extracted from *V. cholerae* strain X25049 by hot phenol/water extraction followed by enzymatic treatment [234]. OSP was coated at ambient temperature overnight on Nunc MaxiSorp plates at a concentration of 1 µg/mL in Dulbecco's phosphate buffered saline (DPBS). Plates were blocked for two hours at 37°C in PBS-1% BSA. mAbs were serially diluted 1:4 in antibody dilution buffer (ADB: PBS-1% BSA-0.05% Tween-20) starting at a concentration of 20 nM. 100 µL of each dilution was added to blocked plates and incubated for 2 hours at 37ºC. In assays measuring relative binding differences between isotypes, 100 µL of HRP-conjugated goat F(ab')2 goat anti-

human lambda or kappa secondary antibody (Southern Biotech) diluted 1:1000 in ADB was added. Assays measuring binding differences only between IgG1 antibodies used HRP-conjugated F(ab')2 goat anti-human IgG Fcγ antibody (Jackson ImmunoResearch) diluted 1:5000 in ADB. Intermediate washes consisted of PBS-0.05% Tween (3X) and PBS (1X). Development was performed using 0.4 mg/ml o-phenylenediamine (OPD) in 0.05 M phosphate-citrate buffer pH 5.0, supplemented with 0.012% hydrogen peroxide before use. Reactions were stopped with 1 M hydrochloric acid and absorbance was measured at 490 nm.

Generation of F(ab)s

F(ab) fragments were generated from IgG1 mAbs by papain digestion using the Pierce F(ab) Preparation Kit (Thermo Fisher) according to manufacturer's instructions. Following protein A purification, F(ab)s were further purified by size exclusion chromatography using a HiLoad 16/600 Superdex 200 pg column at 1 mL/min in PBS. Fractions with a retention volume of 70-75 mLs and 80-90 mLs, corresponding to the high and low molecular weight F(ab) species respectively, were pooled and concentrated with a 10 kDa centrifugal filter (Amicon, EMD Millipore). To assess F(ab) purity and composition, 200 ng of samples were prepared in reducing (2.5% beta-mercaptoethanol) and non-reducing sample loading buffer and heated for 10 min at 95ºC. Samples were then resolved by. SDS-PAGE using Any kD Mini-PROTEAN TGX precast gels (BioRad). Proteins were blotted onto 0.45 µm nitrocellulose membranes at 100 V for 1 hour in Towbin Buffer. Membranes were blocked with Intercept TBS blocking buffer (LI-COR Biosciences). Protein was detected with a directly labeled anti-human IgG (H+L)-AF790 antibody (Jackson ImmunoResearch) and, after drying, the membrane was imaged using a LI-

COR Odyssey CLX infrared imager. Washes between each step consisted of four 5-minute washes in TBS-0.1% Tween 20.

Vibriocidal and agglutination assays

Assays were performed using *V. cholerae* strain O1-Ogawa (X25049). Vibriocidal assays were essentially conducted as previously described [137]. In this study, mAbs were diluted two-fold in 0.9% saline solution starting at 20-40 nM. Vibriocidal EC_{50} values were determined as the concentration of mAb that affected a 50% reduction in the average culture turbidity (OD 595 nm) of media-only controls. Assays utilizing inactivated guinea pig complement were performed as described above but utilized complement that had first been heated for 30 minutes at 56°C before use. Minimum agglutinating titers were determined by diluting mAbs two-fold in PBS starting at a concentration of 100 nM. Bacteria were prepared by growing each culture to mid-log phase (2-3 hours) in bovine heart infusion media. Bacteria were then pelleted at 3,000 x g for 10 min and washed twice in PBS. Immediately before use, bacteria were normalized such that a 1:10 dilution of the sample had an OD 595 nm value of 0.3 ± 0.02 relative to PBS. For each antibody, duplicate measurements were performed in which 25 µL of the bacterial sample was combined with an equal volume of diluted mAbs added to a V-bottom microtiter plate. Plates were sealed with an adhesive film, briefly centrifuged to concentrate contents at the bottom of the well (20 x g, 15 seconds), and then incubated for 20-24 hours at 4°C to allow non-agglutinated bacteria to form a ‘button’ at the bottom of the well. Plates were imaged using a UV imaging system (ChemiDoc, BioRad). Agglutination titers were recorded as the last dilution where bacteria were visibly agglutinated.

Soft-agar motility inhibition assays

Antibody-mediated inhibition of motility was measured using an antibody-infused soft agar bacterial migration assay. Assays were performed in 24 well plates containing 500 µL of LB-0.3% agar. Wells were prepared by performing 2-fold serial dilutions of antibodies in LB media starting at a concentration of 50 nM. Equal volumes of diluted antibody and 45ºC, 0.6% molten LB agar (Fisher; Cat -BP1423) were combined and mixed in a microplate mixer. Plates were allowed to rest overnight at ambient temperature. Wells were stab-inoculated at the top of the well with an inoculation needle dipped in a mid-log phase culture of *V. cholerae* O1-Ogawa (X25049). Plates were then incubated at 30ºC for 7-8 hours until bacterial growth in no-antibody control wells reached the well's mid-point. The minimum effective concentration of antibody was measured as the lowest concentration of antibody that was able to retard bacterial migration relative to no-antibody control wells. For experiments utilizing F(ab) fragments, wells were stabbed inoculated in the center of the well and the diameter of bacterial growth was measured after 7 hours. Assays were performed with duplicate measurements tested on separate plates.

Live-cell *V. cholerae* motility tracking

The motion of the free-swimming cells after treatment with isotype and subclass antibody variants was examined by live-cell microscopy using a Zeiss Axio spinning-disk Observer Z1 microscope equipped with a 37ºC heating chamber. A mid-log culture of the GFP expressing *V. cholerae* O1-Ogawa strain RT4273, derived from classical strain O395, (gift of Ron Taylor's laboratory, Dartmouth) was used at a concentration of approximately 1 x 10^8 CFU/mL (OD=1). This culture was prepared by sub culturing bacteria from an overnight streak plate grown for 2-3 hours in luria broth (LB) shaking at 250 RPM. Equal volumes of bacterial culture and antibody

diluted in LB were gently mixed and then loaded in a u-Slide VI 0.4 Uncoated (Ibidi) chamber slide for direct imaging. Bacteria were detected with a 488 nm laser. Images were collected every 100 ms for 5 to 7.5 seconds. For each experiment, a minimum of 50 cells were analyzed for speed, vector direction, and general motility characteristics. The percentage reduction of the number of motile bacteria was determined relative to a negative influenza HA specific IgG1 control antibody (EM4C04) at a concentration of 20 nM on each 6-chamber slide in order to account for longitudinal differences in the absolute number of motile bacteria due to factors such as cell division during experimentation.

The motility characteristics of bacteria were obtained by our tracking algorithm that detected high intensity bacteria and tracked their movements in a fluorescent image sequence. The local adaptive threshold algorithm was used to binarize the first frame of the image sequence, generating a set of foreground objects with their spatial locations and morphometry features as the initial state components for bacteria representation. In each of the following frames from an image sequence, it was first processed in the same way as the first image frame for a set of “true states”. Next, a set of “particles”, i.e. educated bacteria state guesses, was generated by adding random perturbations to the original states. The weights of the resulting particles were computed by comparisons with the binary image frame after segmentation. The weighted average of all particles of a bacteria state was treated as its estimated state and compared with the true states of all bacteria in the current image frame. With the estimated state of each bacterium, we computed pair wise similarities between the estimated and each true state. If the best similarity is sufficiently good, the true state associated with the best similarity was selected as the state updates for each bacterium. Otherwise, this bacterium was considered moving out of the image focal plane or scope of view. Additionally, those with unselected true

states were considered newly emerging bacteria. By repeating this procedure, the trajectories of bacteria were obtained by the updated spatial state components with step-wise state evolutions. With these bacteria spatial trajectories and the known time interval between adjacent image frames, we computed the derived spatial speed for each bacterium. To distinguish motile and stationary bacteria, we set the speed cutoff value as 5 pixels, about 1% of the image frame size. Software to implement the image analysis is available upon request.

Statistical tests

Graphs and statistical tests were performed using GraphPad Prism software version 8.0. Either a one-way or two-way ANOVA was used to determine statistical significance. Information about the statistics used for each experiment, including sample size, experimental method, and specific statistic test employed, can be found in the relevant results section or figure legend.

Author Contribution:

R.C.K. and O.A. contributed to the acquisition of the data, the analysis of the data, the interpretation of the data, and wrote and approved the final manuscript. A.C., L.E.N., T.R.B, F.Q., R.C.C. S.B.C and E.T.R contributed to critical discussion and manuscript revision. M.K., J.H.B, E.T.R contributed to the generation of critical reagents. H.Y. contributed to the analysis of the data. J.K. contributed to the analysis of the data, the interpretation of the data, and helped draft the work. J.W. designed the study, contributed to the analysis of the data, the interpretation of the data, and wrote and approved the final manuscript.

Declaration of Interests

The authors declare no competing interests.

Correspondence:

Jens Wrammert, Department of Pediatrics; Division of Infection Disease; Emory Vaccine Center, School of Medicine, Emory University, 2015 Uppergate Drive, ECC Building, Room 510, Atlanta, GA 30322; email: jwramme@emory.edu.

Acknowledgments:

We would like to thank to Dr. Hedda Wadermann, Max Plank Institute, for providing the human IgG subclass vectors, Dr. Hugo Mouquet, Institut Pasteur, for providing IgA1, IgA2, and J-chain vectors, and Dr. Lynn Dustin, University of Oxford, for providing the IgM vector. Dr.

Gabriela Kovacikova and the laboratory of Dr. Ron Taylor, Dartmouth, for providing *V. cholerae* strain 4273, and Dr. Pavol Kováč and Dr. Peng Xu, NIDDK, LBC, National Institutes of Health, Bethesda, Maryland, for assistance in generating OSP:BSA. We thank Drs. Neil Anthony and April Reedy of the Emory Integrated Imaging Core for expert technical assistance. And we gratefully acknowledge Dr. Tatiana Chirkova, Grace Mantus, Carson Norwood, and Maurizio Affer for helpful discussions regarding experimental design and manuscript preparation.

Funding Information:

This work was funded in part by R01 AI137127 (J.W.), T32 AI074492 (R.C.K and L.E.N), R01 106878 (E.T.R., F.Q.), D43 TW005572 (T.R.B) and K43 TW010362). Research reported in this publication was supported in part by the Emory University Integrated Cellular Imaging Microscopy Core of the Emory+Children's Pediatric Research Center. The funders had no role in study design, data collection and analysis, decision to publish, or preparation of the manuscript.

Figures and Legends

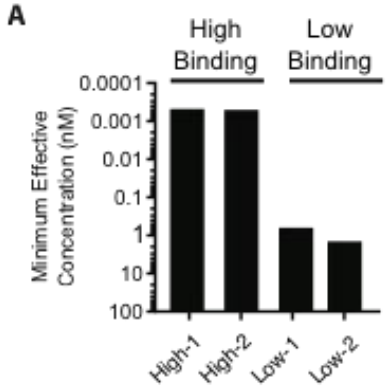

B

mAb ID	Name	Original Isotype
High – 1	29.1.A2	IgG
High – 2	21.2.G1	IgG
Low – 1	31.1.F2	IgM
Low – 2	21.1.D4	IgA

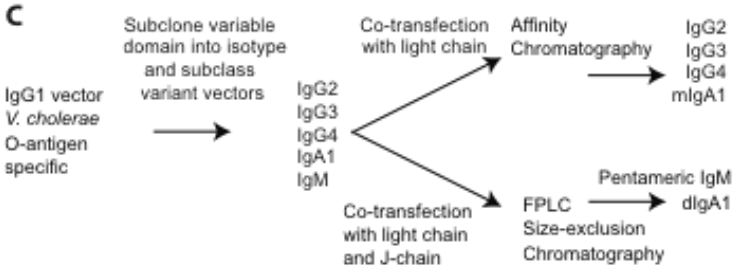

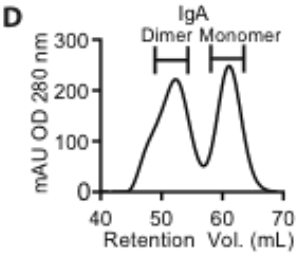

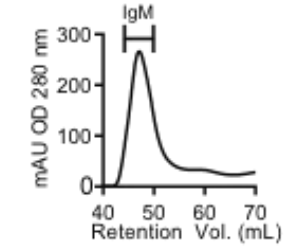

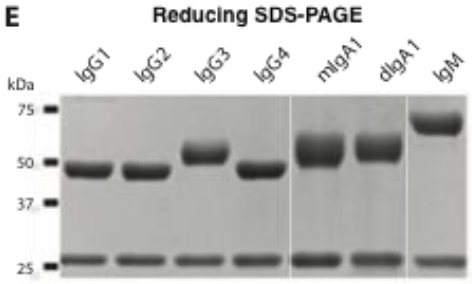

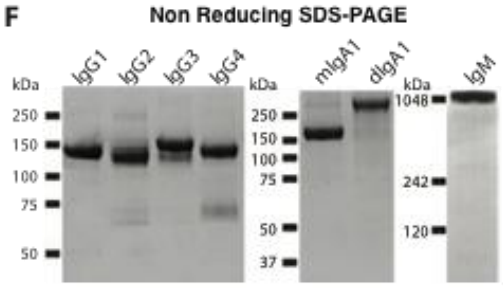

Figure 1: Generation of immunoglobulin isotype and subclass variants from LPS O-antigen specific monoclonal antibodies with differential binding strengths. (A) IgG1 variant binding to O1-Ogawa O-antigen was determined by ELISA. Values represent mAb concentration with signal three times background. (B) Table detailing the original nomenclature and sorted cell isotype of the parent antibody previously reported (See ref. [40]). (C) Flow chart describing the generation of antibody isotype and subclass variants. (D) Representative 280 nm sample absorbance chromatograms of IgM and IgA purification during size-exclusion chromatography. Brackets denote the collected fractions. (E) Reducing SDS-PAGE analysis of isotype and subclass variants of mAb High-1. Heavy (top band) and light (bottom band) chains were resolved using Mini-PROTEAN TGX 10% gels (BioRad). (F) Non-reducing SDS-PAGE analysis of immunoglobulin variants derived from mAb High-1. IgG and IgA antibodies were resolved using NuPAGE 4-12% Bis-Tris Gels with MOPS-SDS running buffer. IgM samples were resolved on a Native PAGE 3-12% Bis-Tris gel with Tris-Acetate SDS running buffer. Data are representative of two or more independent experiments.

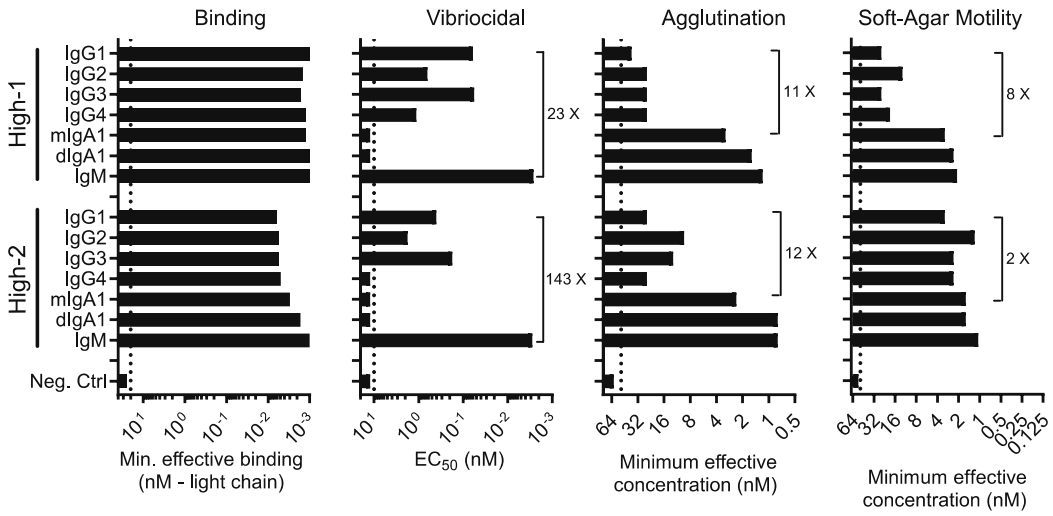

Figure 2: Isotype does not markedly impact the binding properties of high-binding mAbs but differentially affects their functional potency. Quantitative analysis of binding, vibriocidal activity, agglutination potency, and motility inhibition for immunoglobulin variants derived from the two high-binding mAbs. For all analyses an influenza HA-specific human IgG1 antibody (EM4C04) was used as a negative control. Dotted lines indicate the highest tested concentration for each assay (binding = 20 nM; vibriocidal = 10 nM, agglutination = 50 nM, and motility = 25 nM. Vibriocidal values reflect the EC_{50} concentration after baseline subtracting data generated using paired heat-inactivated complement controls. Values represent the mean of duplicate measurements in one experiment and are representative of results from two independent experiments.

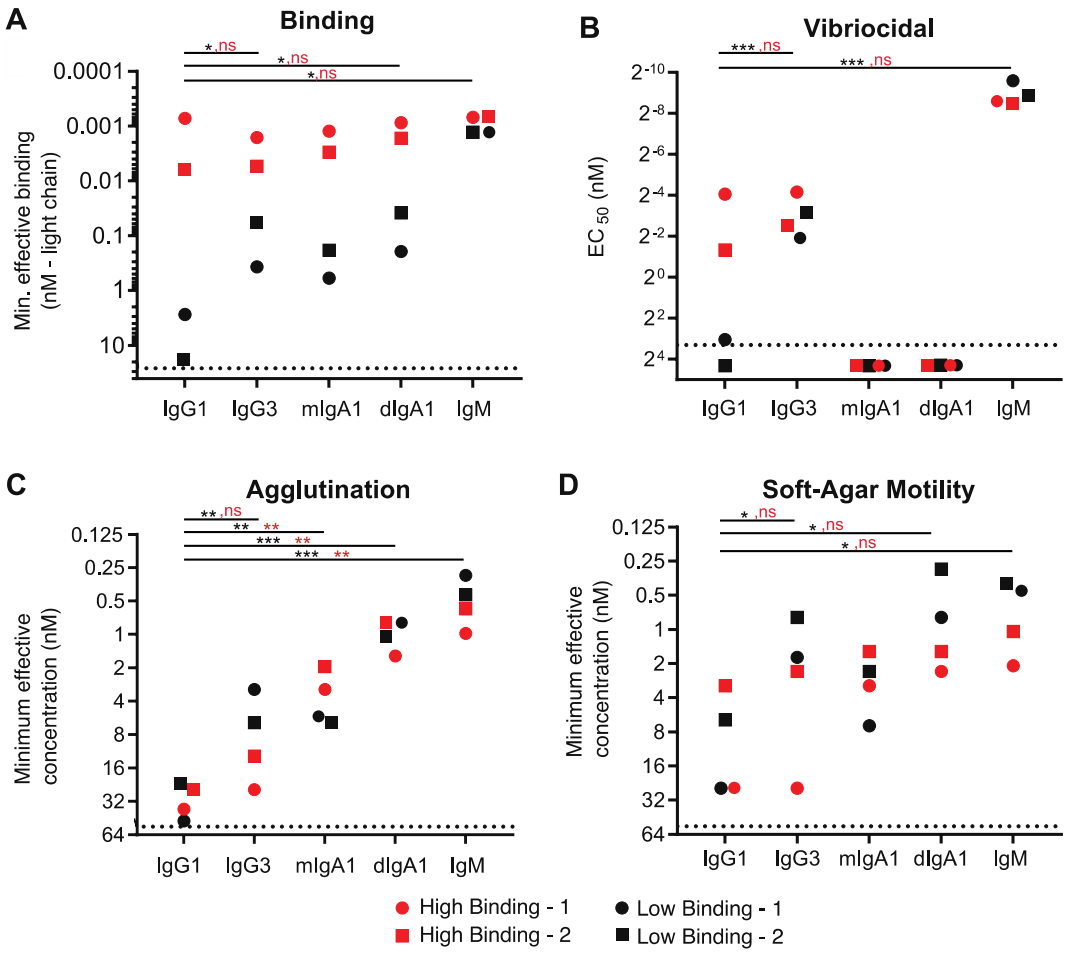
A
Binding
Min. effective binding (nM - light chain)
0.0001
0.001
0.01
0.1
1
10
*,ns
*,ns
*,ns
IgG1
IgG3
mIgA1
dIgA1
IgM
B
Vibriocidal
EC 50 (nM)
2-10
2-8
2-6
2-4
2-2
20
22
24
***,ns
***,ns
IgG1
IgG3
mIgA1
dIgA1
IgM
C
Agglutination
Minimum effective concentration (nM)
0.125
0.25
0.5
1
2
4
8
16
32
64
**,ns
**
**
***
**
***
**
IgG1
IgG3
mIgA1
dIgA1
IgM
D
Soft-Agar Motility
Minimum effective concentration (nM)
0.125
0.25
0.5
1
2
4
8
16
32
64
*,ns
*,ns
*,ns
IgG1
IgG3
mIgA1
dIgA1
IgM
High Binding - 1
High Binding - 2
Low Binding - 1
Low Binding - 2

Figure 3: Low-binding mAb variants displayed functional properties comparable to high-binding mAbs and O-antigen binding was markedly affected by isotype and subclass. (A) Variant binding to O1-Ogawa O-antigen was determined by ELISA. Values represent mAb concentration with signal three times background. (B) Vibriocidal assay EC_{50} values of select antibodies after background subtraction of inactivated complement controls. (C) Values represent the minimum effective mAb concentration that agglutinated bacteria in a microtiter agglutination assay. (D) Values represent the minimum effective mAb concentration that inhibited bacterial migration relative to a no antibody control in a soft-agar motility inhibition assay. The dotted line marks the highest concentration of antibody evaluated (25 nM). The dotted line marks the highest concentration of antibody evaluated (A = 20 nM, B=10 nM, C=50 nM, D=25 nM). Values represent the mean of duplicate measurements and are representative of results from two independent experiments.

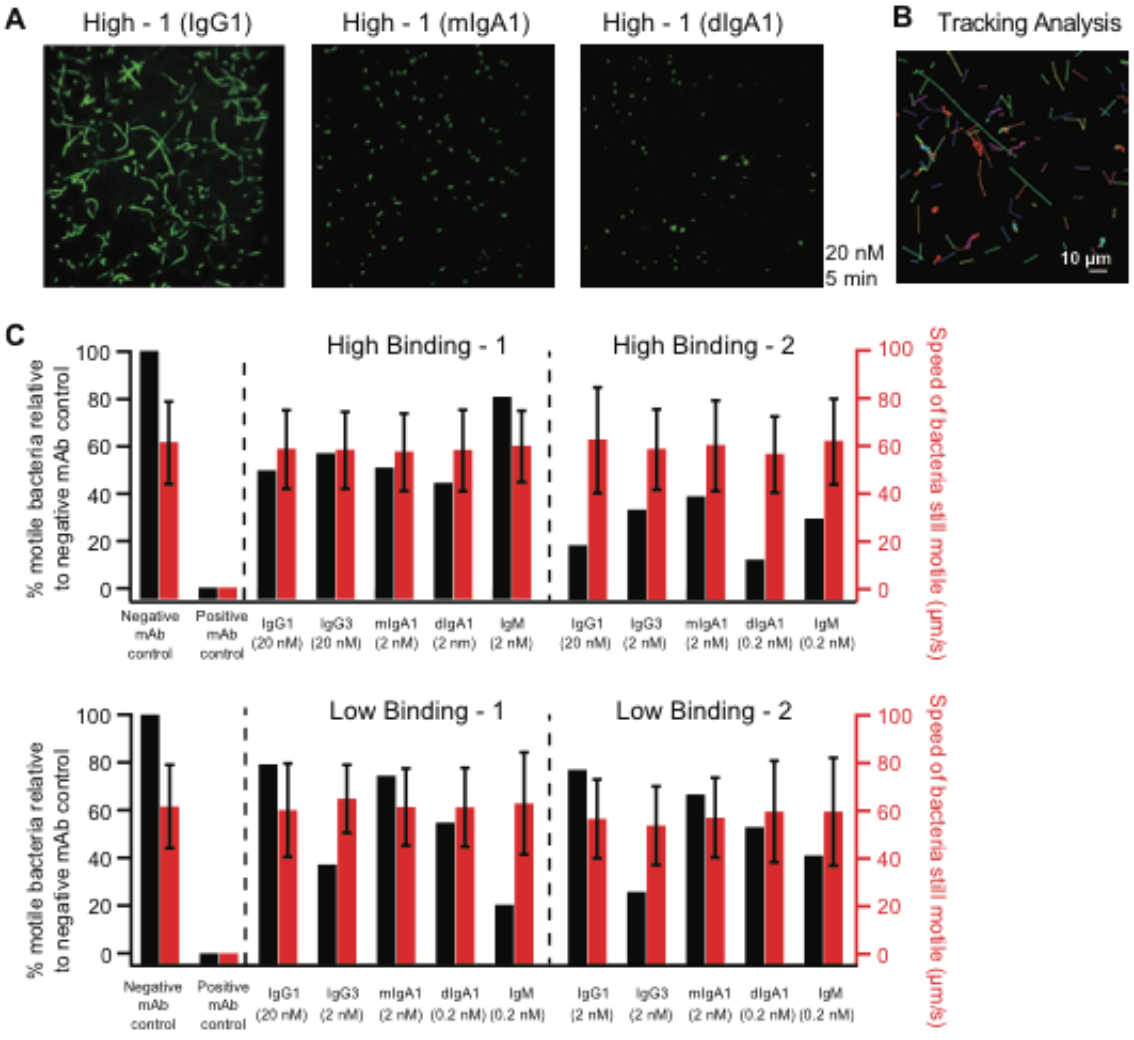
A
High - 1 (IgG1)
High - 1 (mIgA1)
High - 1 (dIgA1)
20 nM
5 min
B
Tracking Analysis
10 µm
C
High Binding - 1
High Binding - 2
% motile bacteria relative to negative mAb control
Speed of bacteria still motile (µm/s)
Negative mAb control
Positive mAb control
IgG1 (20 nM)
IgG3 (20 nM)
mIgA1 (2 nM)
dIgA1 (2 nm)
IgM (2 nM)
IgG1 (20 nM)
IgG3 (2 nM)
mIgA1 (2 nM)
dIgA1 (0.2 nM)
IgM (0.2 nM)
Low Binding - 1
Low Binding - 2
IgG1 (2 nM)
IgG3 (2 nM)
mIgA1 (2 nM)
dIgA1 (0.2 nM)
IgM (0.2 nM)

Figure 4: O-antigen specific mAbs rapidly inhibit motility without affecting the speed of motile bacteria. The motion of a GFP expressing *V. cholerae* O1-Ogawa strain was examined at 37ºC using live-cell confocal microscopy five minutes after 20 nM antibody treatment. (A) (Left) Representative image depicting limited inhibition of motility induced by the IgG1 variant of mAb High-1. (Center) Depicts gain of function by changing the isotype to IgA. (Right) Absence of motility in the presence of dimeric IgA. (B) Representative image of motility tracking analysis over ten frames collected at 100 ms intervals. Individual bacteria are connected by colored lines (C) Antibodies were titrated to a concentration, shown in parentheses, that partially inhibited the number of motile bacteria relative to a paired negative control antibody. The percentage of motile bacteria (left y-axis) in mAb treated samples is shown in black bars. Red bars represent the mean speed (right y-axis) of the remaining motile bacteria, with overlaid bars indicating the standard deviation. EM4C04 (IgG1) was used as a negative control while the IgM variant of mAb Low-1 was used as a positive control at 20 nM. Image series were collected for five seconds at 100 ms intervals. Data in (A) are representative of two independent experiments while data in (C) were collected between three separate experiments.

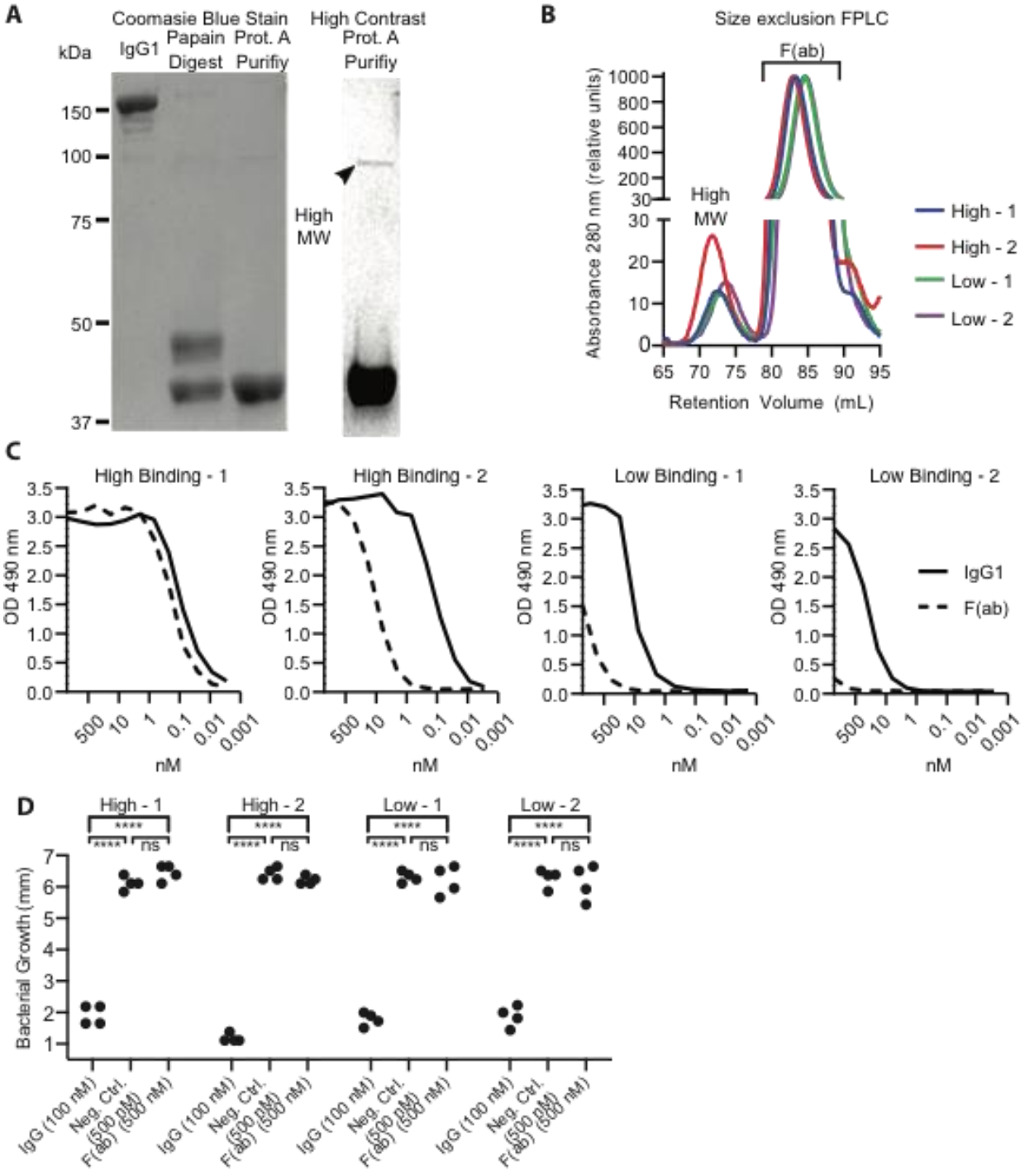
A
Coomasie Blue Stain
kDa
IgG1
Papain Digest
Prot. A Purifiy
High Contrast Prot. A Purifiy
150
100
75
50
37
High MW
B
Size exclusion FPLC
F(ab)
High MW
Absorbance 280 nm (relative units)
Retention Volume (mL)
High - 1
High - 2
Low - 1
Low - 2
C
High Binding - 1
High Binding - 2
Low Binding - 1
Low Binding - 2
OD 490 nm
nM
IgG1
F(ab)
D
High - 1
High - 2
Low - 1
Low - 2
Bacterial Growth (mm)
****
ns
IgG (100 nM)
Neg. Ctrl.
F(ab) (500 nM)

Figure 5: Antigen crosslinking is important to O-antigen binding potency and essential to motility inhibition. (A) Representative coomassie blue stained non-reducing SDS-PAGE gel of F(ab) fragment preparation from IgG1, before papain digestion (left) after papain digestion (center) and after protein A purification (right). A high contrast version of the F(ab) post protein A purification lane is shown as a separate image; arrow indicates a rare ~100 kDa protein. Each lane contains 4 µg of protein. (B) Chromatogram of 280 nm absorbance during F(ab) purification by size-exclusion chromatography. Proteins eluted between 70 and 75 mLs on the HiLoad 16/600 Superdex 200 pg column represent the high-molecular weight (MW) species while those eluted between 80 and 90 mLs represented the F(ab) fraction. Absorbance values are normalized relative to the largest peak to account for loading differences. (C) Binding to Ogawa O-antigen was determined by ELISA for SEC purified F(ab)s (dashed black line) and undigested IgG1 antibody (solid black line). (D) Purified F(ab) fragments were tested at 500 nM in the soft-agar motility inhibition assay. Each assay included 500 nM EM4C04-IgG1 as a negative control and a positive control consisting of the IgG1 form of each antibody at 100 nM. Motility was assessed by measuring the diameter of bacterial growth after incubation at 30ºC for 7 hours. Significance between bracketed samples was determined using a one-way ANOVA. The p-values were not significant (ns) $0.47<p<0.95$. Data shown are from two independent experiments with each sample tested in duplicate.

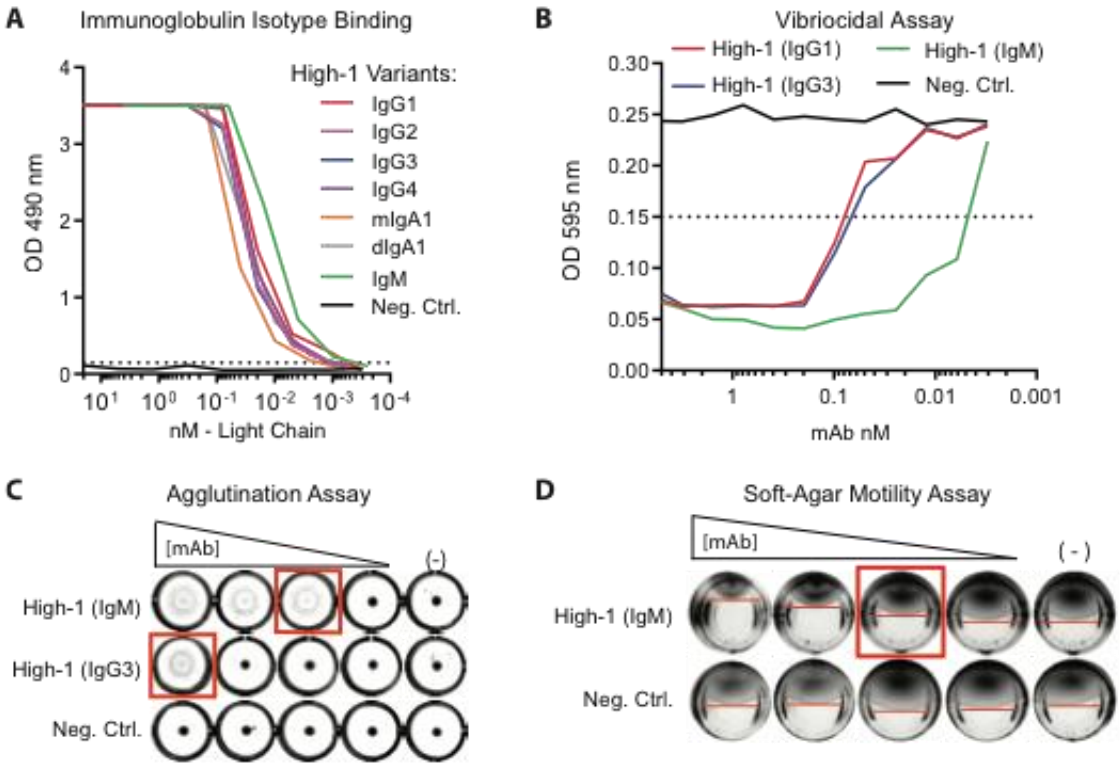
A
Immunoglobulin Isotype Binding
High-1 Variants:
IgG1
IgG2
IgG3
IgG4
mIgA1
dIgA1
IgM
Neg. Ctrl.
OD 490 nm
nM - Light Chain
B
Vibriocidal Assay
High-1 (IgG1)
High-1 (IgM)
High-1 (IgG3)
Neg. Ctrl.
OD 595 nm
mAb nM
C
Agglutination Assay
[mAb]
(-)
High-1 (IgM)
High-1 (IgG3)
Neg. Ctrl.
D
Soft-Agar Motility Assay
[mAb]
(-)
High-1 (IgM)
Neg. Ctrl.

Supplemental Figure S1: Example experimental data from binding and functional analyses. (A-D) Representative functional assays for selected variants of mAb High-1. (A) Binding to Ogawa O-antigen was determined by ELISA. The dotted line marks the absorbance value equalivalent to three times background signal. This threshold was used quantify binding strength in ELISA experiments. (B) Vibriocidal assay EC_{50} values were determined as the concentration of antibody (x-axis) capable of effecting a 50% reduction in bacterial growth relative to no-treatment controls. Higher values on the y-axis correspond to increased culture turbidity as measured by UV absorbance at 595 nm. The dotted-line signifies the EC_{50} threshold (C) Agglutination potency was determined using a microtiter plate-based agglutination assay. The reported minimal effective concentration (red squares) were determined as the lowest concentration of antibody capable of visibly agglutinating approximately 1 x 10^8 CFU of unfixed bacteria. This is evident by the absence of a defined 'button' of settled bacteria as seen in a no antibody control well (-). (D) Motility inhibition was determined using a soft-agar motility assay in which serially diluted mAbs were infused in 0.3% LB-agar. The reported minimal effective concentration (red square) was determined as the lowest concentration of antibody capable of visibly retarding bacterial migration relative to the no treatment control well (-). Red lines denote the leading front of bacterial migration.

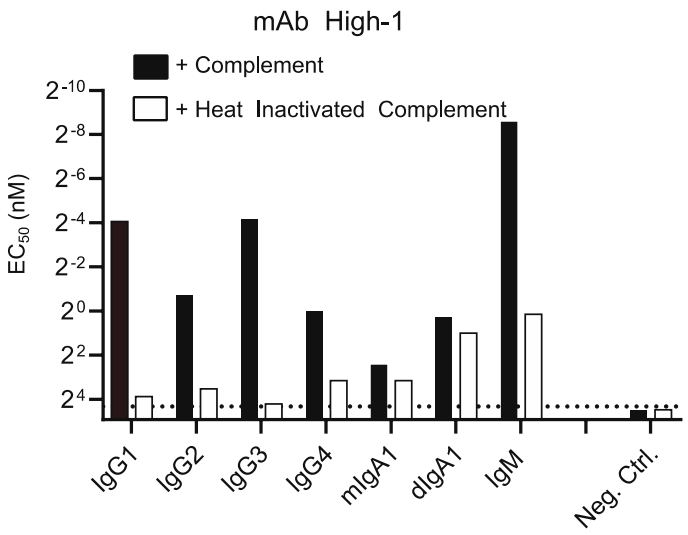

Supplemental Figure S2: Antibodies demonstrate complement independent inhibition of bacterial outgrowth in standard *V. cholerae* vibriocidal assays. EC_{50} values derived from vibriocidal analyses of mAb High-1 variants in which experiments were performed with either fresh 5% guinea pig complment (black bars) or 5% heat-inactivated guinea pig complement (white bars). Complement was inactivated at 56ºC for 30 minutes. EM4C04-IgG1 was used as a negative control. The dotted line at 20 nM denotes the lowest concentration tested in heat-inactivated complement samples. Values represent the mean of duplicate measurements in one experiment and are reprsentative of two independent experiments.

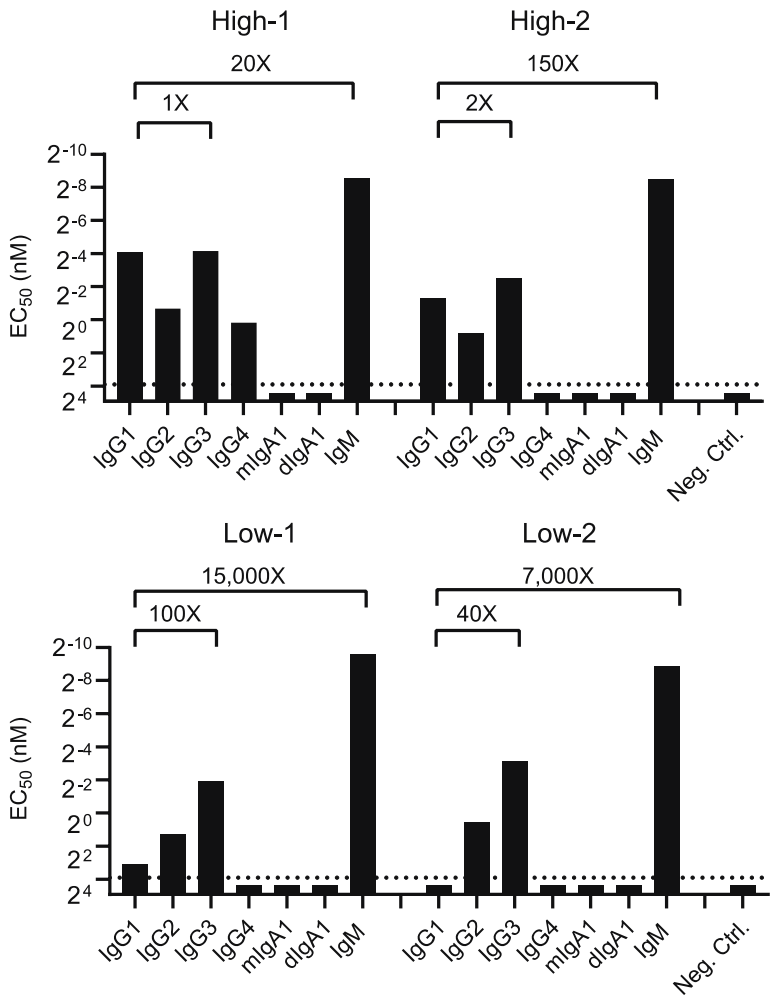

Supplemental Figure S3: IgM variants binding have markedly enhanced vibriocidal capacity for all antibodies. Vibriocidal assay EC_{50} values of antibodies after background subtraction of heat-inactivated complement controls. Brackets above bars represent the fold increase in potency between IgG1 and IgM and IgG1 and IgG3 mAbs. EM4C04-IgG1 was used as a negative control. The dotted line at 10 nM denotes the lowest concentration tested in experiments containing active complement. Values represent the mean of duplicate measurements in one experiment and are representative of two independent experiments.

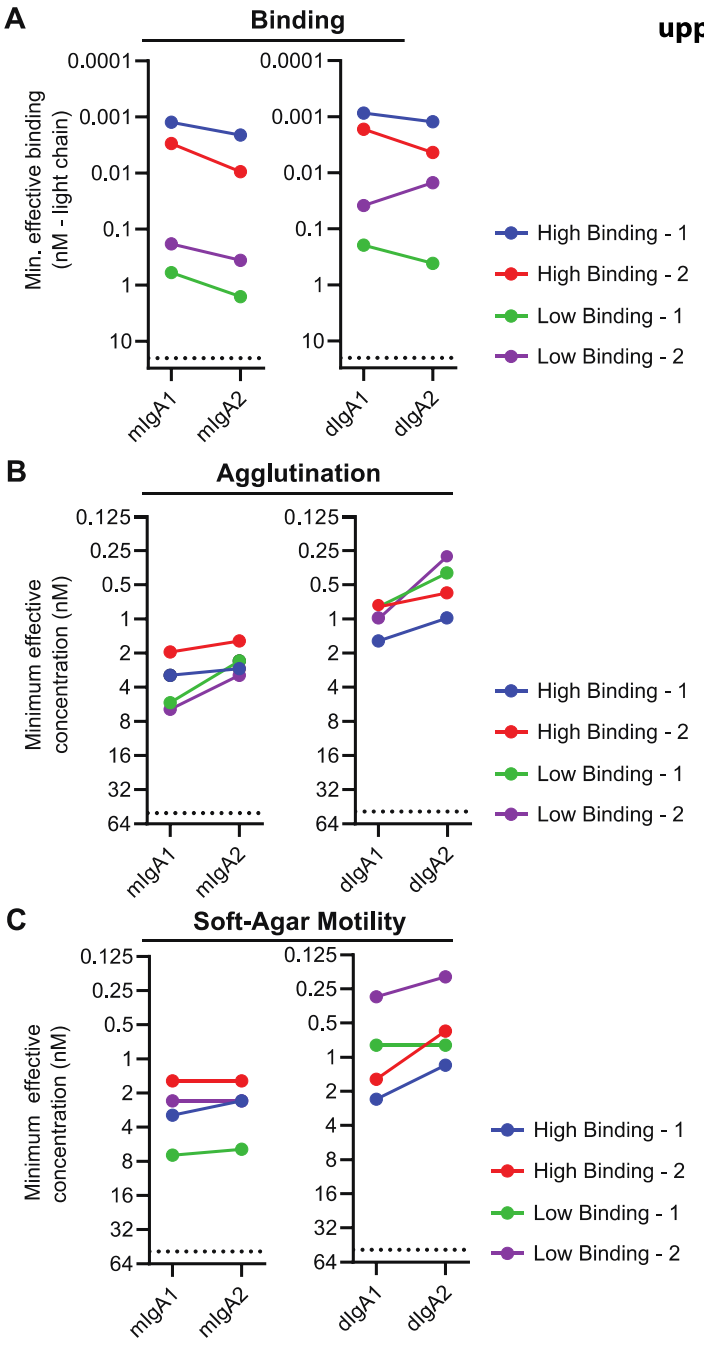
A
Binding
upp
Min. effective binding
(nM - light chain)
0.0001
0.001
0.01
0.1
1
10
mIgA1
mIgA2
dIgA1
dIgA2
High Binding - 1
High Binding - 2
Low Binding - 1
Low Binding - 2
B
Agglutination
Minimum effective
concentration (nM)
0.125
0.25
0.5
1
2
4
8
16
32
64
mIgA1
mIgA2
dIgA1
dIgA2
High Binding - 1
High Binding - 2
Low Binding - 1
Low Binding - 2
C
Soft-Agar Motility
Minimum effective
concentration (nM)
0.125
0.25
0.5
1
2
4
8
16
32
64
mIgA1
mIgA2
dIgA1
dIgA2
High Binding - 1
High Binding - 2
Low Binding - 1
Low Binding - 2

Supplemental Figure S4: IgA2 variants have comparable functional potency to IgA1 antibodies. (A) Binding to Ogawa O-antigen was determined by ELISA. Values represent the mAb concentration with signal three times background. (B) Values represent the minimum effective mAb concentration that agglutinated bacteria in a microtiter agglutination assay. (C) Values represent the minimum effective mAb concentration that inhibited bacterial migration relative to a no-antibody control in a soft-agar motility inhibition assay. The dotted line marks the highest concentration of antibody evaluated (A = 20 nM, B=50 nM, C=25 nM). Values represent the mean of duplicate measurements and are representative of results from two independent experiments.

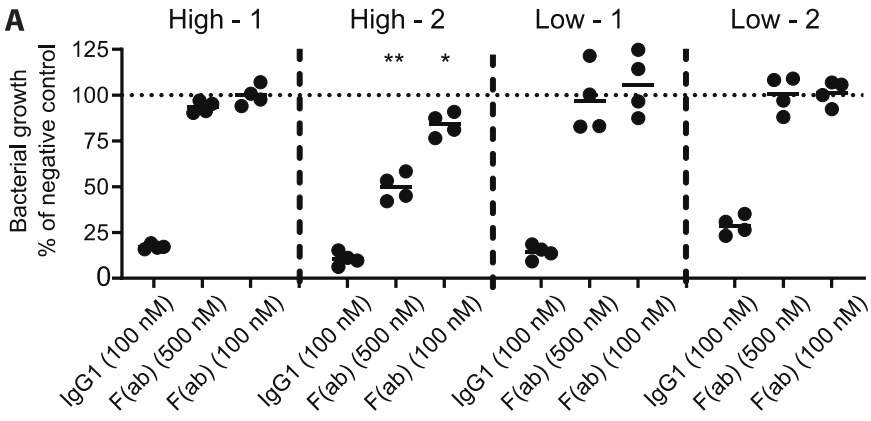
A
High - 1
High - 2
Low - 1
Low - 2
Bacterial growth
% of negative control
125
100
75
50
25
0
**
*
IgG1 (100 nM)
F(ab) (500 nM)
F(ab) (100 nM)

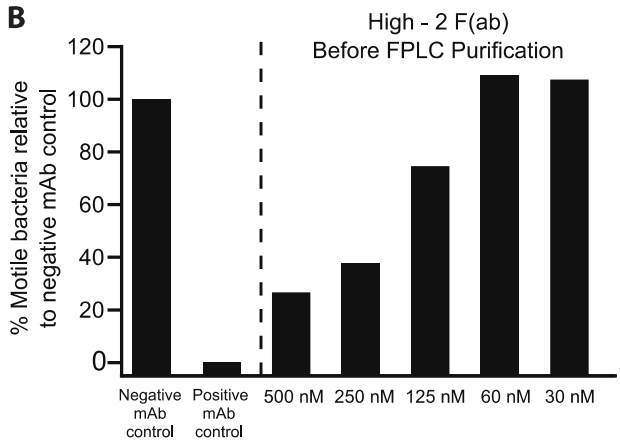
B
High - 2 F(ab)
Before FPLC Purification
% Motile bacteria relative
to negative mAb control
120
100
80
60
40
20
0
Negative mAb control
Positive mAb control
500 nM
250 nM
125 nM
60 nM
30 nM

Supplemental Figure S5. Pre-size exclusion F(ab) preparations derived from mAb High-2 inhibit motility. (A) Motility inhibition was assessed using the soft-agar migration assay. Purified F(ab) fragments were tested at a concentration of 500 nM and 100 nM. Each test plate included 500 nM EM4C04-IgG1 as a negative control and 100 nM of the IgG1 parent of each tested F(ab) at as a positive control. Motility was assessed by measuring the diameter of bacterial growth after incubation at 30ºC for 7 hours. Values are expressed as a percentage of the growth ring diameter of paired negative controls, with the dotted line at 100% indicating equivalent growth to the negative control. Significance was determined using a one-way ANOVA compared to negative control values (*** $p<0.0001$, ** $p=0.004$, * $p=0.07$). Values were obtained in two independent experiments with each sample tested in duplicate. (B) Live-cell confocal microscopy and time-lapsed tracking analysis was used to assess motility inhibition in a concentration dependent manner for mAb High-2 Pre-SEC F(ab) preparations. Bars represent the percentage of motile bacteria relative the negative IgG1 control (EM4C04) at 500 nM. Antibody High-2 (IgG1) was used as a positive control at 100 nM. Data are from one assay and are representative of two independent experiments.

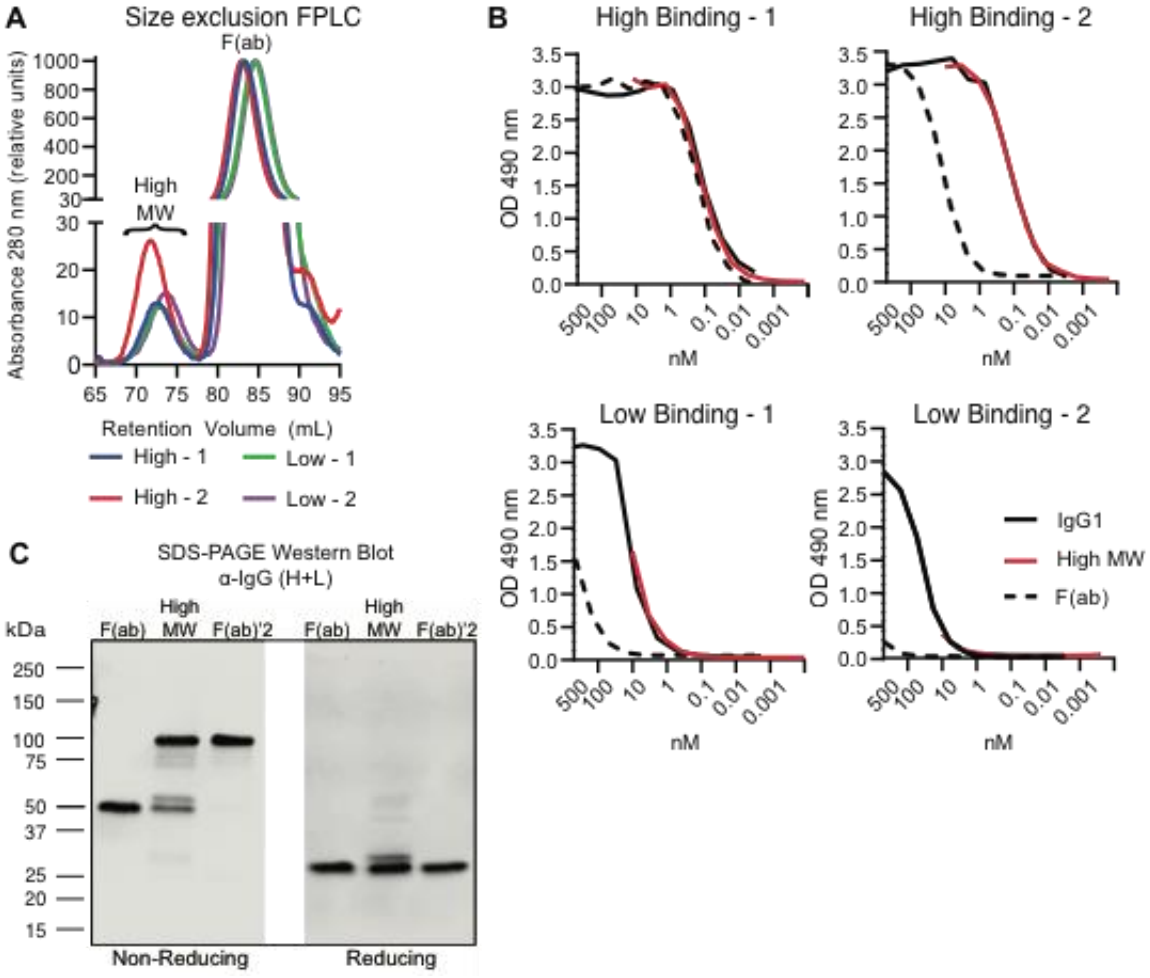
A
Size exclusion FPLC
F(ab)
High MW
Absorbance 280 nm (relative units)
Retention Volume (mL)
High - 1
Low - 1
High - 2
Low - 2
B
High Binding - 1
High Binding - 2
Low Binding - 1
Low Binding - 2
OD 490 nm
nM
IgG1
High MW
F(ab)
C
SDS-PAGE Western Blot
α-IgG (H+L)
kDa
F(ab)
High MW
F(ab)'2
Non-Reducing
Reducing

Supplemental Figure S6. The high molecular weight protein species in conventional F(ab) preparations has binding properties similar to bivalent IgG1 and gel migration characteristics comparable to F(ab)'2 and F(ab) aggregates. (A) Protein sample absorbance at 280 nm during F(ab) purification by size-exclusion chromatography. The high-molecular weight (MW) species is approximately 1.5% to 3% the abundance of the F(ab) population for all four antibodies. (B) Binding to Ogawa O-antigen was determined by ELISA for SEC purified F(ab)s (dashed black line), undigested IgG1 antibody (solid black line), and the purified, 100 kDa, high MW protein species (solid red line). Due to the limited amount of purified high-MW protein (solid red line), binding was measured starting at a reduced of concentration of 10 nM. (C) Representative western blot analysis of the purified F(ab) and high MW proteins relative to F(ab)'2 generated by IdeZ protease digestion of IgG1. Protein was detected using anti-human IgG (H+L)-AF790 antibody using a LiCOR Odyssey imager.

Chapter 5: Discussion

Summary

Vibrio cholerae is the causative agent of the severe acute diarrheal disease cholera. Frequent outbreaks of the disease in addition to its stable presence in numerous countries make it a persistent healthcare threat. Protection against cholera disease is mediated by long lived humoral immune responses that are effective at protecting against subsequent exposure. Despite this, the factors necessary for the generation of these durable immune responses as well as the mechanisms by which protection is conferred are not well defined [104]. The work described in this dissertation helps give critical insight into the nature of the cells likely responsible for both short- and long-term immunity, and the mechanisms by which protection may be mediated.

As highlighted in the research described in chapter 2, exposure to cholerae generates a population of LPS and CTB specific cells shortly following vaccination. Critically, we have shown these antigens induce isotype selectivity with LPS driven primarily by IgM and IgA ASC while the toxin responses were mainly derived from IgG ASC. IgM, and to a lesser extent IgA, plasmablasts also expressed high levels of the gut homing receptor CCR9. These findings suggest that it is the LPS specific cells which are most likely to home to the mucosa and mediate protection in this location. This finding could help explain the lack of correlation between antitoxin responses and protection against disease. Additionally, it highlights the need for cholera vaccines to induce a population of gut homing IgM and IgA cells following vaccination to develop protective mucosal immunity. The early serum responses seen up to day 30 are likely derived from the early plasmablasts response. Peripheral titers at 90- and 365-days post vaccination did not correlate with these cells, which may indicate that they do not contribute to long term peripheral immunity. The source of these long-lived peripheral titers and their relationship with intestinal responses needs further examination. Studies examining rotavirus

infection in mice have shown a clear link between mucosal homing B cells and protection against intestinal infections [93]. Therefore, it would be useful to examine the link between the early gut homing ASC responses and long-term intestinal cholera immunity as they may be more reliable markers of protection compared to peripheral vibriocidal titers.

The single cell analysis approaches utilized on the vaccine induced plasmablasts described in chapter 3 shows that the LPS specific cells are largely gut homing. A surprisingly large number of the LPS specific antibodies induced following vaccination had high numbers of mutations. Additionally, the number of mutations positively correlated with the antibody's affinity towards LPS. Taken together, this finding indicates that a polysaccharide is capable of inducing affinity maturation in humans. The source of these highly mutated plasmablasts is also of great interest, as they could arise from both naïve and memory precursors. These mutated plasmablasts could be indicative of highly efficient SHM of naïve cells via germinal center reactions. Alternatively, these cells may arise from cross reactive memory B cell precursors [188]. Identifying the source of these highly mutated cells may provide insights both into long term immune responses and may also explain the difference in response to the cholera antigens we observed in our cohort. These analyses also highlight the role that V gene usage has in determining affinity to antigens and may also help explain why the response to cholera disease and vaccination is so heterogenous.

Finally, the work on determining the mechanisms behind humoral cholera as described in chapter 4 highlights the role that isotype, affinity, and epitope have in antibody function. Isotype had a profound impact on the ability of low affinity antibodies to interact with the OSP of *V. cholerae*. Changing the isotype from IgG to IgA or IgM resulted in significant increases in both affinity and functional capacity of the antibodies. This rise in functionally could not solely be

explained by increased avidity, as even monomeric IgA and IgG3 resulted in significant gain of function. These findings may highlight the role that antibody hinge flexibility and orientation may have on affinity and functionality. Additionally, while many mechanisms of action have been proposed, our study demonstrated that human derived antibodies were able to arrest bacterial mobility at a single cell level. This effect required crosslinking as F (ab) derived from these antibodies had no effect. These findings also indicate that epitope plays an important role in this process, as even high affinity clones could have poor motility inhibition ability. It appears that the epitope the antibodies are interacting with on the LPS has a profound impact on their ability to inhibit the bacteria. Future work building on the findings described in this dissertation will provide even more insight into cholera-based immunity.

Future Directions

It is clear that cholera immunity is driven by mucosal immune responses that target the OSP of the bacteria. Several animal models have shown that the presence of these specific antibodies within the intestine is key to providing protection against infection. It is reasonable to assume a similar mechanism may be occurring in human immunity to cholera disease as well. Identification of the intestinal humoral responses that mediate this effect is necessary to shed insight on the factors required for durable immunity. It is becoming increasingly clear that the peripheral markers typically used to determine immunity are not able to accurately predict long term protection. The reason for this is likely a disconnect between the peripheral and mucosal immune compartments. Both animal models and human studies have shown that the immune responses observed in the periphery are not always reflective of the responses seen in the intestinal tissue [54, 93]. Therefore, it is important to understand the links between systemic and intestinal cholera immune responses. Identifying the source and nature of the peripheral

vibriocidal titers seen six months past exposure would also provide key insight in cholera immunity. Early vibriocidal responses in naïve individuals are driven by IgM titers, but these titers decline rapidly post exposure. Therefore, the vibriocidal activity at later time points may possibly be driven by LPS specific IgG titers, but the source of these ASC has yet to be identified. It would be worthwhile to examine tissues such as the bone marrow known to contain LLPC to see if these LPS specific cells are located in this area. This would be very important if the source of these vibriocidal antibodies is not IgM ASC, but IgG ASC, which are not known to play a large role in intestinal immunity.

Next, it is important to investigate the nature of the long-lived response seen in the mucosa. Studies in patients have identified the presence of cholera specific cells, both for LPS and CTB, within the mucosa long after the initial infection [127]. Detection of LPS specific cells was likely limited by the detection methods utilized in that study, nevertheless they do provide definitive evidence of LPS specific LLPC. Our research has shown that a majority of the early plasmablasts response consist of highly mutated gut homing cells. It is unclear how these early plasmablasts are able to contribute to the LLPC pool located in the mucosa. One approach to identify links between these two compartments would be to identify shared clones which could show a link between the acute phase and long term protective immune responses. This information would also help identify markers of the early plasmablasts that could be indicative of the potential to develop into mucosal LLPC. These findings would have important ramifications for both cholera as well as B cell immunology.

Cholera specific MBC responses can be detected following exposure but they only weakly correlate with immunity. Prior studies have shown that for MBC to mediate effective immunity following an intestinal infection the cells must be able to travel to the intestinal tissue.

Therefore, another important avenue of study should focus on examining the gut homing potential of antigen specific MBC following exposure. Failure to generate sufficient gut homing MBC responses may explain the weak and conflicting correlations prior studies have reported on peripheral MBC and immunity to infection [122].

The existence of tissue resident MBC and the role they play in immunity is another area of active research. Like other tissues, the gut has a population of tissue resident MBC [94]. Importantly, gut resident MBC displayed a completely different phenotypic profile compared to their blood counterparts. The contribution of these cells to mucosa immunity in the context of cholera still needs to be elucidated. Upon exposure to *V. cholerae,* symptom onset can occur rapidly in as little as 10 hours. Within this timeframe, it is unlikely that the MBC seen in periphery can differentiate in time to mount effective immune responses. Tissue resident MBC, particularly their ability to rapidly differentiate into IgM ASC and their presence in the immediate vicinity of the pathogen, provide an avenue of rapid protection. Therefore, identifying if these cells are produced, their longevity, and contribution to human cholera immunity would provide key insight into the durability of the response.

Our analysis on mucosal homing plasmablasts generated during a primary exposure showed highly mutated antibodies, which may be indicative of very efficient germinal center SHM of naïve B cells. Another possibility is that these plasmablasts originated from a memory B cell precursor. Our cohort was cholera naïve, therefore these cells originating from an MBC precursor is an intriguing prospect. The intestinal immune cells are constantly exposed to a multitude of foreign antigens [90]. While the intestine is largely non inflammatory, these microbes still induce humoral responses. Indeed, many of the commensals are covered with sIgA and sIgM which are used to regulate gut homeostasis [182]. This results in the presence of a

multitude of antigen experienced IgM and IgA MBC. Studies have also shown that while many of these cells are antigen specific, a significant proportion of them are polyreactive. Therefore, it is possible that these cells can respond not only to antigens from commensal microbes but also related pathogenic ones. Identifying the presence of antibodies from intestinal MBC or LLPC in naïve donors that are polyreactive could be useful in predicting who will have a more robust response vaccination. Additionally, cholera specific antibodies can be used to screen for commensal bacteria that have cross reactive OSP for use as potential immunization agents. This could also help explain a phenomenon we observed in our cohort where some donors had the peak of their response 10 days post vaccination. This later timepoint could be indicative of a true naïve response, compared to donors who peaked on day 7 post immunization. Therefore, it would also be illuminating to compare the repertoire and SHM of plasmablasts generated on day 7 compared to day 10.

There are many proposed mechanisms of antibody mediated cholerae immunity including agglutination, enchaining, and motility inhibition. Likely, immunity is driven by a combination of these factors. However, our group and others have demonstrated that antibodies are able to inhibit cholera motility at a single cell level. This is critical to protection because immotile cholera strains are severely restricted in their ability to cause disease. This mechanism also provides an avenue of protection without requiring large groups of bacteria to be present like agglutination does. This provides an avenue for antibodies to rapidly control the bacteria before they are able to proliferate within the intestinal tissue. The precise mechanism behind motility inhibition needs further study. The most likely explanations are bacterial stress responses, flagellar wrapping, and proton motive force ablation. Bacterial stress responses to antibody binding have been examined, however the authors of that study did not observe an increase in

any stress related gene transcripts [145]. Given the speed at which motility arrest occurs means it's more likely that control is occurring at the post transcriptional level. Flagellar wrapping is another possibility, though given the speed and force at which the flagella rotates it is unclear if the antibodies can exert the force necessary to completely impede its movement. Finally, there is proton motive force ablation. In *V. cholerae*, flagellar movement is powered by a sodium concentration gradient and loss of this this gradient leads to cessation of bacterial motility. Analysis from a study examining *Cronobacter turicensis* has identified O-antigen specific antibodies that bind to the bacterial membrane and lead to the abolishment of the PMF, thereby causing cessation of bacterial movement[236]. This effect is predicated on opening small pores in the bacterial membrane resulting in a loss of polarity. Our own lab has identified several antibodies that appear to exert this effect in *V. cholerae*, but further studies need to be undertaken to identify the role of antibodies altering bacteria membrane potential.

We have also described how isotypes and subclass can have a profound impact on the binding and functional properties of the antibodies. IgM and IgA in particular were exceptionally effective in enhancing the binding and functional capabilities. The likely reason for this rise in efficacy is the increased avidity associated with the pentameric and dimeric antibodies. However, avidity alone could not explain the enhanced functionality we observed. Switching the constant domain to IgG3 and mIgA also resulted in gains of function, likely due to the increased flexibility of the Fab region provided by the extended hinge region. The reason why this results in increased functionally must also be investigated. Given the need for cross linking to effectively inhibit motility, it is possible that the increased flexibility of the hinge groups allows the antibodies to bind different LPS molecules. Ascertaining where on the OSP that antibodies

bind to and correlating that with functional capacity is crucial to understanding the mechanisms behind antibody mediated immunity of *V. cholerae*.

Conclusion

Humoral responses to cholera disease are known to be the primary driver of immunity. Yet, the factors that are important for the induction and durability of cholera immunity have not been thoroughly elucidated. The studies described in this dissertation help to shed key insight on early factors that may better correlate with long term intestinal immunity. They provide critical insight on the nature of the cells likely responsible for providing protection at the mucosa. Finally, they provide understanding on the mechanisms of antibody mediated immunity to the bacteria. These findings also have broader applications on mucosal vaccination and human B cell intestinal immunology. Most importantly, millions of people in communities worldwide suffer from cholera disease. The work of the studies presented in this dissertation are part of larger research efforts that the broader scientific community is utilizing to generate improvements in the effectiveness of treatment, vaccination, and prevention of cholera disease.

References

1. Cooper MD. A life of adventure in immunobiology. Annu Rev Immunol. 2010;28:1-19. Epub 2009/12/09. doi: 10.1146/annurev-immunol-030409-101248. PubMed PMID: 19968560.

2. Cooper MD, Raymond DA, Peterson RD, South MA, Good RA. The functions of the thymus system and the bursa system in the chicken. J Exp Med. 1966;123(1):75-102. Epub 1966/01/01. PubMed PMID: 5323079; PubMed Central PMCID: PMCPMC2138128.

3. Cooper MD, Peterson RD, Good RA. Delineation of the Thymic and Bursal Lymphoid Systems in the Chicken. Nature. 1965;205:143-6. Epub 1965/01/09. PubMed PMID: 14276257.

4. Cambier JC, Gauld SB, Merrell KT, Vilen BJ. B-cell anergy: from transgenic models to naturally occurring anergic B cells? Nat Rev Immunol. 2007;7(8):633-43. Epub 2007/07/21. doi: 10.1038/nri2133. PubMed PMID: 17641666; PubMed Central PMCID: PMCPMC3714009.

5. Sellars M, Kastner P, Chan S. Ikaros in B cell development and function. World J Biol Chem. 2011;2(6):132-9. Epub 2011/07/19. doi: 10.4331/wjbc.v2.i6.132. PubMed PMID: 21765979; PubMed Central PMCID: PMCPMC3135860.

6. Bain G, Maandag EC, Izon DJ, Amsen D, Kruisbeek AM, Weintraub BC, et al. E2A proteins are required for proper B cell development and initiation of immunoglobulin gene rearrangements. Cell. 1994;79(5):885-92. Epub 1994/12/02. PubMed PMID: 8001125.

7. Cambier JC, Campbell KS. Signal transduction by B lymphocyte receptors: structure-function relationships of membrane immunoglobulins and associated molecules. Semin Immunol. 1990;2(2):139-49. Epub 1990/03/01. PubMed PMID: 1966612.

8. Yu W, Nagaoka H, Jankovic M, Misulovin Z, Suh H, Rolink A, et al. Continued RAG expression in late stages of B cell development and no apparent re-induction after immunization. Nature. 1999;400(6745):682-7. Epub 1999/08/24. doi: 10.1038/23287. PubMed PMID: 10458165.

9. Hardy RR, Hayakawa K. B cell development pathways. Annu Rev Immunol. 2001;19:595-621. Epub 2001/03/13. doi: 10.1146/annurev.immunol.19.1.595. PubMed PMID: 11244048.

10. Hozumi N, Tonegawa S. Evidence for somatic rearrangement of immunoglobulin genes coding for variable and constant regions. 1976 [classical article]. J Immunol. 2004;173(7):4260-4. Epub 2004/09/24. PubMed PMID: 15383553.

11. Meier JT, Lewis SM. P nucleotides in V(D)J recombination: a fine-structure analysis. Mol Cell Biol. 1993;13(2):1078-92. Epub 1993/02/01. doi: 10.1128/mcb.13.2.1078. PubMed PMID: 8380891; PubMed Central PMCID: PMCPMC358993.

12. Briney B, Inderbitzin A, Joyce C, Burton DR. Commonality despite exceptional diversity in the baseline human antibody repertoire. Nature. 2019;566(7744):393-7. Epub 2019/01/22. doi: 10.1038/s41586-019-0879-y. PubMed PMID: 30664748; PubMed Central PMCID: PMCPMC6411386.

13. Soto C, Bombardi RG, Branchizio A, Kose N, Matta P, Sevy AM, et al. High frequency of shared clonotypes in human B cell receptor repertoires. Nature. 2019;566(7744):398-402. Epub 2019/02/15. doi: 10.1038/s41586-019-0934-8. PubMed PMID: 30760926; PubMed Central PMCID: PMCPMC6949180.

14. Sandel PC, Monroe JG. Negative selection of immature B cells by receptor editing or deletion is determined by site of antigen encounter. Immunity. 1999;10(3):289-99. Epub 1999/04/16. doi: 10.1016/s1074-7613(00)80029-1. PubMed PMID: 10204485.

15. Pelanda R, Torres RM. Central B-cell tolerance: where selection begins. Cold Spring Harb Perspect Biol. 2012;4(4):a007146. Epub 2012/03/02. doi: 10.1101/cshperspect.a007146. PubMed PMID: 22378602; PubMed Central PMCID: PMCPMC3312675.

16. Dornmair K, Goebels N, Weltzien HU, Wekerle H, Hohlfeld R. T-cell-mediated autoimmunity: novel techniques to characterize autoreactive T-cell receptors. Am J Pathol. 2003;163(4):1215-26. Epub 2003/09/26. doi: 10.1016/S0002-9440(10)63481-5. PubMed PMID: 14507631; PubMed Central PMCID: PMCPMC1868314.

17. Vermi W, Lonardi S, Bosisio D, Uguccioni M, Danelon G, Pileri S, et al. Identification of CXCL13 as a new marker for follicular dendritic cell sarcoma. J Pathol. 2008;216(3):356-64. Epub 2008/09/16. doi: 10.1002/path.2420. PubMed PMID: 18792075.

18. Heesters BA, Myers RC, Carroll MC. Follicular dendritic cells: dynamic antigen libraries. Nat Rev Immunol. 2014;14(7):495-504. Epub 2014/06/21. doi: 10.1038/nri3689. PubMed PMID: 24948364.

19. Heesters BA, Chatterjee P, Kim YA, Gonzalez SF, Kuligowski MP, Kirchhausen T, et al. Endocytosis and recycling of immune complexes by follicular dendritic cells enhances B cell antigen binding and activation. Immunity. 2013;38(6):1164-75. Epub 2013/06/19. doi: 10.1016/j.immuni.2013.02.023. PubMed PMID: 23770227; PubMed Central PMCID: PMCPMC3773956.

20. Allende ML, Tuymetova G, Lee BG, Bonifacino E, Wu YP, Proia RL. S1P1 receptor directs the release of immature B cells from bone marrow into blood. J Exp Med. 2010;207(5):1113-24. Epub 2010/04/21. doi: 10.1084/jem.20092210. PubMed PMID: 20404103; PubMed Central PMCID: PMCPMC2867276.

21. Bortnick A, Allman D. What is and what should always have been: long-lived plasma cells induced by T cell-independent antigens. J Immunol. 2013;190(12):5913-8. Epub 2013/06/12. doi: 10.4049/jimmunol.1300161. PubMed PMID: 23749966; PubMed Central PMCID: PMCPMC4234153.

22. Batista FD, Harwood NE. The who, how and where of antigen presentation to B cells. Nat Rev Immunol. 2009;9(1):15-27. Epub 2008/12/17. doi: 10.1038/nri2454. PubMed PMID: 19079135.

23. Krieg AM, Yi AK, Matson S, Waldschmidt TJ, Bishop GA, Teasdale R, et al. CpG motifs in bacterial DNA trigger direct B-cell activation. Nature. 1995;374(6522):546-9. Epub 1995/04/06. doi: 10.1038/374546a0. PubMed PMID: 7700380.

24. De Silva NS, Klein U. Dynamics of B cells in germinal centres. Nat Rev Immunol. 2015;15(3):137-48. Epub 2015/02/07. doi: 10.1038/nri3804. PubMed PMID: 25656706; PubMed Central PMCID: PMCPMC4399774.

25. Scharer CD, Patterson DG, Mi T, Price MJ, Hicks SL, Boss JM. Antibody-secreting cell destiny emerges during the initial stages of B-cell activation. Nat Commun. 2020;11(1):3989. Epub 2020/08/12. doi: 10.1038/s41467-020-17798-x. PubMed PMID: 32778653; PubMed Central PMCID: PMCPMC7417592.

26. Stavnezer J, Guikema JE, Schrader CE. Mechanism and regulation of class switch recombination. Annu Rev Immunol. 2008;26:261-92. Epub 2008/03/29. doi: 10.1146/annurev.immunol.26.021607.090248. PubMed PMID: 18370922; PubMed Central PMCID: PMCPMC2707252.

27. Muramatsu M, Kinoshita K, Fagarasan S, Yamada S, Shinkai Y, Honjo T. Class switch recombination and hypermutation require activation-induced cytidine deaminase (AID), a potential RNA editing enzyme. Cell. 2000;102(5):553-63. Epub 2000/09/28. doi: 10.1016/s0092-8674(00)00078-7. PubMed PMID: 11007474.

28. Roco JA, Mesin L, Binder SC, Nefzger C, Gonzalez-Figueroa P, Canete PF, et al. Class-Switch Recombination Occurs Infrequently in Germinal Centers. Immunity. 2019;51(2):337-50 e7. Epub 2019/08/04. doi: 10.1016/j.immuni.2019.07.001. PubMed PMID: 31375460; PubMed Central PMCID: PMCPMC6914312.

29. Stavnezer J, Schrader CE. IgH chain class switch recombination: mechanism and regulation. J Immunol. 2014;193(11):5370-8. Epub 2014/11/21. doi: 10.4049/jimmunol.1401849. PubMed PMID: 25411432; PubMed Central PMCID: PMCPMC4447316.

30. Kurosaki T, Kometani K, Ise W. Memory B cells. Nat Rev Immunol. 2015;15(3):149-59. Epub 2015/02/14. doi: 10.1038/nri3802. PubMed PMID: 25677494.

31. Takemori T, Kaji T, Takahashi Y, Shimoda M, Rajewsky K. Generation of memory B cells inside and outside germinal centers. Eur J Immunol. 2014;44(5):1258-64. Epub 2014/03/13. doi: 10.1002/eji.201343716. PubMed PMID: 24610726.

32. Schwickert TA, Victora GD, Fooksman DR, Kamphorst AO, Mugnier MR, Gitlin AD, et al. A dynamic T cell-limited checkpoint regulates affinity-dependent B cell entry into the germinal center. J Exp Med. 2011;208(6):1243-52. Epub 2011/05/18. doi: 10.1084/jem.20102477. PubMed PMID: 21576382; PubMed Central PMCID: PMCPMC3173244.

33. Gitlin AD, Shulman Z, Nussenzweig MC. Clonal selection in the germinal centre by regulated proliferation and hypermutation. Nature. 2014;509(7502):637-40. Epub 2014/05/09. doi: 10.1038/nature13300. PubMed PMID: 24805232; PubMed Central PMCID: PMCPMC4271732.

34. Crotty S. T follicular helper cell differentiation, function, and roles in disease. Immunity. 2014;41(4):529-42. Epub 2014/11/05. doi: 10.1016/j.immuni.2014.10.004. PubMed PMID: 25367570; PubMed Central PMCID: PMCPMC4223692.

35. Chaudhuri J, Tian M, Khuong C, Chua K, Pinaud E, Alt FW. Transcription-targeted DNA deamination by the AID antibody diversification enzyme. Nature. 2003;422(6933):726-30. Epub 2003/04/15. doi: 10.1038/nature01574. PubMed PMID: 12692563.

36. Caron G, Le Gallou S, Lamy T, Tarte K, Fest T. CXCR4 expression functionally discriminates centroblasts versus centrocytes within human germinal center B cells. J Immunol. 2009;182(12):7595-602. Epub 2009/06/06. doi: 10.4049/jimmunol.0804272. PubMed PMID: 19494283.

37. Allen CD, Ansel KM, Low C, Lesley R, Tamamura H, Fujii N, et al. Germinal center dark and light zone organization is mediated by CXCR4 and CXCR5. Nat Immunol. 2004;5(9):943-52. Epub 2004/08/10. doi: 10.1038/ni1100. PubMed PMID: 15300245.

38. Chappell CP, Draves KE, Giltiay NV, Clark EA. Extrafollicular B cell activation by marginal zone dendritic cells drives T cell-dependent antibody responses. J Exp Med. 2012;209(10):1825-40. Epub 2012/09/12. doi: 10.1084/jem.20120774. PubMed PMID: 22966002; PubMed Central PMCID: PMCPMC3457737.

39. Priyamvada L, Cho A, Onlamoon N, Zheng NY, Huang M, Kovalenkov Y, et al. B Cell Responses during Secondary Dengue Virus Infection Are Dominated by Highly Cross-Reactive, Memory-Derived Plasmablasts. J Virol. 2016;90(12):5574-85. doi: 10.1128/JVI.03203-15. PubMed PMID: 27030262; PubMed Central PMCID: PMCPMC4886779.

40. Kauffman RC, Bhuiyan TR, Nakajima R, Mayo-Smith LM, Rashu R, Hoq MR, et al. Single-Cell Analysis of the Plasmablast Response to Vibrio cholerae Demonstrates Expansion of Cross-

Reactive Memory B Cells. MBio. 2016;7(6). doi: 10.1128/mBio.02021-16. PubMed PMID: 27999163; PubMed Central PMCID: PMCPMC5181778.

41. Fairfax KA, Kallies A, Nutt SL, Tarlinton DM. Plasma cell development: from B-cell subsets to long-term survival niches. Semin Immunol. 2008;20(1):49-58. Epub 2008/01/29. doi: 10.1016/j.smim.2007.12.002. PubMed PMID: 18222702.

42. Halliley JL, Kyu S, Kobie JJ, Walsh EE, Falsey AR, Randall TD, et al. Peak frequencies of circulating human influenza-specific antibody secreting cells correlate with serum antibody response after immunization. Vaccine. 2010;28(20):3582-7. Epub 2010/03/20. doi: 10.1016/j.vaccine.2010.02.088. PubMed PMID: 20298818; PubMed Central PMCID: PMCPMC2956140.

43. Cho A, Bradley B, Kauffman R, Priyamvada L, Kovalenkov Y, Feldman R, et al. Robust memory responses against influenza vaccination in pemphigus patients previously treated with rituximab. JCI Insight. 2017;2(12). Epub 2017/06/15. doi: 10.1172/jci.insight.93222. PubMed PMID: 28614800; PubMed Central PMCID: PMCPMC5470882.

44. Aktar A, Rahman MA, Afrin S, Faruk MO, Uddin T, Akter A, et al. O-Specific Polysaccharide-Specific Memory B Cell Responses in Young Children, Older Children, and Adults Infected with Vibrio cholerae O1 Ogawa in Bangladesh. Clin Vaccine Immunol. 2016;23(5):427-35. doi: 10.1128/CVI.00647-15. PubMed PMID: 27009211; PubMed Central PMCID: PMCPMC4860469.

45. Priyamvada L, Quicke KM, Hudson WH, Onlamoon N, Sewatanon J, Edupuganti S, et al. Human antibody responses after dengue virus infection are highly cross-reactive to Zika virus. Proc Natl Acad Sci U S A. 2016;113(28):7852-7. doi: 10.1073/pnas.1607931113. PubMed PMID: 27354515; PubMed Central PMCID: PMCPMC4948328.

46. MacLennan IC, Toellner KM, Cunningham AF, Serre K, Sze DM, Zuniga E, et al. Extrafollicular antibody responses. Immunol Rev. 2003;194:8-18. Epub 2003/07/09. PubMed PMID: 12846803.

47. Garimalla S, Nguyen DC, Halliley JL, Tipton C, Rosenberg AF, Fucile CF, et al. Differential transcriptome and development of human peripheral plasma cell subsets. JCI Insight. 2019;4(9). Epub 2019/05/03. doi: 10.1172/jci.insight.126732. PubMed PMID: 31045577; PubMed Central PMCID: PMCPMC6538338.

48. Racine R, Chatterjee M, Winslow GM. CD11c expression identifies a population of extrafollicular antigen-specific splenic plasmablasts responsible for CD4 T-independent antibody responses during intracellular bacterial infection. J Immunol. 2008;181(2):1375-85. Epub 2008/07/09. PubMed PMID: 18606692; PubMed Central PMCID: PMCPMC2645789.

49. Lee SK, Rigby RJ, Zotos D, Tsai LM, Kawamoto S, Marshall JL, et al. B cell priming for extrafollicular antibody responses requires Bcl-6 expression by T cells. J Exp Med. 2011;208(7):1377-88. Epub 2011/06/29. doi: 10.1084/jem.20102065. PubMed PMID: 21708925; PubMed Central PMCID: PMCPMC3135363.

50. Arumugakani G, Stephenson SJ, Newton DJ, Rawstron A, Emery P, Doody GM, et al. Early Emergence of CD19-Negative Human Antibody-Secreting Cells at the Plasmablast to Plasma Cell Transition. J Immunol. 2017;198(12):4618-28. Epub 2017/05/12. doi: 10.4049/jimmunol.1501761. PubMed PMID: 28490574; PubMed Central PMCID: PMCPMC5458329.

51. Slifka MK, Antia R, Whitmire JK, Ahmed R. Humoral immunity due to long-lived plasma cells. Immunity. 1998;8(3):363-72. Epub 1998/04/07. PubMed PMID: 9529153.

52. Nguyen DC, Garimalla S, Xiao H, Kyu S, Albizua I, Galipeau J, et al. Factors of the bone marrow microniche that support human plasma cell survival and immunoglobulin secretion. Nat Commun. 2018;9(1):3698. Epub 2018/09/14. doi: 10.1038/s41467-018-05853-7. PubMed PMID: 30209264; PubMed Central PMCID: PMCPMC6135805.

53. Halliley JL, Tipton CM, Liesveld J, Rosenberg AF, Darce J, Gregoretti IV, et al. Long-Lived Plasma Cells Are Contained within the CD19(-)CD38(hi)CD138(+) Subset in Human Bone Marrow. Immunity. 2015;43(1):132-45. Epub 2015/07/19. doi: 10.1016/j.immuni.2015.06.016. PubMed PMID: 26187412; PubMed Central PMCID: PMCPMC4680845.

54. Landsverk OJ, Snir O, Casado RB, Richter L, Mold JE, Reu P, et al. Antibody-secreting plasma cells persist for decades in human intestine. J Exp Med. 2017;214(2):309-17. doi: 10.1084/jem.20161590. PubMed PMID: 28104812; PubMed Central PMCID: PMCPMC5294861.

55. Mesin L, Di Niro R, Thompson KM, Lundin KE, Sollid LM. Long-lived plasma cells from human small intestine biopsies secrete immunoglobulins for many weeks in vitro. J Immunol.

2011;187(6):2867-74. Epub 2011/08/16. doi: 10.4049/jimmunol.1003181. PubMed PMID: 21841131.

56. Nguyen DC, Joyner CJ, Sanz I, Lee FE. Factors Affecting Early Antibody Secreting Cell Maturation Into Long-Lived Plasma Cells. Front Immunol. 2019;10:2138. Epub 2019/10/02. doi: 10.3389/fimmu.2019.02138. PubMed PMID: 31572364; PubMed Central PMCID: PMCPMC6749102.

57. Hebeis BJ, Klenovsek K, Rohwer P, Ritter U, Schneider A, Mach M, et al. Activation of virus-specific memory B cells in the absence of T cell help. J Exp Med. 2004;199(4):593-602. Epub 2004/02/11. doi: 10.1084/jem.20030091. PubMed PMID: 14769849; PubMed Central PMCID: PMCPMC2211828.

58. Viant C, Weymar GHJ, Escolano A, Chen S, Hartweger H, Cipolla M, et al. Antibody Affinity Shapes the Choice between Memory and Germinal Center B Cell Fates. Cell. 2020;183(5):1298-311 e11. Epub 2020/10/31. doi: 10.1016/j.cell.2020.09.063. PubMed PMID: 33125897; PubMed Central PMCID: PMCPMC7722471.

59. Weisel FJ, Zuccarino-Catania GV, Chikina M, Shlomchik MJ. A Temporal Switch in the Germinal Center Determines Differential Output of Memory B and Plasma Cells. Immunity. 2016;44(1):116-30. Epub 2016/01/23. doi: 10.1016/j.immuni.2015.12.004. PubMed PMID: 26795247; PubMed Central PMCID: PMCPMC4724390.

60. Mesin L, Schiepers A, Ersching J, Barbulescu A, Cavazzoni CB, Angelini A, et al. Restricted Clonality and Limited Germinal Center Reentry Characterize Memory B Cell Reactivation by

Boosting. Cell. 2020;180(1):92-106 e11. Epub 2019/12/24. doi: 10.1016/j.cell.2019.11.032. PubMed PMID: 31866068; PubMed Central PMCID: PMCPMC6958527.

61. Zuccarino-Catania GV, Sadanand S, Weisel FJ, Tomayko MM, Meng H, Kleinstein SH, et al. CD80 and PD-L2 define functionally distinct memory B cell subsets that are independent of antibody isotype. Nat Immunol. 2014;15(7):631-7. Epub 2014/06/02. doi: 10.1038/ni.2914. PubMed PMID: 24880458; PubMed Central PMCID: PMCPMC4105703.

62. Lutz J, Dittmann K, Bosl MR, Winkler TH, Wienands J, Engels N. Reactivation of IgG-switched memory B cells by BCR-intrinsic signal amplification promotes IgG antibody production. Nat Commun. 2015;6:8575. Epub 2016/01/28. doi: 10.1038/ncomms9575. PubMed PMID: 26815242; PubMed Central PMCID: PMCPMC4633962.

63. Weisel FJ, Appelt UK, Schneider AM, Horlitz JU, van Rooijen N, Korner H, et al. Unique requirements for reactivation of virus-specific memory B lymphocytes. J Immunol. 2010;185(7):4011-21. Epub 2010/08/27. doi: 10.4049/jimmunol.1001540. PubMed PMID: 20739675.

64. Pandey M, Wykes MN, Hartas J, Good MF, Batzloff MR. Long-term antibody memory induced by synthetic peptide vaccination is protective against Streptococcus pyogenes infection and is independent of memory T cell help. J Immunol. 2013;190(6):2692-701. Epub 2013/02/13. doi: 10.4049/jimmunol.1202333. PubMed PMID: 23401589; PubMed Central PMCID: PMCPMC3594626.

65. Aiba Y, Kometani K, Hamadate M, Moriyama S, Sakaue-Sawano A, Tomura M, et al. Preferential localization of IgG memory B cells adjacent to contracted germinal centers. Proc Natl Acad Sci U S A. 2010;107(27):12192-7. Epub 2010/06/16. doi: 10.1073/pnas.1005443107. PubMed PMID: 20547847; PubMed Central PMCID: PMCPMC2901464.

66. Amanna IJ, Carlson NE, Slifka MK. Duration of humoral immunity to common viral and vaccine antigens. N Engl J Med. 2007;357(19):1903-15. Epub 2007/11/09. doi: 10.1056/NEJMoa066092. PubMed PMID: 17989383.

67. Burlen O, Coutinho A, Freitas AA. Long-lasting thymus-independent immune responses to anti-idiotype lipopolysaccharide conjugates require continuous B cell renewal. Eur J Immunol. 1988;18(9):1433-9. Epub 1988/09/01. doi: 10.1002/eji.1830180920. PubMed PMID: 3262522.

68. Bortnick A, Chernova I, Quinn WJ, 3rd, Mugnier M, Cancro MP, Allman D. Long-lived bone marrow plasma cells are induced early in response to T cell-independent or T cell-dependent antigens. J Immunol. 2012;188(11):5389-96. Epub 2012/04/25. doi: 10.4049/jimmunol.1102808. PubMed PMID: 22529295; PubMed Central PMCID: PMCPMC4341991.

69. Foote JB, Mahmoud TI, Vale AM, Kearney JF. Long-term maintenance of polysaccharide-specific antibodies by IgM-secreting cells. J Immunol. 2012;188(1):57-67. Epub 2011/11/26. doi: 10.4049/jimmunol.1100783. PubMed PMID: 22116821; PubMed Central PMCID: PMCPMC3244511.

70. Koh CY, Yuan D. The functional relevance of NK-cell-mediated upregulation of antigen-specific IgG2a responses. Cell Immunol. 2000;204(2):135-42. Epub 2000/11/09. doi: 10.1006/cimm.2000.1703. PubMed PMID: 11069721.

71. Taillardet M, Haffar G, Mondiere P, Asensio MJ, Gheit H, Burdin N, et al. The thymus-independent immunity conferred by a pneumococcal polysaccharide is mediated by long-lived plasma cells. Blood. 2009;114(20):4432-40. Epub 2009/09/22. doi: 10.1182/blood-2009-01-200014. PubMed PMID: 19767510.

72. Alugupalli KR, Leong JM, Woodland RT, Muramatsu M, Honjo T, Gerstein RM. B1b lymphocytes confer T cell-independent long-lasting immunity. Immunity. 2004;21(3):379-90. Epub 2004/09/11. doi: 10.1016/j.immuni.2004.06.019. PubMed PMID: 15357949.

73. Obukhanych TV, Nussenzweig MC. T-independent type II immune responses generate memory B cells. J Exp Med. 2006;203(2):305-10. Epub 2006/02/16. doi: 10.1084/jem.20052036. PubMed PMID: 16476769; PubMed Central PMCID: PMCPMC2118207.

74. Yang Y, Ghosn EE, Cole LE, Obukhanych TV, Sadate-Ngatchou P, Vogel SN, et al. Antigen-specific memory in B-1a and its relationship to natural immunity. Proc Natl Acad Sci U S A. 2012;109(14):5388-93. Epub 2012/03/17. doi: 10.1073/pnas.1121627109. PubMed PMID: 22421135; PubMed Central PMCID: PMCPMC3325686.

75. Di Niro R, Lee SJ, Vander Heiden JA, Elsner RA, Trivedi N, Bannock JM, et al. Salmonella Infection Drives Promiscuous B Cell Activation Followed by Extrafollicular Affinity Maturation.

Immunity. 2015;43(1):120-31. Epub 2015/07/19. doi: 10.1016/j.immuni.2015.06.013. PubMed PMID: 26187411; PubMed Central PMCID: PMCPMC4523395.

76. Lu LL, Suscovich TJ, Fortune SM, Alter G. Beyond binding: antibody effector functions in infectious diseases. Nat Rev Immunol. 2018;18(1):46-61. Epub 2017/10/25. doi: 10.1038/nri.2017.106. PubMed PMID: 29063907; PubMed Central PMCID: PMCPMC6369690.

77. Vidarsson G, Dekkers G, Rispens T. IgG subclasses and allotypes: from structure to effector functions. Front Immunol. 2014;5:520. Epub 2014/11/05. doi: 10.3389/fimmu.2014.00520. PubMed PMID: 25368619; PubMed Central PMCID: PMCPMC4202688.

78. Schroeder HW, Jr., Cavacini L. Structure and function of immunoglobulins. J Allergy Clin Immunol. 2010;125(2 Suppl 2):S41-52. Epub 2010/03/05. doi: 10.1016/j.jaci.2009.09.046. PubMed PMID: 20176268; PubMed Central PMCID: PMCPMC3670108.

79. Mora JR, von Andrian UH. Differentiation and homing of IgA-secreting cells. Mucosal Immunol. 2008;1(2):96-109. Epub 2008/12/17. doi: 10.1038/mi.2007.14. PubMed PMID: 19079167.

80. Jertborn M, Svennerholm AM, Holmgren J. Saliva, breast milk, and serum antibody responses as indirect measures of intestinal immunity after oral cholera vaccination or natural disease. J Clin Microbiol. 1986;24(2):203-9. Epub 1986/08/01. PubMed PMID: 3528211; PubMed Central PMCID: PMCPMC268875.

81. Pabst O. New concepts in the generation and functions of IgA. Nat Rev Immunol. 2012;12(12):821-32. doi: 10.1038/nri3322. PubMed PMID: 23103985.

82. Mathias A, Corthesy B. Recognition of gram-positive intestinal bacteria by hybridoma- and colostrum-derived secretory immunoglobulin A is mediated by carbohydrates. J Biol Chem. 2011;286(19):17239-47. Epub 2011/04/02. doi: 10.1074/jbc.M110.209015. PubMed PMID: 21454510; PubMed Central PMCID: PMCPMC3089566.

83. Steffen U, Koeleman CA, Sokolova MV, Bang H, Kleyer A, Rech J, et al. IgA subclasses have different effector functions associated with distinct glycosylation profiles. Nat Commun. 2020;11(1):120. Epub 2020/01/09. doi: 10.1038/s41467-019-13992-8. PubMed PMID: 31913287; PubMed Central PMCID: PMCPMC6949214.

84. Breedveld A, van Egmond M. IgA and FcalphaRI: Pathological Roles and Therapeutic Opportunities. Front Immunol. 2019;10:553. Epub 2019/04/16. doi: 10.3389/fimmu.2019.00553. PubMed PMID: 30984170; PubMed Central PMCID: PMCPMC6448004.

85. Brandtzaeg P, Farstad IN, Johansen FE, Morton HC, Norderhaug IN, Yamanaka T. The B-cell system of human mucosae and exocrine glands. Immunol Rev. 1999;171:45-87. Epub 1999/12/03. PubMed PMID: 10582165.

86. Yamanaka T, Straumfors A, Morton H, Fausa O, Brandtzaeg P, Farstad I. M cell pockets of human Peyer's patches are specialized extensions of germinal centers. Eur J Immunol.

2001;31(1):107-17. Epub 2001/02/13. doi: 10.1002/1521-4141(200101)31:1<107::AID-IMMU107>3.0.CO;2-4. PubMed PMID: 11169444.

87. Mora JR, Iwata M, Eksteen B, Song SY, Junt T, Senman B, et al. Generation of gut-homing IgA-secreting B cells by intestinal dendritic cells. Science. 2006;314(5802):1157-60. Epub 2006/11/18. doi: 10.1126/science.1132742. PubMed PMID: 17110582.

88. Boursier L, Dunn-Walters DK, Spencer J. Characteristics of IgVH genes used by human intestinal plasma cells from childhood. Immunology. 1999;97(4):558-64. Epub 1999/08/24. PubMed PMID: 10457207; PubMed Central PMCID: PMCPMC2326878.

89. Palm NW, de Zoete MR, Cullen TW, Barry NA, Stefanowski J, Hao L, et al. Immunoglobulin A coating identifies colitogenic bacteria in inflammatory bowel disease. Cell. 2014;158(5):1000-10. Epub 2014/08/30. doi: 10.1016/j.cell.2014.08.006. PubMed PMID: 25171403; PubMed Central PMCID: PMCPMC4174347.

90. Spencer J, Sollid LM. The human intestinal B-cell response. Mucosal Immunol. 2016;9(5):1113-24. Epub 2016/07/28. doi: 10.1038/mi.2016.59. PubMed PMID: 27461177.

91. Magri G, Comerma L, Pybus M, Sintes J, Llige D, Segura-Garzon D, et al. Human Secretory IgM Emerges from Plasma Cells Clonally Related to Gut Memory B Cells and Targets Highly Diverse Commensals. Immunity. 2017;47(1):118-34 e8. Epub 2017/07/16. doi: 10.1016/j.immuni.2017.06.013. PubMed PMID: 28709802; PubMed Central PMCID: PMCPMC5519504.

92. Lindner C, Thomsen I, Wahl B, Ugur M, Sethi MK, Friedrichsen M, et al. Diversification of memory B cells drives the continuous adaptation of secretory antibodies to gut microbiota. Nat Immunol. 2015;16(8):880-8. Epub 2015/07/07. doi: 10.1038/ni.3213. PubMed PMID: 26147688.

93. Williams MB, Rose JR, Rott LS, Franco MA, Greenberg HB, Butcher EC. The memory B cell subset responsible for the secretory IgA response and protective humoral immunity to rotavirus expresses the intestinal homing receptor, alpha4beta7. J Immunol. 1998;161(8):4227-35. Epub 1998/10/21. PubMed PMID: 9780197.

94. Weisel NM, Weisel FJ, Farber DL, Borghesi LA, Shen Y, Ma W, et al. Comprehensive analyses of B-cell compartments across the human body reveal novel subsets and a gut-resident memory phenotype. Blood. 2020;136(24):2774-85. Epub 2020/08/05. doi: 10.1182/blood.2019002782. PubMed PMID: 32750113; PubMed Central PMCID: PMCPMC7731793.

95. Lemke A, Kraft M, Roth K, Riedel R, Lammerding D, Hauser AE. Long-lived plasma cells are generated in mucosal immune responses and contribute to the bone marrow plasma cell pool in mice. Mucosal Immunol. 2016;9(1):83-97. Epub 2015/05/07. doi: 10.1038/mi.2015.38. PubMed PMID: 25943272.

96. Glass RI, Becker S, Huq MI, Stoll BJ, Khan MU, Merson MH, et al. Endemic cholera in rural Bangladesh, 1966-1980. Am J Epidemiol. 1982;116(6):959-70. PubMed PMID: 7148820.

97. Ali M, Nelson AR, Lopez AL, Sack DA. Updated Global Burden of Cholera in Endemic Countries. Plos Neglect Trop D. 2015;9(6). doi: ARTN e0003832

10.1371/journal.pntd.0003832. PubMed PMID: WOS:000357398100034; PubMed Central PMCID: PMCPMC4455997.

98. Qadri F, Islam T, Clemens JD. Cholera in Yemen - An Old Foe Rearing Its Ugly Head. N Engl J Med. 2017. Epub 2017/11/02. doi: 10.1056/NEJMp1712099. PubMed PMID: 29091747.

99. Teoh SL, Kotirum S, Hutubessy R, Chaiyakunapruk N. Global Economic Evaluation of Oral Cholera Vaccine: A Systematic Review. Hum Vaccin Immunother. 2017:0. Epub 2017/11/04. doi: 10.1080/21645515.2017.1392422. PubMed PMID: 29099647.

100. Azman AS, Rudolph KE, Cummings DA, Lessler J. The incubation period of cholera: a systematic review. J Infect. 2013;66(5):432-8. doi: 10.1016/j.jinf.2012.11.013. PubMed PMID: 23201968; PubMed Central PMCID: PMCPMC3677557.

101. Glass RI, Svennerholm AM, Khan MR, Huda S, Huq MI, Holmgren J. Seroepidemiological Studies of El-Tor Cholera in Bangladesh - Association of Serum Antibody-Levels with Protection. Journal of Infectious Diseases. 1985;151(2):236-42. PubMed PMID: WOS:A1985AAS1200006.

102. Kabir S. Critical analysis of compositions and protective efficacies of oral killed cholera vaccines. Clin Vaccine Immunol. 2014;21(9):1195-205. Epub e. doi: 10.1128/CVI.00378-14. PubMed PMID: 25056361; PubMed Central PMCID: PMCPMC4178583.

103. Yoon SS, Mekalanos JJ. 2,3-butanediol synthesis and the emergence of the Vibrio cholerae El Tor biotype. Infect Immun. 2006;74(12):6547-56. doi: 10.1128/IAI.00695-06. PubMed PMID: 17015461; PubMed Central PMCID: PMCPMC1698044.

104. Clemens JD, Nair GB, Ahmed T, Qadri F, Holmgren J. Cholera. Lancet. 2017;390(10101):1539-49. Epub 2017/03/18. doi: 10.1016/S0140-6736(17)30559-7. PubMed PMID: 28302312.

105. Guentzel MN, Berry LJ. Motility as a virulence factor for Vibrio cholerae. Infect Immun. 1975;11(5):890-7. Epub 1975/05/01. PubMed PMID: 1091563; PubMed Central PMCID: PMCPMC415153.

106. Bharati K, Ganguly NK. Cholera toxin: a paradigm of a multifunctional protein. Indian J Med Res. 2011;133:179-87. Epub 2011/03/19. PubMed PMID: 21415492; PubMed Central PMCID: PMCPMC3089049.

107. Mekalanos JJ, Collier RJ, Romig WR. Enzymic activity of cholera toxin. II. Relationships to proteolytic processing, disulfide bond reduction, and subunit composition. J Biol Chem. 1979;254(13):5855-61. PubMed PMID: 221485.

108. Carpenter CC, Sack RB, Feeley JC, Steenberg RW. Site and characteristics of electrolyte loss and effect of intraluminal glucose in experimental canine cholera. J Clin Invest. 1968;47(5):1210-20. Epub 1968/05/01. doi: 10.1172/JCI105810. PubMed PMID: 5645863; PubMed Central PMCID: PMCPMC297273.

109. Banwell JG, Pierce NF, Mitra RC, Brigham KL, Caranasos GJ, Keimowitz RI, et al. Intestinal fluid and electrolyte transport in human cholera. J Clin Invest. 1970;49(1):183-95. Epub 1970/01/01. doi: 10.1172/JCI106217. PubMed PMID: 5409804; PubMed Central PMCID: PMCPMC322456.

110. Faruque SM, Biswas K, Udden SM, Ahmad QS, Sack DA, Nair GB, et al. Transmissibility of cholera: in vivo-formed biofilms and their relationship to infectivity and persistence in the environment. Proc Natl Acad Sci U S A. 2006;103(16):6350-5. Epub 2006/04/08. doi: 10.1073/pnas.0601277103. PubMed PMID: 16601099; PubMed Central PMCID: PMCPMC1458881.

111. Silva AJ, Benitez JA. Vibrio cholerae Biofilms and Cholera Pathogenesis. PLoS Negl Trop Dis. 2016;10(2):e0004330. Epub 2016/02/06. doi: 10.1371/journal.pntd.0004330. PubMed PMID: 26845681; PubMed Central PMCID: PMCPMC4741415.

112. David LA, Weil A, Ryan ET, Calderwood SB, Harris JB, Chowdhury F, et al. Gut microbial succession follows acute secretory diarrhea in humans. MBio. 2015;6(3):e00381-15. doi: 10.1128/mBio.00381-15. PubMed PMID: 25991682; PubMed Central PMCID: PMCPMC4442136.

113. Lippi D, Gotuzzo E, Caini S. Cholera. Microbiol Spectr. 2016;4(4). Epub 2016/10/12. doi: 10.1128/microbiolspec.PoH-0012-2015. PubMed PMID: 27726771.

114. Levine MM, Nalin DR, Craig JP, Hoover D, Bergquist EJ, Waterman D, et al. Immunity of cholera in man: relative role of antibacterial versus antitoxic immunity. Trans R Soc Trop Med Hyg. 1979;73(1):3-9. PubMed PMID: 442179.

115. Mosley WH, Ahmad S, Benenson AS, Ahmed A. The relationship of vibriocidal antibody titre to susceptibility to cholera in family contacts of cholera patients. Bull World Health Organ. 1968;38(5):777-85. PubMed PMID: 5303331; PubMed Central PMCID: PMCPMC2554681.

116. Benenson AS, Saad A, Mosley WH. Serological studies in cholera. 2. The vibriocidal antibody response of cholera patients determined by a microtechnique. Bull World Health Organ. 1968;38(2):277-85. PubMed PMID: 5302303; PubMed Central PMCID: PMCPMC2554323.

117. Chen WH, Cohen MB, Kirkpatrick BD, Brady RC, Galloway D, Gurwith M, et al. Single-dose Live Oral Cholera Vaccine CVD 103-HgR Protects Against Human Experimental Infection With Vibrio cholerae O1 El Tor. Clin Infect Dis. 2016;62(11):1329-35. doi: 10.1093/cid/ciw145. PubMed PMID: 27001804; PubMed Central PMCID: PMCPMC4872293.

118. Tacket CO, Losonsky G, Nataro JP, Cryz SJ, Edelman R, Kaper JB, et al. Onset and duration of protective immunity in challenged volunteers after vaccination with live oral cholera vaccine CVD 103-HgR. J Infect Dis. 1992;166(4):837-41. PubMed PMID: 1527420.

119. Clemens JD, van Loon F, Sack DA, Chakraborty J, Rao MR, Ahmed F, et al. Field trial of oral cholera vaccines in Bangladesh: serum vibriocidal and antitoxic antibodies as markers of the risk of cholera. J Infect Dis. 1991;163(6):1235-42. PubMed PMID: 2037789.

120. Levine MM, Black RE, Clements ML, Cisneros L, Nalin DR, Young CR. Duration of infection-derived immunity to cholera. J Infect Dis. 1981;143(6):818-20. PubMed PMID: 7252264.

121. Rahman A, Rashu R, Bhuiyan TR, Chowdhury F, Khan AI, Islam K, et al. Antibody-secreting cell responses after Vibrio cholerae O1 infection and oral cholera vaccination in adults

in Bangladesh. Clin Vaccine Immunol. 2013;20(10):1592-8. doi: 10.1128/CVI.00347-13. PubMed PMID: 23945156; PubMed Central PMCID: PMCPMC3807192.

122. Harris AM, Bhuiyan MS, Chowdhury F, Khan AI, Hossain A, Kendall EA, et al. Antigen-specific memory B-cell responses to Vibrio cholerae O1 infection in Bangladesh. Infect Immun. 2009;77(9):3850-6. doi: 10.1128/IAI.00369-09. PubMed PMID: 19528207; PubMed Central PMCID: PMCPMC2738048.

123. Kopp ZA, Jain U, Van Limbergen J, Stadnyk AW. Do antimicrobial peptides and complement collaborate in the intestinal mucosa? Front Immunol. 2015;6:17. doi: 10.3389/fimmu.2015.00017. PubMed PMID: 25688244; PubMed Central PMCID: PMCPMC4311685.

124. Johnson RA, Uddin T, Aktar A, Mohasin M, Alam MM, Chowdhury F, et al. Comparison of immune responses to the O-specific polysaccharide and lipopolysaccharide of Vibrio cholerae O1 in Bangladeshi adult patients with cholera. Clin Vaccine Immunol. 2012;19(11):1712-21. doi: 10.1128/CVI.00321-12. PubMed PMID: 22993410; PubMed Central PMCID: PMCPMC3491541.

125. Uddin T, Aktar A, Xu P, Johnson RA, Rahman MA, Leung DT, et al. Immune responses to O-specific polysaccharide and lipopolysaccharide of Vibrio cholerae O1 Ogawa in adult Bangladeshi recipients of an oral killed cholera vaccine and comparison to responses in patients with cholera. Am J Trop Med Hyg. 2014;90(5):873-81. doi: 10.4269/ajtmh.13-0498. PubMed PMID: 24686738; PubMed Central PMCID: PMCPMC4015581.

126. Yang JS, An SJ, Jang MS, Song M, Han SH. IgM specific to lipopolysaccharide of Vibrio cholerae is a surrogate antibody isotype responsible for serum vibriocidal activity. PLoS One. 2019;14(3):e0213507. Epub 2019/03/08. doi: 10.1371/journal.pone.0213507. PubMed PMID: 30845262; PubMed Central PMCID: PMCPMC6405115.

127. Uddin T, Harris JB, Bhuiyan TR, Shirin T, Uddin MI, Khan AI, et al. Mucosal immunologic responses in cholera patients in Bangladesh. Clin Vaccine Immunol. 2011;18(3):506-12. doi: 10.1128/CVI.00481-10. PubMed PMID: 21248157; PubMed Central PMCID: PMCPMC3067383.

128. Blanc P, Moro-Sibilot L, Barthly L, Jagot F, This S, de Bernard S, et al. Mature IgM-expressing plasma cells sense antigen and develop competence for cytokine production upon antigenic challenge. Nat Commun. 2016;7:13600. Epub 2016/12/08. doi: 10.1038/ncomms13600. PubMed PMID: 27924814; PubMed Central PMCID: PMCPMC5150646.

129. Pinto D, Montani E, Bolli M, Garavaglia G, Sallusto F, Lanzavecchia A, et al. A functional BCR in human IgA and IgM plasma cells. Blood. 2013;121(20):4110-4. Epub 2013/04/04. doi: 10.1182/blood-2012-09-459289. PubMed PMID: 23550036.

130. Tengvall S, Lundgren A, Quiding-Jarbrink M, Svennerholm AM. BAFF, stimulatory DNA and IL-15 stimulates IgA(+) memory B cells and provides a novel approach for analysis of memory responses to mucosal vaccines. Vaccine. 2010;28(33):5445-50. Epub 2010/06/16. doi: 10.1016/j.vaccine.2010.06.001. PubMed PMID: 20547203.

131. van Splunter M, van Hoffen E, Floris-Vollenbroek EG, Timmerman H, de Bos EL, Meijer B, et al. Oral cholera vaccination promotes homing of IgA(+) memory B cells to the large intestine

and the respiratory tract. Mucosal Immunol. 2018. Epub 2018/02/23. doi: 10.1038/s41385-018-0006-7. PubMed PMID: 29467446.

132. Patel SM, Rahman MA, Mohasin M, Riyadh MA, Leung DT, Alam MM, et al. Memory B cell responses to Vibrio cholerae O1 lipopolysaccharide are associated with protection against infection from household contacts of patients with cholera in Bangladesh. Clin Vaccine Immunol. 2012;19(6):842-8. doi: 10.1128/CVI.00037-12. PubMed PMID: 22518009; PubMed Central PMCID: PMCPMC3370438.

133. Cash RA, Music SI, Libonati JP, Snyder MJ, Wenzel RP, Hornick RB. Response of man to infection with Vibrio cholerae. I. Clinical, serologic, and bacteriologic responses to a known inoculum. J Infect Dis. 1974;129(1):45-52. Epub 1974/01/01. doi: 10.1093/infdis/129.1.45. PubMed PMID: 4809112.

134. Elson CO, Ealding W. Generalized systemic and mucosal immunity in mice after mucosal stimulation with cholera toxin. J Immunol. 1984;132(6):2736-41. Epub 1984/06/01. PubMed PMID: 6233359.

135. Dallas WS, Falkow S. Amino acid sequence homology between cholera toxin and Escherichia coli heat-labile toxin. Nature. 1980;288(5790):499-501. Epub 1980/12/04. doi: 10.1038/288499a0. PubMed PMID: 7003397.

136. Domenighini M, Pizza M, Jobling MG, Holmes RK, Rappuoli R. Identification of errors among database sequence entries and comparison of correct amino acid sequences for the heat-labile enterotoxins of Escherichia coli and Vibrio cholerae. Mol Microbiol.

1995;15(6):1165-7. Epub 1995/03/01. doi: 10.1111/j.1365-2958.1995.tb02289.x. PubMed PMID: 7623669.

137. Harris JB, LaRocque RC, Chowdhury F, Khan AI, Logvinenko T, Faruque AS, et al. Susceptibility to Vibrio cholerae infection in a cohort of household contacts of patients with cholera in Bangladesh. PLoS Negl Trop Dis. 2008;2(4):e221. doi: 10.1371/journal.pntd.0000221. PubMed PMID: 18398491; PubMed Central PMCID: PMCPMC2271133.

138. Levine MM, Chen WH, Kaper JB, Lock M, Danzig L, Gurwith M. PaxVax CVD 103-HgR single-dose live oral cholera vaccine. Expert Rev Vaccines. 2017;16(3):197-213. doi: 10.1080/14760584.2017.1291348. PubMed PMID: 28165831.

139. Chowdhury F, Khan AI, Harris JB, LaRocque RC, Chowdhury MI, Ryan ET, et al. A comparison of clinical and immunologic features in children and older patients hospitalized with severe cholera in Bangladesh. Pediatr Infect Dis J. 2008;27(11):986-92. doi: 10.1097/INF.0b013e3181783adf. PubMed PMID: 18833030; PubMed Central PMCID: PMCPMC2749325.

140. Bhuiyan TR, Lundin SB, Khan AI, Lundgren A, Harris JB, Calderwood SB, et al. Cholera caused by Vibrio cholerae O1 induces T-cell responses in the circulation. Infect Immun. 2009;77(5):1888-93. Epub 2009/02/25. doi: 10.1128/IAI.01101-08. PubMed PMID: 19237532; PubMed Central PMCID: PMCPMC2681774.

141. Leung DT, Rahman MA, Mohasin M, Patel SM, Aktar A, Khanam F, et al. Memory B cell and other immune responses in children receiving two doses of an oral killed cholera vaccine

compared to responses following natural cholera infection in Bangladesh. Clin Vaccine Immunol. 2012;19(5):690-8. Epub 2012/03/24. doi: 10.1128/CVI.05615-11. PubMed PMID: 22441386; PubMed Central PMCID: PMCPMC3346319.

142. Leitch GJ, Iwert ME, Burrows W. Experimental cholera in the rabbit ligated ileal loop: toxin-induced water and ion movement. J Infect Dis. 1966;116(3):303-12. Epub 1966/06/01. PubMed PMID: 5940329.

143. Sawasvirojwong S, Srimanote P, Chatsudthipong V, Muanprasat C. An Adult Mouse Model of Vibrio cholerae-induced Diarrhea for Studying Pathogenesis and Potential Therapy of Cholera. PLoS Negl Trop Dis. 2013;7(6):e2293. Epub 2013/07/05. doi: 10.1371/journal.pntd.0002293. PubMed PMID: 23826402; PubMed Central PMCID: PMCPMC3694821.

144. Kojima S, Yamamoto K, Kawagishi I, Homma M. The polar flagellar motor of Vibrio cholerae is driven by an Na+ motive force. J Bacteriol. 1999;181(6):1927-30. Epub 1999/03/12. PubMed PMID: 10074090; PubMed Central PMCID: PMCPMC93596.

145. Baranova DE, Willsey GG, Levinson KJ, Smith C, Wade J, Mantis NJ. Transcriptional profiling of Vibrio cholerae O1 following exposure to human anti- lipopolysaccharide monoclonal antibodies. Pathog Dis. 2020;78(4). Epub 2020/06/27. doi: 10.1093/femspd/ftaa029. PubMed PMID: 32589220; PubMed Central PMCID: PMCPMC7371154.

146. Levinson KJ, De Jesus M, Mantis NJ. Rapid effects of a protective O-polysaccharide-specific monoclonal IgA on Vibrio cholerae agglutination, motility, and surface morphology. Infect Immun. 2015;83(4):1674-83. doi: 10.1128/IAI.02856-14. PubMed PMID: 25667263; PubMed Central PMCID: PMCPMC4363435.

147. Wang Z, Lazinski DW, Camilli A. Immunity Provided by an Outer Membrane Vesicle Cholera Vaccine Is Due to O-Antigen-Specific Antibodies Inhibiting Bacterial Motility. Infect Immun. 2017;85(1). doi: 10.1128/IAI.00626-16. PubMed PMID: 27795359; PubMed Central PMCID: PMCPMC5203661.

148. Levine MM, Kaper JB, Herrington D, Ketley J, Losonsky G, Tacket CO, et al. Safety, immunogenicity, and efficacy of recombinant live oral cholera vaccines, CVD 103 and CVD 103-HgR. Lancet. 1988;2(8609):467-70. PubMed PMID: 2900401.

149. Kaper JB, Lockman H, Baldini MM, Levine MM. A Recombinant Live Oral Cholera Vaccine. Bio/Technology. 1984;2(4):345-9. doi: 10.1038/nbt0484-345.

150. Cryz SJ, Jr., Levine MM, Losonsky G, Kaper JB, Althaus B. Safety and immunogenicity of a booster dose of Vibrio cholerae CVD 103-HgR live oral cholera vaccine in Swiss adults. Infect Immun. 1992;60(9):3916-7. PubMed PMID: 1500200; PubMed Central PMCID: PMCPMC257409.

151. Migasena S, Pitisuttitham P, Prayurahong B, Suntharasamai P, Supanaranond W, Desakorn V, et al. Preliminary assessment of the safety and immunogenicity of live oral cholera

vaccine strain CVD 103-HgR in healthy Thai adults. Infect Immun. 1989;57(11):3261-4. PubMed PMID: 2807523; PubMed Central PMCID: PMCPMC259791.

152. Tacket CO, Kotloff KL, Losonsky G, Nataro JP, Michalski J, Kaper JB, et al. Volunteer studies investigating the safety and efficacy of live oral El Tor Vibrio cholerae O1 vaccine strain CVD 111. Am J Trop Med Hyg. 1997;56(5):533-7. PubMed PMID: 9180604.

153. Taylor DN, Tacket CO, Losonsky G, Castro O, Gutierrez J, Meza R, et al. Evaluation of a bivalent (CVD 103-HgR/CVD 111) live oral cholera vaccine in adult volunteers from the United States and Peru. Infect Immun. 1997;65(9):3852-6. PubMed PMID: 9284163; PubMed Central PMCID: PMCPMC175550.

154. Su-Arehawaratana P, Singharaj P, Taylor DN, Hoge C, Trofa A, Kuvanont K, et al. Safety and immunogenicity of different immunization regimens of CVD 103-HgR live oral cholera vaccine in soldiers and civilians in Thailand. J Infect Dis. 1992;165(6):1042-8. PubMed PMID: 1583321.

155. Wasserman SS, Losonsky GA, Noriega F, Tacket CO, Castaneda E, Levine MM. Kinetics of the vibriocidal antibody response to live oral cholera vaccines. Vaccine. 1994;12(11):1000-3. PubMed PMID: 7975839.

156. Lagos R, Avendano A, Prado V, Horwitz I, Wasserman S, Losonsky G, et al. Attenuated live cholera vaccine strain CVD 103-HgR elicits significantly higher serum vibriocidal antibody titers in persons of blood group O. Infect Immun. 1995;63(2):707-9. PubMed PMID: 7822046; PubMed Central PMCID: PMCPMC173056.

157. Losonsky GA, Tacket CO, Wasserman SS, Kaper JB, Levine MM. Secondary Vibrio cholerae-specific cellular antibody responses following wild-type homologous challenge in people vaccinated with CVD 103-HgR live oral cholera vaccine: changes with time and lack of correlation with protection. Infect Immun. 1993;61(2):729-33. PubMed PMID: 8423098; PubMed Central PMCID: PMCPMC302786.

158. Viret JF, Favre D, Wegmuller B, Herzog C, Que JU, Cryz SJ, Jr., et al. Mucosal and systemic immune responses in humans after primary and booster immunizations with orally administered invasive and noninvasive live attenuated bacteria. Infect Immun. 1999;67(7):3680-5. PubMed PMID: 10377160; PubMed Central PMCID: PMCPMC116565.

159. Clements ML, Levine MM, Young CR, Black RE, Lim YL, Robins-Browne RM, et al. Magnitude, kinetics, and duration of vibriocidal antibody responses in North Americans after ingestion of Vibrio cholerae. J Infect Dis. 1982;145(4):465-73. PubMed PMID: 7069227.

160. Alam MM, Riyadh MA, Fatema K, Rahman MA, Akhtar N, Ahmed T, et al. Antigen-specific memory B-cell responses in Bangladeshi adults after one- or two-dose oral killed cholera vaccination and comparison with responses in patients with naturally acquired cholera. Clin Vaccine Immunol. 2011;18(5):844-50. doi: 10.1128/CVI.00562-10. PubMed PMID: 21346055; PubMed Central PMCID: PMCPMC3122537.

161. Bhuiyan TR, Hoq MR, Nishat NS, Al Mahbuba D, Rashu R, Islam K, et al. Enumeration of Gut-Homing beta7-Positive, Pathogen-Specific Antibody-Secreting Cells in Whole Blood from Enterotoxigenic Escherichia coli- and Vibrio cholerae-Infected Patients, Determined Using an

Enzyme-Linked Immunosorbent Spot Assay Technique. Clin Vaccine Immunol. 2015;23(1):27-36. Epub 2015/10/30. doi: 10.1128/CVI.00526-15. PubMed PMID: 26512047; PubMed Central PMCID: PMCPMC4711085.

162. Svennerholm AM, Holmgren J. Synergistic protective effect in rabbits of immunization with Vibrio cholerae lipopolysaccharide and toxin/toxoid. Infect Immun. 1976;13(3):735-40. Epub 1976/03/01. doi: 10.1128/IAI.13.3.735-740.1976. PubMed PMID: 1270131; PubMed Central PMCID: PMCPMC420671.

163. Black RE, Levine MM, Clements ML, Young CR, Svennerholm AM, Holmgren J. Protective efficacy in humans of killed whole-vibrio oral cholera vaccine with and without the B subunit of cholera toxin. Infect Immun. 1987;55(5):1116-20. PubMed PMID: 3552989; PubMed Central PMCID: PMCPMC260477.

164. Karlsson SL, Ax E, Nygren E, Kallgard S, Blomquist M, Ekman A, et al. Development of stable Vibrio cholerae O1 Hikojima type vaccine strains co-expressing the Inaba and Ogawa lipopolysaccharide antigens. PLoS One. 2014;9(11):e108521. doi: 10.1371/journal.pone.0108521. PubMed PMID: 25397871; PubMed Central PMCID: PMCPMC4232259.

165. Santé WHOOmdl. Weekly Epidemiological Record. Weekly Epidemiological Record = Relevé épidémiologique hebdomadaire. 2020; 95 (37)(37): 441 - 8. Epub 11 September 2020.

166. Mosley WH, McCormack WM, Ahmed A, Chowdhury AK, Barui RK. Report of the 1966-67 cholera vaccine field trial in rural East Pakistan. 2. Results of the serological surveys in the

study population--the relationship of case rate to antibody titre and an estimate of the inapparent infection rate with Vibrio cholerae. Bull World Health Organ. 1969;40(2):187-97. PubMed PMID: 5306539; PubMed Central PMCID: PMCPMC2554605.

167. Saha D, LaRocque RC, Khan AI, Harris JB, Begum YA, Akramuzzaman SM, et al. Incomplete correlation of serum vibriocidal antibody titer with protection from Vibrio cholerae infection in urban Bangladesh. J Infect Dis. 2004;189(12):2318-22. doi: 10.1086/421275. PubMed PMID: 15181581.

168. Sina C, Kemper C, Derer S. The intestinal complement system in inflammatory bowel disease: Shaping intestinal barrier function. Semin Immunol. 2018;37:66-73. Epub 2018/03/01. doi: 10.1016/j.smim.2018.02.008. PubMed PMID: 29486961.

169. Jain U, Otley AR, Van Limbergen J, Stadnyk AW. The complement system in inflammatory bowel disease. Inflamm Bowel Dis. 2014;20(9):1628-37. Epub 2014/05/17. doi: 10.1097/MIB.0000000000000056. PubMed PMID: 24831561.

170. Herzog C. Successful comeback of the single-dose live oral cholera vaccine CVD 103-HgR. Travel Med Infect Dis. 2016;14(4):373-7. doi: 10.1016/j.tmaid.2016.07.003. PubMed PMID: 27425792.

171. Chen WH, Greenberg RN, Pasetti MF, Livio S, Lock M, Gurwith M, et al. Safety and immunogenicity of single-dose live oral cholera vaccine strain CVD 103-HgR, prepared from new master and working cell banks. Clin Vaccine Immunol. 2014;21(1):66-73. doi: 10.1128/CVI.00601-13. PubMed PMID: 24173028; PubMed Central PMCID: PMCPMC3910924.

172. Cabrera A, Lepage JE, Sullivan KM, Seed SM. Vaxchora: A Single-Dose Oral Cholera Vaccine. Ann Pharmacother. 2017;51(7):584-9. Epub 2017/06/18. doi: 10.1177/1060028017698162. PubMed PMID: 28622736.

173. Suharyono, Simanjuntak C, Totosudirjo H, Witham N, Punjabi N, Burr D, et al. Safety and immunogenicity of single-dose live oral cholera vaccine CVD 103-HgR in 5-9-year-old Indonesian children. The Lancet. 1992;340(8821):689-94. doi: 10.1016/0140-6736(92)92231-4.

174. Sack RB, Barua D, Saxena R, Carpenter CC. Vibriocidal and agglutinating antibody patterns in cholera patients. J Infect Dis. 1966;116(5):630-40. Epub 1966/12/01. doi: 10.1093/infdis/116.5.630. PubMed PMID: 5957269.

175. Herrington DA, Hall RH, Losonsky G, Mekalanos JJ, Taylor RK, Levine MM. Toxin, toxin-coregulated pili, and the toxR regulon are essential for Vibrio cholerae pathogenesis in humans. J Exp Med. 1988;168(4):1487-92. Epub 1988/10/01. PubMed PMID: 2902187; PubMed Central PMCID: PMCPMC2189073.

176. Heiman KE, Mody RK, Johnson SD, Griffin PM, Gould LH. Escherichia coli O157 Outbreaks in the United States, 2003-2012. Emerg Infect Dis. 2015;21(8):1293-301. Epub 2015/07/23. doi: 10.3201/eid2108.141364. PubMed PMID: 26197993; PubMed Central PMCID: PMCPMC4517704.

177. Scallan E, Hoekstra RM, Angulo FJ, Tauxe RV, Widdowson MA, Roy SL, et al. Foodborne illness acquired in the United States--major pathogens. Emerg Infect Dis. 2011;17(1):7-15. Epub

2011/01/05. doi: 10.3201/eid1701.P11101. PubMed PMID: 21192848; PubMed Central PMCID: PMCPMC3375761.

178. Jackson SM, Wilson PC, James JA, Capra JD. Human B cell subsets. Adv Immunol. 2008;98:151-224. Epub 2008/09/06. doi: 10.1016/S0065-2776(08)00405-7. PubMed PMID: 18772006.

179. Habtezion A, Nguyen LP, Hadeiba H, Butcher EC. Leukocyte Trafficking to the Small Intestine and Colon. Gastroenterology. 2016;150(2):340-54. Epub 2015/11/10. doi: 10.1053/j.gastro.2015.10.046. PubMed PMID: 26551552; PubMed Central PMCID: PMCPMC4758453.

180. Hammerschmidt SI, Ahrendt M, Bode U, Wahl B, Kremmer E, Forster R, et al. Stromal mesenteric lymph node cells are essential for the generation of gut-homing T cells in vivo. J Exp Med. 2008;205(11):2483-90. Epub 2008/10/15. doi: 10.1084/jem.20080039. PubMed PMID: 18852290; PubMed Central PMCID: PMCPMC2571923.

181. Houston SA, Cerovic V, Thomson C, Brewer J, Mowat AM, Milling S. The lymph nodes draining the small intestine and colon are anatomically separate and immunologically distinct. Mucosal Immunol. 2016;9(2):468-78. Epub 2015/09/04. doi: 10.1038/mi.2015.77. PubMed PMID: 26329428.

182. Berkowska MA, Schickel JN, Grosserichter-Wagener C, de Ridder D, Ng YS, van Dongen JJ, et al. Circulating Human CD27-IgA+ Memory B Cells Recognize Bacteria with Polyreactive Igs.

J Immunol. 2015;195(4):1417-26. doi: 10.4049/jimmunol.1402708. PubMed PMID: 26150533; PubMed Central PMCID: PMCPMC4595932.

183. Kim L, Martinez CJ, Hodgson KA, Trager GR, Brandl JR, Sandefer EP, et al. Systemic and mucosal immune responses following oral adenoviral delivery of influenza vaccine to the human intestine by radio controlled capsule. Sci Rep. 2016;6:37295. doi: 10.1038/srep37295. PubMed PMID: 27881837; PubMed Central PMCID: PMCPMC5121599 Vaxart, the sponsor of the study. The authors EPS and WJD work for a contract research organization that ran the study for the sponsor.

184. Crotty S, Aubert RD, Glidewell J, Ahmed R. Tracking human antigen-specific memory B cells: a sensitive and generalized ELISPOT system. J Immunol Methods. 2004;286(1-2):111-22. Epub 2004/04/17. doi: 10.1016/j.jim.2003.12.015. PubMed PMID: 15087226.

185. Saha A, Rosewell A, Hayen A, MacIntyre CR, Qadri F. Improving immunization approaches to cholera. Expert Rev Vaccines. 2017;16(3):235-48. Epub 2016/11/03. doi: 10.1080/14760584.2017.1249470. PubMed PMID: 27805467.

186. Wrammert J, Smith K, Miller J, Langley WA, Kokko K, Larsen C, et al. Rapid cloning of high-affinity human monoclonal antibodies against influenza virus. Nature. 2008;453(7195):667-71. doi: 10.1038/nature06890. PubMed PMID: 18449194; PubMed Central PMCID: PMCPMC2515609.

187. Wang J, Villeneuve S, Zhang J, Lei P, Miller CE, Lafaye P, et al. On the antigenic determinants of the lipopolysaccharides of Vibrio cholerae O:1, serotypes Ogawa and Inaba. J Biol Chem. 1998;273(5):2777-83. PubMed PMID: 9446585.

188. Giesecke C, Meyer T, Durek P, Maul J, Preiss J, Jacobs JFM, et al. Simultaneous Presence of Non- and Highly Mutated Keyhole Limpet Hemocyanin (KLH)-Specific Plasmablasts Early after Primary KLH Immunization Suggests Cross-Reactive Memory B Cell Activation. J Immunol. 2018;200(12):3981-92. Epub 2018/05/08. doi: 10.4049/jimmunol.1701728. PubMed PMID: 29735481.

189. Mayo-Smith LM, Simon JK, Chen WH, Haney D, Lock M, Lyon CE, et al. The Live Attenuated Cholera Vaccine CVD 103-HgR Primes Responses to the Toxin-Coregulated Pilus Antigen TcpA in Subjects Challenged with Wild-Type Vibrio cholerae. Clin Vaccine Immunol. 2017;24(1). Epub 2016/11/17. doi: 10.1128/CVI.00470-16. PubMed PMID: 27847368; PubMed Central PMCID: PMCPMC5216439.

190. Provenzano D, Lauriano CM, Klose KE. Characterization of the role of the ToxR-modulated outer membrane porins OmpU and OmpT in Vibrio cholerae virulence. J Bacteriol. 2001;183(12):3652-62. Epub 2001/05/24. doi: 10.1128/JB.183.12.3652-3662.2001. PubMed PMID: 11371530; PubMed Central PMCID: PMCPMC95243.

191. Hapfelmeier S, Lawson MA, Slack E, Kirundi JK, Stoel M, Heikenwalder M, et al. Reversible microbial colonization of germ-free mice reveals the dynamics of IgA immune

responses. Science. 2010;328(5986):1705-9. Epub 2010/06/26. doi: 10.1126/science.1188454. PubMed PMID: 20576892; PubMed Central PMCID: PMCPMC3923373.

192. Bishop AL, Schild S, Patimalla B, Klein B, Camilli A. Mucosal immunization with Vibrio cholerae outer membrane vesicles provides maternal protection mediated by antilipopolysaccharide antibodies that inhibit bacterial motility. Infect Immun. 2010;78(10):4402-20. Epub 2010/08/04. doi: 10.1128/IAI.00398-10. PubMed PMID: 20679439; PubMed Central PMCID: PMCPMC2950341.

193. Kauffman RC, Adekunle O, Yu H, Cho A, Nyhoff LE, Kelly M, et al. Impact of Immunoglobulin Isotype and Epitope on the Functional Properties of Vibrio cholerae O-Specific Polysaccharide-Specific Monoclonal Antibodies. mBio. 2021;12(2). Epub 2021/04/22. doi: 10.1128/mBio.03679-20. PubMed PMID: 33879588; PubMed Central PMCID: PMCPMC8092325.

194. Price MJ, Hicks SL, Bradley JE, Randall TD, Boss JM, Scharer CD. IgM, IgG, and IgA Influenza-Specific Plasma Cells Express Divergent Transcriptomes. J Immunol. 2019;203(8):2121-9. Epub 2019/09/11. doi: 10.4049/jimmunol.1900285. PubMed PMID: 31501259; PubMed Central PMCID: PMCPMC6783370.

195. Mackworth-Young CG, Harmer IJ, Mageed RA. The role of antigen in the selection of the human V3-23 immunoglobulin heavy chain variable region gene. Clin Exp Immunol. 2003;134(3):420-5. Epub 2003/11/25. doi: 10.1111/j.1365-2249.2003.02319.x. PubMed PMID: 14632746; PubMed Central PMCID: PMCPMC1808894.

196. Mroczek ES, Ippolito GC, Rogosch T, Hoi KH, Hwangpo TA, Brand MG, et al. Differences in the composition of the human antibody repertoire by B cell subsets in the blood. Front Immunol. 2014;5:96. Epub 2014/03/29. doi: 10.3389/fimmu.2014.00096. PubMed PMID: 24678310; PubMed Central PMCID: PMCPMC3958703.

197. Blaser MJ, Falkow S. What are the consequences of the disappearing human microbiota? Nat Rev Microbiol. 2009;7(12):887-94. Epub 2009/11/10. doi: 10.1038/nrmicro2245. PubMed PMID: 19898491.

198. Smith K, Garman L, Wrammert J, Zheng NY, Capra JD, Ahmed R, et al. Rapid generation of fully human monoclonal antibodies specific to a vaccinating antigen. Nat Protoc. 2009;4(3):372-84. Epub 2009/02/28. doi: 10.1038/nprot.2009.3. PubMed PMID: 19247287; PubMed Central PMCID: PMCPMC2750034.

199. Koelle K, Rodo X, Pascual M, Yunus M, Mostafa G. Refractory periods and climate forcing in cholera dynamics. Nature. 2005;436(7051):696-700. Epub 2005/08/05. doi: 10.1038/nature03820. PubMed PMID: 16079845.

200. Svennerholm AM, Jertborn M, Gothefors L, Karim AM, Sack DA, Holmgren J. Mucosal antitoxic and antibacterial immunity after cholera disease and after immunization with a combined B subunit-whole cell vaccine. J Infect Dis. 1984;149(6):884-93. PubMed PMID: 6736680.

201. Koelle K, Pascual M, Yunus M. Serotype cycles in cholera dynamics. Proc Biol Sci. 2006;273(1603):2879-86. doi: 10.1098/rspb.2006.3668. PubMed PMID: 17015366; PubMed Central PMCID: PMCPMC1664638.

202. Bi Q, Ferreras E, Pezzoli L, Legros D, Ivers LC, Date K, et al. Protection against cholera from killed whole-cell oral cholera vaccines: a systematic review and meta-analysis. Lancet Infect Dis. 2017;17(10):1080-8. doi: 10.1016/S1473-3099(17)30359-6. PubMed PMID: 28729167; PubMed Central PMCID: PMCPMC5639147.

203. Ramamurthy T, Garg S, Sharma R, Bhattacharya SK, Nair GB, Shimada T, et al. Emergence of novel strain of Vibrio cholerae with epidemic potential in southern and eastern India. Lancet. 1993;341(8846):703-4. Epub 1993/03/13. doi: 10.1016/0140-6736(93)90480-5. PubMed PMID: 8095620.

204. Gustafsson B, Holme T. Immunological characterization of Vibrio cholerae O:1 lipopolysaccharide, O-side chain, and core with monoclonal antibodies. Infect Immun. 1985;49(2):275-80. PubMed PMID: 2410362; PubMed Central PMCID: PMCPMC262010.

205. Aktar A, Rahman MA, Afrin S, Akter A, Uddin T, Yasmin T, et al. Plasma and memory B cell responses targeting O-specific polysaccharide (OSP) are associated with protection against Vibrio cholerae O1 infection among household contacts of cholera patients in Bangladesh. PLoS Negl Trop Dis. 2018;12(4):e0006399. doi: 10.1371/journal.pntd.0006399. PubMed PMID: 29684006; PubMed Central PMCID: PMCPMC5912711.

206. Stokes CR, Soothill JF, Turner MW. Immune exclusion is a function of IgA. Nature. 1975;255(5511):745-6. Epub 1975/06/26. doi: 10.1038/255745a0. PubMed PMID: 1169692.

207. Binsker U, Lees JA, Hammond AJ, Weiser JN. Immune exclusion by naturally acquired secretory IgA against pneumococcal pilus-1. J Clin Invest. 2020;130(2):927-41. Epub 2019/11/07. doi: 10.1172/JCI132005. PubMed PMID: 31687974; PubMed Central PMCID: PMCPMC6994158.

208. Williams RC, Gibbons RJ. Inhibition of bacterial adherence by secretory immunoglobulin A: a mechanism of antigen disposal. Science. 1972;177(4050):697-9. PubMed PMID: 5054144.

209. Moor K, Diard M, Sellin ME, Felmy B, Wotzka SY, Toska A, et al. High-avidity IgA protects the intestine by enchaining growing bacteria. Nature. 2017;544(7651):498-502. doi: 10.1038/nature22058. PubMed PMID: 28405025.

210. Forbes SJ, Eschmann M, Mantis NJ. Inhibition of Salmonella enterica serovar typhimurium motility and entry into epithelial cells by a protective antilipopolysaccharide monoclonal immunoglobulin A antibody. Infect Immun. 2008;76(9):4137-44. Epub 2008/07/16. doi: 10.1128/IAI.00416-08. PubMed PMID: 18625740; PubMed Central PMCID: PMCPMC2519396.

211. Charles RC, Kelly M, Tam JM, Akter A, Hossain M, Islam K, et al. Humans Surviving Cholera Develop Antibodies against Vibrio cholerae O-Specific Polysaccharide That Inhibit Pathogen Motility. mBio. 2020;11(6). Epub 2020/11/19. doi: 10.1128/mBio.02847-20. PubMed PMID: 33203761; PubMed Central PMCID: PMCPMC7683404.

212. Haney DJ, Lock MD, Simon JK, Harris J, Gurwith M. Antibody-Based Correlates of Protection Against Cholera Analysis of a Challenge Study in a Cholera-Naive Population. Clin Vaccine Immunol. 2017. doi: 10.1128/CVI.00098-17. PubMed PMID: 28566334; PubMed Central PMCID: PMCPMC5583470.

213. Losonsky GA, Yunyongying J, Lim V, Reymann M, Lim YL, Wasserman SS, et al. Factors influencing secondary vibriocidal immune responses: relevance for understanding immunity to cholera. Infect Immun. 1996;64(1):10-5. PubMed PMID: 8557325; PubMed Central PMCID: PMCPMC173720.

214. Riordan SM, McIver CJ, Wakefield D, Andreopoulos PC, Duncombe VM, Bolin TD, et al. Local and systemic complement activity in small intestinal bacterial overgrowth. Dig Dis Sci. 1997;42(6):1128-36. PubMed PMID: 9201072.

215. Kerr MA. The structure and function of human IgA. Biochem J. 1990;271(2):285-96. PubMed PMID: 2241915; PubMed Central PMCID: PMCPMC1149552.

216. Shamsuzzaman S, Ahmed T, Mannoor K, Begum YA, Bardhan PK, Sack RB, et al. Robust gut associated vaccine-specific antibody-secreting cell responses are detected at the mucosal surface of Bangladeshi subjects after immunization with an oral killed bivalent V. cholerae O1/O139 whole cell cholera vaccine: comparison with other mucosal and systemic responses. Vaccine. 2009;27(9):1386-92. doi: 10.1016/j.vaccine.2008.12.041. PubMed PMID: 19146897.

217. Liu C, Morrow J. Biosimilars of monoclonal antibodies : a practical guide to manufacturing, preclinical, and clinical development. Hoboken, New Jersey: John Wiley & Sons, Inc.,; 2017.

218. Atsumi T, McCarter L, Imae Y. Polar and lateral flagellar motors of marine Vibrio are driven by different ion-motive forces. Nature. 1992;355(6356):182-4. doi: 10.1038/355182a0. PubMed PMID: 1309599.

219. Roux KH, Strelets L, Michaelsen TE. Flexibility of human IgG subclasses. J Immunol. 1997;159(7):3372-82. PubMed PMID: WOS:A1997XY46100035.

220. Villeneuve S, Souchon H, Riottot MM, Mazie JC, Lei P, Glaudemans CP, et al. Crystal structure of an anti-carbohydrate antibody directed against Vibrio cholerae O1 in complex with antigen: molecular basis for serotype specificity. Proc Natl Acad Sci U S A. 2000;97(15):8433-8. Epub 2000/07/06. doi: 10.1073/pnas.060022997. PubMed PMID: 10880560; PubMed Central PMCID: PMCPMC26965.

221. Roche MI, Lu Z, Hui JH, Sharon J. Characterization of monoclonal antibodies to terminal and internal O-antigen epitopes of Francisella tularensis lipopolysaccharide. Hybridoma (Larchmt). 2011;30(1):19-28. Epub 2011/04/07. doi: 10.1089/hyb.2010.0083. PubMed PMID: 21466282; PubMed Central PMCID: PMCPMC3119334.

222. Lu Z, Rynkiewicz MJ, Yang CY, Madico G, Perkins HM, Wang Q, et al. The binding sites of monoclonal antibodies to the non-reducing end of Francisella tularensis O-antigen accommodate mainly the terminal saccharide. Immunology. 2013;140(3):374-89. Epub

2013/07/13. doi: 10.1111/imm.12150. PubMed PMID: 23844703; PubMed Central PMCID: PMCPMC3800442.

223. Leitner DR, Feichter S, Schild-Prufert K, Rechberger GN, Reidl J, Schild S. Lipopolysaccharide modifications of a cholera vaccine candidate based on outer membrane vesicles reduce endotoxicity and reveal the major protective antigen. Infect Immun. 2013;81(7):2379-93. Epub 2013/05/01. doi: 10.1128/IAI.01382-12. PubMed PMID: 23630951; PubMed Central PMCID: PMCPMC3697601.

224. Forbes SJ, Martinelli D, Hsieh C, Ault JG, Marko M, Mannella CA, et al. Association of a protective monoclonal IgA with the O antigen of Salmonella enterica serovar Typhimurium impacts type 3 secretion and outer membrane integrity. Infect Immun. 2012;80(7):2454-63. Epub 2012/04/05. doi: 10.1128/IAI.00018-12. PubMed PMID: 22473607; PubMed Central PMCID: PMCPMC3416483.

225. Schauer K, Lehner A, Dietrich R, Kleinsteuber I, Canals R, Zurfluh K, et al. A Cronobacter turicensis O1 Antigen-Specific Monoclonal Antibody Inhibits Bacterial Motility and Entry into Epithelial Cells. Infection and Immunity. 2015;83(3):876-87. doi: 10.1128/Iai.02211-14. PubMed PMID: WOS:000351230200003.

226. Levinson KJ, Giffen SR, Pauly MH, Kim DH, Bohorov O, Bohorova N, et al. Plant-based production of two chimeric monoclonal IgG antibodies directed against immunodominant epitopes of Vibrio cholerae lipopolysaccharide. J Immunol Methods. 2015;422:111-7. doi:

10.1016/j.jim.2015.04.001. PubMed PMID: 25865265; PubMed Central PMCID: PMCPMC4458452.

227. Wold AE, Mestecky J, Tomana M, Kobata A, Ohbayashi H, Endo T, et al. Secretory immunoglobulin A carries oligosaccharide receptors for Escherichia coli type 1 fimbrial lectin. Infect Immun. 1990;58(9):3073-7. Epub 1990/09/01. doi: 10.1128/IAI.58.9.3073-3077.1990. PubMed PMID: 2201644; PubMed Central PMCID: PMCPMC313613.

228. Furtado PB, Whitty PW, Robertson A, Eaton JT, Almogren A, Kerr MA, et al. Solution structure determination of monomeric human IgA2 by X-ray and neutron scattering, analytical ultracentrifugation and constrained modelling: a comparison with monomeric human IgA1. J Mol Biol. 2004;338(5):921-41. Epub 2004/04/28. doi: 10.1016/j.jmb.2004.03.007. PubMed PMID: 15111057.

229. Boehm MK, Woof JM, Kerr MA, Perkins SJ. The Fab and Fc fragments of IgA1 exhibit a different arrangement from that in IgG: a study by X-ray and neutron solution scattering and homology modelling. J Mol Biol. 1999;286(5):1421-47. Epub 1999/03/05. doi: 10.1006/jmbi.1998.2556. PubMed PMID: 10064707.

230. Lorin V, Mouquet H. Efficient generation of human IgA monoclonal antibodies. J Immunol Methods. 2015;422:102-10. doi: 10.1016/j.jim.2015.04.010. PubMed PMID: 25910833.

231. Charles ED, Orloff MI, Dustin LB. A flow cytometry-based strategy to identify and express IgM from VH1-69+ clonal peripheral B cells. J Immunol Methods. 2011;363(2):210-20.

doi: 10.1016/j.jim.2010.09.022. PubMed PMID: 20875420; PubMed Central PMCID: PMCPMC3003765.

232. Kobayashi K. Studies on human secretory IgA comparative studies of the IgA-bound secretory piece and the free secretory piece protein. Immunochemistry. 1971;8(9):785-800. Epub 1971/09/01. doi: 10.1016/0019-2791(71)90446-0. PubMed PMID: 5002714.

233. Miller F, Metzger H. Characterization of a Human Macroglobulin. I. The Molecular Weight of Its Subunit. J Biol Chem. 1965;240:3325-33. Epub 1965/08/01. PubMed PMID: 14328368.

234. Xu P, Alam MM, Kalsy A, Charles RC, Calderwood SB, Qadri F, et al. Simple, direct conjugation of bacterial O-SP-core antigens to proteins: development of cholera conjugate vaccines. Bioconjug Chem. 2011;22(10):2179-85. doi: 10.1021/bc2001984. PubMed PMID: 21899371; PubMed Central PMCID: PMCPMC3197769.

235. Sayeed MA, Bufano MK, Xu P, Eckhoff G, Charles RC, Alam MM, et al. A Cholera Conjugate Vaccine Containing O-specific Polysaccharide (OSP) of V. cholerae O1 Inaba and Recombinant Fragment of Tetanus Toxin Heavy Chain (OSP:rTTHc) Induces Serum, Memory and Lamina Proprial Responses against OSP and Is Protective in Mice. PLoS Negl Trop Dis. 2015;9(7):e0003881. doi: 10.1371/journal.pntd.0003881. PubMed PMID: 26154421; PubMed Central PMCID: PMCPMC4495926.

236. Schauer K, Lehner A, Dietrich R, Kleinsteuber I, Canals R, Zurfluh K, et al. A Cronobacter turicensis O1 antigen-specific monoclonal antibody inhibits bacterial motility and entry into

epithelial cells. Infect Immun. 2015;83(3):876-87. Epub 2014/12/24. doi: 10.1128/IAI.02211-14. PubMed PMID: 25534937; PubMed Central PMCID: PMCPMC4333459.